UNIVERSIDADE DO ALGARVE

PREDICTIVE CONTROL OF HVAC SYSTEMS IN BUILDINGS

Shabnam Pesteh

Dissertação

Mestrado Integrado em Engenharia Electrónica e Telecomunicações

Trabalho efectuado sob a orientação de:

Prof. Dra. António Eduardo de Barros Ruano

2015

Declaration of Authorship

I, Shabnam Pesteh, declare that this thesis titled, 'Predictive Control of HVAC Systems in Buildings' and the work presented in it are my own. Authors and works consulted during the realization of this work are properly cited and included in the reference listing.

Signed: 

Date: 30/09.2015

Abstract

This thesis deals with the development of Model Based Predictive Control (MBPC) techniques for costs efficient building climate control. Because a large apportionment of the world's energy is spent in buildings and refurbishments are expensive, there is a vigorous motivation for a more cost efficient control. The aim is to utilize control alternatives in order to optimize building Heating, Ventilation, and Air Conditioning (HVAC) by using MBPC with weather and comfort level predictions considering the occupied periods.

A significant characteristic in building climate control is the uncertainty in the weather predictions. In addition, comfort constraints do not have to be satisfied at all times, but can be described as constraints that have to be satisfied. MBPC is a control methodology which is applied by its capability to deal with constrained control problems employing models for predicting the future behavior of a system and utilizing optimization approaches to determine the control input.

The thesis starts with the state-of-the-art methods in building climate control following with a background MBPC methodology and its required materials in which the theoretical and practical developments are presented.

This thesis introduces three investigations in the topic of building climate control:

The first investigation is concerned with the energy consumption estimation in the objective function according to the number of indoor units supplied by a single external machine as this dissertation studies a multi-zone building. The data yielded by this study provided convincing evidence that the energy consumption is independent from the deviation of the average inside air temperature over the integration period to its setpoints which was aforementioned in the previous version of this work [1]. This issue will be addressed in this thesis by dynamic and static modelings.

The second investigation is concerned with the reduction of peak electricity demand by incorporating electricity tariffs straightly in the objective function of the MBPC setup therefore reducing electricity economical costs.

Finally, an investigation of the importance of occupancy consideration in building climate control is outlined. The previous MBPC approach suffered from not being able to assure thermal comfort conditions in the time that the occupants start entering the room, therefore not maintaining the comfort for the whole occupancy periods. A MBPC

controller which controls the building with a pre-defined occupancy schedule is employed as a benchmark. Three approaches are considered to solve this issue.

The first two approaches include two varied time scheduled MBPC methodologies with some improvements in the optimization algorithm in order to activate the control algorithm only if the room is predicted to be outside thermal comfort within the occupied hours.

The last but not least improvement introduced to aforementioned MBPC algorithm is to modify the search procedure of the optimization algorithm, Branch-and-Band (BaB) approach, in order to not apply the control constraints for the nodes of the tree that are placed outside of occupied hours. The simulation findings suggest that the modified MBPC algorithm outperforms current control practice regarding both cost efficiency and occupant comfort.

Resumo

Esta dissertação insere-se no âmbito de desenvolvimento de Modelos de Controlo Preditivos (MBPC) que visam controlar o clima de um edifício tendo em conta a otimização de custos. Uma considerável parte da energia consumida pelo planeta recai em consumos relacionados com edifícios e, consequentemente, este facto desperta uma motivação justificada para controlar os custos de uma forma eficiente. O objetivo passa por utilizar alternativas de controlo de forma a optimizar o Aquecimento, Ventilação e Ar Condicionado (HVAC) usando MBPC, considerando períodos de ocupação para prever níveis de clima e conforto no edifício.

Uma característica significante no controlo do clima de um edifício reside na incerteza na predição do clima. Além disso, restrições em termos dos níveis de conforto não precisam de ser necessariamente satisfeitas a todo o momento. São portanto classificadas como restrições de ocasião. MBPC consiste numa metodologia de controlo caracterizada pela sua capacidade de lidar com problemas de controlo com restrições, que façam uso de modelos preditivos para estimar comportamentos futuros de um sistema, utilizando técnicas de optimização para gerar a acção de controlo (entrada do sistema).

Esta tese inicia-se com uma visão geral do estado da arte, nomeadamente dos métodos utilizados para controlar o clima de um edifício. De seguida, a metodologia MBPC é introduzida e são apresentados os materiais indispensáveis ao desenvolvimento prático e teórico dos trabalhos aqui apresentados.

Este trabalho introduz três investigações concentradas no âmbito o controlo do clima de um edifício:

Inicialmente a investigação focou-se na estimação de consumos energéticos na função objectivo em função do número de unidades interiores, disponibilizado por uma única máquina externa, na medida em que esta dissertação estuda edifícios multi-zona .

A segunda investigação faz referência à redução do pico de demanda de electricidade ao incorporar tarifas de eletricidade, directamen na função objectivo da configuração do MBPC.

Por último, a investigação direcionou-se para o impacto que a ocupação tem no controlo do clima de um edifício. A metodologia MBPC tem como objectivo garantir que o edifício se encontra em conforto térmico no momento da entrada dos ocupantes, bem como manter os níveis de conforto ao longo da sua estadia.

Como benchmark foi utilizado um controlador MBPC que procede ao controlo do edifício com um calendário de ocupação pré-definido. Três abordagens são consideradas para resolver este problema.

As duas primeiras abordagens incluem duas variações do da metodologia MBPC com algumas melhoria no algoritmo de optimização, de forma a activar o algoritmo de controlo apenas caso seja estimado que o edifício vá estar fora dos níveis de conforto adequados durante as horas de ocupação.

Por último, o procedimento de procura do algoritmo de optimização, Branch-and-Band (BaB), foi alterado. A restrições de controlo não foram aplicadas aos nós localizados fora de horas de ocupação, de forma a diminuir o consumo de energia. As simulações revelam que o algoritmo MBPC modificado apresenta uma maior performance comparativamente ao anterior, tanto em eficiência de custos como em níveis de conforto.

Acknowledgements

Firstly, I would like to express my sincere gratitude to my advisor Professor António Eduardo de Barros Ruano for the continuous support of my master study and related research, for his patience, motivation, and immense knowledge. I would also like to thank him for providing an excellent working environment and for bringing interesting and diverse people together. I am very grateful for having been part of such an inspiring and motivating environment as the Centre for Intelligent Systems (CSI) in UAlg Portugal.

My thanks go also to all members of the QREN SIDT 38798 and FCT project, who shared with me their expertise on meteorology, building physics, and building control. I am grateful for the privilege of having experienced the work on an industry project and meeting people, who showed me a different perspective on many questions.

Shabnam Pesteh
Faro, September 2015

Contents

Declaration of Authorship **i**

Abstract **iii**

Resumo **v**

Acknowledgements **vii**

Contents **viii**

List of Figures **x**

List of Tables **xiii**

Abbreviations **xv**

Symbols **xvii**

1 Introduction **1**
1.1 Objectives . . . 3
1.2 Contributions and publications . . . 5
1.3 Thesis structure . . . 5

2 State-of-the-Art **7**
2.1 HVAC control . . . 7
2.2 Thermal comfort representation . . . 9
2.3 Energy peak reduction . . . 9
2.4 Thesis contribution . . . 10

3 Background **12**
3.1 Experimental environment . . . 13
3.2 Model based predictive control (MBPC) . . . 14
3.3 Thermal comfort constraint . . . 15
3.4 Model structure . . . 18
3.4.1 Artificial neural network (ANN) . . . 18
3.4.1.1 Radial basis function networks . . . 19
3.5 PMV model . . . 24
3.6 Predictive models . . . 25

3.7 Optimization algorithm: Branch-and-Band (BaB) 26
3.7.1 Branch-and-Band algorithm implementation 29

4 Energy Estimation Methodology 34
4.1 Previous energy estimation method 35
4.2 Dynamics energy estimation modeling 36
4.2.1 Autoregressive exogenous models (ARX) 37
4.2.2 Model structure 39
4.2.3 One-at-a-time running internal machine 40
4.2.4 Two-at-a-time running internal machine 42
4.2.5 Three-at-a-time running internal machine 44
4.2.6 Four-at-a-time running internal machine 45
4.3 Static energy estimation modeling 46
4.4 Simulation results 49
4.5 Concluding remarks 57

5 Objective Function Study 58
5.1 Objective function definition 59
5.2 Previous objective function 60
5.3 Dynamic model objective function 60
5.4 Static model objective function 62
5.5 Cost-oriented objective function 62
5.5.1 Real-Time Pricing 63
5.5.2 Formulation 63
5.6 Simulation results 66
5.7 Concluding remarks 75

6 Modified Model-based Predictive Control 76
6.1 Occupation period scheduling plan 77
6.2 Scheduled MBPC 4 hours 79
6.3 Scheduled MBPC 2 hours 80
6.4 Modified MBPC Algorithm 80
6.5 Simulation results 82
6.6 Concluding remarks 90

7 Conclusions and future works 92
7.1 Conclusions 92
7.2 Future work 93

List of Figures

3.1 Overview on the map floor 2. 13
3.2 Overview of the experimental set up used from [1]. 14
3.3 Model based predictive control strategy obtained from [2]. 15
3.4 Block diagram of a learning process with a teacher. Adapted from [3] . . 19
3.5 Plotting of $s(x) = x^2$. In this case Γ is the bi dimensional plot of the output as a function of the input. 21
3.6 Branch and bound tree structure for MBPC obtained from [2]. 27
3.7 Branch and band implementation diagram. 33

4.1 External unit energy consumption trend profile while switching on/off the HVAC system. 36
4.2 Model identification process. 37
4.3 Response of each developed model for one working internal machine. . . . 40
4.4 Model estimated output compared with the energy consumption trend in one-at-a-time running internal machine case. 42
4.5 Response of each developed model for two working internal machines. . . 42
4.6 Model estimated output compared with the energy consumption trend in two-at-a-time running internal machine case. 43
4.7 Response of each developed model for three working internal machines. . 44
4.8 Model estimated output compared with the energy consumption trend in three-at-a-time running internal machine case. 45
4.9 Response of each developed model for four working internal machines. . . 46
4.10 Model estimated output compared with the energy consumption trend in four-at-a-time running internal machine case. 47
4.11 Energy consumption trend profile distinguished by the number of indoor units that are working simultaneously. 47
4.12 Static energy estimation modeling. 48
4.13 A comparison on energy consumption estimation methods within 'experiment 1' while there is only one internal machine working. 49
4.14 A comparison on energy consumption estimation methods within 'experiment 2' while there is only one internal machine working. 50
4.15 A comparison on energy consumption estimation methods within 'experiment 3' while there is only one internal machine working. 50
4.16 A comparison on energy consumption estimation methods within 'experiment 4' while there are only two internal machines working. 52
4.17 A comparison on energy consumption estimation methods within 'experiment 5' while there are only two internal machines working. 52
4.18 A comparison on energy consumption estimation methods within 'experiment 6' while there are only two internal machines working. 53

4.19 A comparison on energy consumption estimation methods within 'experiment 7' while there are three internal machines working simultaneously. . 53
4.20 A comparison on energy consumption estimation methods within 'experiment 8' while there are three internal machines working simultaneously. . 54
4.21 A comparison on energy consumption estimation methods within 'experiment 9' while there are three internal machines working simultaneously. . 54
4.22 A comparison on energy consumption estimation methods within 'experiment 10' while all the four internal machines are working simultaneously. 55
4.23 A comparison on energy consumption estimation methods within 'experiment 11' while all the four internal machines are working simultaneously. 56
4.24 A comparison on energy consumption estimation methods within 'experiment 12' while all the four internal machines are working simultaneously. 56

5.1 Real-time pricing unit electric rate daily range at summer and winter peaks. 64
5.2 Upper plot: OAT (in green) and IAT evolution using the old cost function (in blue), dynamic model (in pink) and static model (in sea green) objective functions. Lower plot: setpoint temperature evolution using the old, dynamic and static objective functions with same specified colors for experiment 1. 67
5.3 PMV evolution of experiment 1 using specified objective functions. 67
5.4 Upper plot: OAT (in green) and IAT evolution using the old cost function (in blue), dynamic model (in pink) and static model (in sea green) objective functions. Lower plot: setpoint temperature evolution using the old, dynamic and static objective functions with same specified colors for experiment 2. 68
5.5 PMV evolution of experiment 2 using specified objective functions. 69
5.6 Upper plot: OAT (in green) and IAT evolution using the old cost function (in blue), dynamic model (in pink) and static model (in sea green) objective functions. Lower plot: setpoint temperature evolution using the old, dynamic and static objective functions with same specified colors for experiment 3. 70
5.7 PMV evolution of experiment 3 using specified objective functions. 70
5.8 Upper plot: OAT (in green) and IAT evolution using the energy-oriented (in pink) and cost-oriented (in blue) objective functions. Lower plot: setpoint temperature evolution using the energy-oriented (in pink) and cost-oriented (in blue) objective functions for experiment 1. 71
5.9 A comparison between PMV evolution of energy-oriented and cost-oriented objective function for experiment 1. 72
5.10 Upper plot: OAT (in green) and IAT evolution using the energy-oriented (in pink) and cost-oriented (in blue) objective functions. Lower plot: setpoint temperature evolution using the energy-oriented (in pink) and cost-oriented (in blue) objective functions for experiment 2. 73
5.11 A comparison between PMV evolution of energy-oriented and cost-oriented objective function for experiment 2. 73
5.12 Upper plot: OAT (in green) and IAT evolution using the energy-oriented (in pink) and cost-oriented (in blue) objective functions. Lower plot: setpoint temperature evolution using the energy-oriented (in pink) and cost-oriented (in blue) objective functions for experiment 3. 74

5.13 A comparison between PMV evolution of energy-oriented and cost-oriented objective function for experiment 3. 74

6.1 Sample trend data of HVACs on/off status of 4 indoor units without occupation scheduling plan consideration. In order the plot to be discernible, indoor units A, B, C and D on/off states are distinguished in different levels of 0.9, 1, 1.1 and 1.2 respectively. 77
6.2 Sample trend data of thermal comfort without 4 indoor units without occupation scheduling plan consideration. 78
6.3 Sample trend data of the energy consumption and its related cost without 4 indoor units without occupation scheduling plan consideration. 78
6.4 A comparison between HVAC system on/off state applying different MBPC methodologies developed in this work compared with the MBPC with regular BaB algorithm for experiment 1. In order the plot to be discernible, standard MBPC, scheduled MBPC 4 hours, scheduled MBPC 2 hours and modified MBPC on/off states are distinguished in different levels of 0.9, 1, 1.1 and 1.2 respectively. 85
6.5 PMV evolution employing different MBPC methodologies developed in this work compared to the standard MBPC within the occupation period for experiment 1. 85
6.6 A comparison between HVAC system on/off state applying different MBPC methodologies developed in this work compared with the MBPC with regular BaB algorithm for experiment 2. In order the plot to be discernible, standard MBPC, scheduled MBPC 4 hours, scheduled MBPC 2 hours and modified MBPC on/off states are distinguished in different levels of 0.9, 1, 1.1 and 1.2 respectively. 87
6.7 PMV evolution employing different MBPC methodologies developed in this work compared to the standard MBPC within the occupation period for experiment 2. 87

List of Tables

3.1 The ASHRAE thermal sensation scale 16
3.2 Input–output structure for room climate summer models. 26
3.3 Input–output structure for room climate winter models. 26

4.1 Static rates of the energy consumption for the experimental external units. 48
4.2 Energy estimation method evaluation within 3 different experiments in case that only one internal unit connected to the external machine is running. 49
4.3 Energy estimation method accuracy for 3 different experiments while only one internal unit is working. 51
4.4 Energy estimation method evaluation within 3 different experiments in case that only two internal units connected to the external machine are running. 51
4.5 Energy estimation method accuracy for 3 different experiments while only two internal units are working. 52
4.6 Energy estimation method evaluation within 3 different experiments in case that three internal units connected to the external machine are running. 55
4.7 Energy estimation method accuracy for 3 different experiments while three internal units are working. 55
4.8 Energy estimation method evaluation within 3 different experiments in case that all the four internal units connected to the external machine are running. 56
4.9 Energy estimation method accuracy for 3 different experiments while all the four internal units are working. 57

5.1 Tariff timetable specified in UAlg contract with EDP. 63
5.2 UAlg electricity active power rate charges specified in UAlg contract with EDP. 64
5.3 Coefficient values calculated for the objective function in (5.16) 65
5.4 Energy consumption and expense of different objective functions related to experiment 2. 69
5.5 Energy consumption and expense of different objective functions related to experiment 3. 71
5.6 Energy consumption and expense of energy-oriented and cost-oriented objective functions related to experiment 2. 72
5.7 Energy consumption and expense of energy-oriented and cost-oriented objective functions related to experiment 3. 75

6.1 Energy consumptions and their corresponding prices employing different MBPC methodologies developed in this work compared to the standard MBPC distinguished in two parts of 4 hours prior to occupation and within occupation for experiment 1. 86
6.2 Energy consumptions and their corresponding prices employing different MBPC methodologies developed in this work compared to the standard MBPC distinguished in two parts of 4 hours prior to occupation and within occupation for experiment 2. 88
6.3 Energy consumption and corresponding price saving percentages employing different MBPC methodologies developed in this work compared to the standard MBPC within 4 presented experiments. 90

Abbreviations

MBPC	**M**odel **B**ased **P**redictive **C**ontrol
BaB	**B**ranch and **B**and
UAlg	**U**niversity of **A**lgarve
AC	**A**ir **C**onditioning
HVAC	**H**eating **V**entilating and **A**ir **C**onditioning
ARX	**A**ut **R**regressive **E**xogenous
ASHRAE	**A**merican **S**ociety of **H**eating, **R**efrigerating, and **A**ir-conditioning **E**ngineers
SISO	**S**ingle **I**nput **S**ingle **O**utput
MSE	**M**ean **S**quared **E**rror
FPE	**F**inal **P**rediction **E**rror
NRMSE	**N**ormalized **M**ean **S**quare **E**rror
RTP	**R**eal **T**ime **P**ricing
EDP	**E**nergias **D**e **P**ortugal
TIP	**T**emperature **I**ntegration **P**eriod days
PPD	data **P**oints **P**er **D**ay
EMC	**E**nergy **M**anagement **C**ontrol
MOGA	**M**ulti **O**bjective **G**enetic **A**lgorithm
CSI	**C**entro de **S**istemas **I**nteligentes
FCT	**F**aculdade de **C**iências e **T**ecnologia
RBF	**R**adial **B**asis **F**unction
NN	**N**eural **N**etworks
ANN	**A**rtificial **N**eural **N**etwork
RFH	**R**adiant **F**loor **H**eating
SQP	**S**equential **Q**uadratic **P**rogramming
TABS	**T**hermally **A**ctivated **B**uilding **S**ystems

BCVTB	**B**uilding **C**ontrols **V**irtual **T**est **B**ed
MRT	**M**ean **R**adiant **T**emperature
PMV	**P**redicted **M**ean **V**ote
WSN	**W**ireless **S**ensor **N**etwork
VRF	**V**ariable **R**efrigerant **F**low
LM	**L**evenberg **M**arquardt
PRBS	**P**seudo **R**andom **B**inary **S**ignals
RMSE	**R**oot **M**ean **S**quared **E**rror
MLP	**M**ulti **L**ayer **P**erceptron
BS	**B**-**S**plines
TCP/IP	**T**ransmission **C**ontrol **P**rotocol/**I**nternet **P**rotocol

Symbols

ζ	Constant-rate of energy consumption
NP_{TI}	Number of data points within the integration period
$\bar{T}_{\varepsilon}$	Deviation of setpoint from average room temperature
Υ	Accuracy
C_e	Energy cost
C_d	Demand cost
T_e	Energy rate tariff
ND	Number of days of the invoice
k	Time instant
PH	Prediction horizon
CH	Control horizon
u	Control action
U	Sequence of control actions
υ_{PH}	Space of all sequences of size PH
nao	Number of possible control actions
NA	Number of actuators
PA	Matrix of nao possible control combinations for the NA actuators
$\jmath$	Accumulated cost
$\hat{J}_e$	cost of selecting one control action
T_{sp}	Air-conditioner setpoint temperature
T_{ai}	Inside air temperature
H_{ai}	Inside air humidity
T_{ao}	Outside air temperature
H_{ao}	Outside air humidity
R_{sg}	Global solar radiation

Θ	PMV index
Θ_T	Threshold value for the PMV index
E	Energy consumption
P	Energy price
N_u	Number of inputs
N_y	Number of outputs
ε	White noise disturbance
δ	Matrix of white noise disturbance values
n_a	Order of the auto-regressive part of ARX model
n_b	Order of the moving average part of ARX model plus one
A	Matrix of the orders of the auto-regressive part of ARX model
B	Matrix of the orders of the moving average part of ARX model
d	Temporal delay
N	Number of samples
e	Error
G	Transfer function
V	Loss function
S	Number of estimated parameters
ι	Length of estimation dataset
Ω_{pr}	Number of steps in occupation period
t_{os}	Start of occupation interval
t_{oe}	End of occupation interval
D_{os}	Time duration to start of occupation interval
D_{oe}	Time duration to end of occupation interval
C_{ign}	Ignore control algorithm
N_I	Number of occupation time intervals within a specified time
$\varkappa$	Cost-oriented objective function coefficients
N_{IM}	Number of simultaneously operating internal machines
Γ	PMV failure
$\hbar_\Gamma$	PMV failure percentage
Λ	Efficiency percentage
M	Metabolic rate
W	Work activity

P_a	Partial water vapor pressure
$\bar{T}_r$	Mean radiant temperature
T_{cl}	Surface temperature of clothing
h_c	Convective heat transfer coefficient
V_a	Air velocity
I_{cl}	Clothing thermal resistance
f_{cl}	Ratio of body surface area covered by clothes to the naked surface area
T_g	Globe temperature
D	Globe diameter
D^t	Training dataset
D^v	Validation dataset
ϵ	Globe emissivity coefficient
φ	Gaussian function
n	Number of neurons
p	Number of patterns
Φ	Interpolation matrix
w_i	Adjustable weight of the network
ρ	Generalization parameter
Γ	Hypersurface mapping an input to an output domain
$\vartheta(.)$	Radial basis function

This thesis is dedicated to my parents for their endless love, support and encouragement

1

Introduction

The increased interest in building climate control both in academia as well as from industry and policy makers is due to several developments. The world is facing a drastic need to reduce its energy consumption while a large part of today's energy in industrialized countries is consumed in buildings. In the European Community, the primary energy consumption in buildings accounts for about 40% of all energy consumed and, with country variations, half of this energy is spent in air conditioning [4]. When energy costs soared during the energy crisis of the early 1970 s, the building envelope was tightened to reduce uncontrolled air leakage, and outdoor air supply was sharply reduced in many mechanically ventilated buildings and commercial aircraft. Since then there has been growing concern and uncertainty with the quality of the indoor environment due to commonly attributed adverse effects on comfort, health and productivity [5]. The use of advanced control techniques, and in particular, model-based predictive control (MBPC) for heating, ventilating, and air conditioning systems (HVACs) is to offer a huge potential of reducing energy consumption and the related costs inside buildings.

The Center for Intelligent Systems (CSI) is a research center in the Faculty of Sciences and Technology (FCT) of the University of Algarve (UAlg) located in the South of Portugal. ROLEAR SA is a company in Algarve that provides automation solutions for hydraulic systems, electricity and compressed air activity. Some years ago, ROLEAR SA and UAlg started a collaboration aiming to conduct a research in the field of HVAC

systems control. The aim of this project is to propose and implement a commercial solution based on MBPC while minimizing the energy consumption and costs. This Master thesis is a result of the predictive control part as a sub-project from that collaboration. In the other words, the optimization system manipulates the inside climate in order to achieve the following goals:

- Maintain the room in thermal comfort.
- Minimize energy consumption and costs.

Given the contradictory nature of the goals and the characteristics of the control system, the control problem can be characterized as a discrete optimization problem. At each time instant k, the controller must find the best set of discrete control actions which optimizes the required goals and restrictions.

Previous studies indicate that thermal comfort is strongly related to the thermal balance of the body [6]. This balance is influenced by environmental parameters like as air temperature, T_{ai}, and mean radiant temperature, $\bar{T}_r$, relative air velocity, V_a, and relative humidity, H_{ai}, as well as personal parameters like as activity level or metabolic rate[1], M, and clothing thermal resistance[2] (T_{cl}). Several publications have appeared in recent years documenting the methods for predicting the degree of thermal comfort. However Fanger's comfort equation and his practical concepts of Predicted Mean Vote (PMV) is the most used and accepted among the research community [6].

PMV value is to be controlled to be maintained within specified boundaries. MBPC is an advanced method of process control that has been successfully applied in many areas due to its ability to handle constrained control problems. This feature let us to maintain the PMV index within the thermal comfort zone.

MBPC leads to energy savings in building climate control beneficing from the aforementioned capability to incorporate weather forecasts. This rudimentary feature allows the system to use the low energy cost actuations to prepare the building for the future weather conditions and the high energy cost actuations can be avoided as much as possible. However the weather forecasts are not straightforward thereby the control algorithm needs to be designed in order to be able to tackle with the uncertainties and disturbances.

Benefiting from electricity grids and dynamic electricity tariffs, the peak electricity demands can be reduced. Price profiles can be used as an economic incentive for consumers

[1] unit: $1Met = 58^{W}/_{m^2}$
[2] unit: $1clo = 0.155^{m^2 \cdot K}/_{W}$

to shift their electricity demand in time to lower their energy costs. Employing MBPC methodology, the correspondent price profile can be directly incorporated in the formulation of the optimization problem. This work incorporates the economical terms in the formulation of the objective function in order to minimize the energy expenses inside the building.

Another point that has been taken into consideration in this work is that according to building standards, providing thermal comfort is only essential within the occupation periods; therefore the control algorithm can allow for violations during predefined hours of no occupancy based on the building scheduling timetable [7].

1.1 Objectives

The purpose of this thesis if to find a commercial solution based on MBPC to maintain the thermal comfort within a forecast horizon, while minimizing the required energy as well as the energy expenses in the presence of disturbances (i.e. fluctuations in climate and changes in the thermal load due to the occupation and use of equipment).

The existing air conditioning system is managed by a centralized management system. Several variables that reflect the state of the existing air conditioning systems in various experimental rooms are observed through an interface system so that the HVAC systems can be controlled remotely.

The model-based predictive control can be formulated in many ways. In this case, the energy spent by air conditioning system is minimized by ensuring that the PMV remains in the thermal comfort zone (ASHRAE standard [8] recommends a range between -0.5 and $+0.5$, corresponding to less than 10% the occupants feel dissatisfied) over the forecast horizon (i.e. the PMV values over the forecast horizon, are considered a restriction).

In the current version of the method, the energy consumption is estimated as the deviation of the average inside air temperature over the integration period to HVAC system setpoint in case the the AC is operating; otherwise the energy is estimated as zero. A better estimate of the power consumption can be obtained by modeling the energy consumption either by taking into account the steady state energy consumption when the HVAC system turns on according to the number of indoor units running simultaneously, or by dynamic modeling of the energy consumption according to the number of HVAC systems that are working at the same time. Analyzing the consumption profile, an approximation to the steady state consumption can be added to the objective function [9], thereby improving the estimation of energy expenditure. The estimated energy expenditure, computed this way then, is to be translated into economic costs. This can be done,

as proposed in [10] by incorporating the electricity tariffs into the MBPC objective function so that electricity tariff price forecasting are used to provide the MBPC controller with the necessary estimated time-varying costs for the whole prediction horizon.

Controlling HVAC systems is essentially an optimization problem involving a balance between the energy costs and maintaining thermal comfort. Its formulation usually involves multiple conflicting goals subject to a variable number of restrictions. An optimal solution is hardly attainable mainly because of two reasons: an analytical solution is not possible; an optimal solution obtained by searching the solutions space may not be attained in useful real-time. In situations like this, the use of search based optimization algorithms have proven to provide optimal or near-optimal solutions in useful time. To solve this problem, a variety of methods like genetic algorithms, genetic programming and branch-and-bound methods have been used. This study uses the branch-and-bound (BaB) method.

The second part of this thesis allow the system to ensure technical comfort only just during periods of time when it is expected that the room is occupied. This can be achieved by restricting the amount that the control action can take during the control horizon. In order to achieve this goal, three methods are developed in this work. The first two use a scheduling approach to start the control respectively 4 hours and 2 hours before the expected occupation period. The predictive control algorithm can be implemented by keeping the initial value of zero control, i.e., considering the HVAC system off. Therefore if the thermal comfort is ensured during the periods of room usage time by mean of the models forecast, then this implies that there is no need to turn on the air conditioning system at that moment. Otherwise, the predictive control system executes in order to ensure the thermal comfort within the occupation period.

In the third approach, the branch-and-band search algorithm which finds the best control sequence within the control horizon is modified to only examine the restriction condition of thermal comfort for the nodes located in the occupation period. It means that there is no limitation of thermal comfort for the instants outside the occupation hours. In this way not only the room will be in thermal comfort when the occupants enter, but also the energy consumption and its correspondent prices significantly reduce.

All the modifications to the predictive control algorithm will be tested in real time in the equipped rooms of the Faculty of Sciences and Technology of the University of Algarve, in the south of Portugal.

1.2 Contributions and publications

The first contribution of the thesis is towards the CSI research center who has data acquisition and control hardware as well as a software implementation allowing easy specification of simple forms of control and the execution of more elaborate control algorithms. Furthermore the identification of the predictive models was done using a Multi-Objective Genetic Algorithm (MOGA) utterly implemented in CSI research center.

The branch-and-bound structured search method with a restricted formulation was proposed to solve the model-based predictive control problem formulated. A rule based control space reduction methodology was proposed in order to adaptively reduce the number of available discrete control alternatives, to further reduce the computational load involved in the search for the optimal solution. The work carried out in order to obtain cost-oriented objective function produced the following publications:

A.E. Ruano, S. Silva, S. Pesteh, P.M. Ferreira, H. Duarte, G. Mestre, H. Khosravani, R. Horta, "Improving a neural networks based HVAC predictive control approach",IEEE international symposium on intelligent signal processing (WISP), 2015.

A. E. Ruano, G. Mestre, H. Duarte, S. Silva, S. Pesteh, H. Khosravani, P.M. Ferreira, R. Horta,"A Neural-Network based Intelligent Weather Station",IEEE international symposium on intelligent signal processing (WISP), 2015.

Regarding the energy estimation methods and the correspondent objective functions developed in this thesis as well as the proposed control methodologies, i.e. scheduled MBPC and modified BaB algorithm, no publications have been submitted yet.

1.3 Thesis structure

This thesis is divided in seven chapters, each dedicated to a subject, or subjects, that were considered to be better described using the adopted divisions. Chapter 2 begins by presenting an overview of the state-of-the-art in controlling HVAC systems. A special attention is given to the predictive control methodology specifically. Chapter 3 gives some background on current control practice in building climate control and provides the positioning of the work.

Chapter 4 starts with the energy estimation method used in the previous work and its limitations and then discusses two different formulations for estimating the external energy consumption of the external device which supplies the air with desired temperature

to multiple indoor units connected to the correspondent outside machine, in view of applying them to objective function. Furthermore, the effectiveness of energy estimation methodologies is investigated by means of some simulation scenarios.

Chapter 5 starts with the objective function used in the previous work followed by two new developed energy-oriented objective functions based on the estimations done for the energy in chapter 4. In the second phase of this chapter, real-time pricing is used to develop a cost-oriented objective function in order to reduce the prices of energy. This chapter is concluded by means of some simulations using real data extracted from databases evaluating the best objective function for the control system.

In chapter 6 the influence of occupancy information on building climate control is assessed. Taking advantage of these informations, the MBPC algorithm can be initialized some specified time prior to occupation to provide thermal comfort only within prescheduled occupation periods. This method is investigated by initializing the MBPC 4 hours prior to occupation. By running some simulations, this time reduced to 2 hours as the system was capable of providing thermal comfort in 2 hours. The last methodology developed in order to improve the MBPC strategy, was to modify the BaB search algorithm. The assessment procedure for the developed control strategies as well as the regular MBPC are carried out within a set of simulations.

Chapter 7, the last, presents the conclusions from the work presented and discussed in the thesis, and finishes by pointing out some future work directions which should be followed in order to further improve and explore the contributions of this thesis.

2

State-of-the-Art

In large buildings, Energy Management Control (EMC) systems are used to control the HVAC systems and building operation [11]. Two important functions of EMC systems are (i) local control and (ii) supervisory control of HVAC systems [12]. The local control loop is designed to maintain stability and setpoint tracking, taking into consideration the dynamics of the local process environment. Several such local controllers are supervised by a central supervisory controller. The function of the supervisory controller is to optimize the global operation of HVAC systems. The supervisory controller (i) receives predicted weather and occupancy patterns, time-based building operation schedules, time-of-day energy price differentials and process inputs/outputs; (ii) computes the optimal operating strategies by using the above information and updated system models; and (iii) downloads the computed time varying setpoints to the local controllers for implementation. The focus of this thesis is on supervisory control task. Therefore in the following sections, the related works are briefly mentioned in a structured way.

2.1 HVAC control

An important issue in intelligent HVAC control systems is the weather predictions and their uncertainty. Predominantly, predictive methodologies are unearthed to be more

efficient and comprising compared to the conventional strategies in buildings thermal control [13], [14], [15], [16], [17] and [18].

One of the first researches of formulating thermal storage as an optimization problem has been presented in [13] where three phases are distinguished in control of a simple solar domestic hot water system for constant predefined times of the day. Two controllers was employed in this work. One utilizes weather predictions and another one was based on stochastic dynamic programming. The optimization problem was solved considering the weather forecast using statistics and two energy rates. According to the simulation results presented, predictive control approach lead to lower energy consumptions compared to non-predictive methodologies.

A study on control of active and passive building thermal storage was done in [18]. They utilize a short-term weather predictor based on the real weather data. Then an optimization problem is solved using time-of-use differentiated electricity prices without demand charges over a finite horizon and only the first action is sent to the actuators. The optimization is repeated over a shifted prediction horizon at the next time step. It was observed in this work that the cost savings relative to conventional building operation can be substantial.

The authors in [16] have applied a forecasting model of outdoor air temperature in a predictive control technique for intermittently heated Radiant Floor Heating (RFH) systems. The purpose of control is to decide the adequate time to supply the heat to the floor. In the conventional intermittent control approach, the decision is based on the past experiences. The experimental results demonstrate that total energy consumption can be reduced by minimum of 10% for cold winter months compared to the existing conventional control strategy.

In this context, [19], [20], [21] and [22] propound the view that there are uncertainties in the predictions. A stochastic occupancy model has been incorporated in [19] with the aim of improving mean energy efficiency while respecting thermal comfort conditions. Comfort index considered in this work is based on the difference between room air temperature and the reference temperature of HVAC system. A scaling factor based on the probability of occupancy is considered in their formulation.

Alternatively, [20] draws a research on stochastic Gaussian predictive modeling of building weather and load disturbances. The authors have reformulated the MBPC problem into a nonlinear program with the goal of minimizing energy consumption while providing thermal comfort. This optimization problem is solved by tailored Sequential Quadratic Programming (SQP) and second order cone constraint (conic).

Further research in this area may include [21] that utilizes the stochastic MBPC and weather predictions in order to to solve a non-convex optimization problem with the aim of increasing the energy efficiency. The disturbances are then considered over the control loop feedback. In order to analyze thermal comfort conditions probabilistic constraints formulation, customarily called chance constraints have been employed in the optimization process to deal with the uncertainties.

Finally [22] appraise dynamical learning of uncertain variables such as the outside temperature, the occupancy and the solar radiation from real data instead of using the assumptions on their distributions. Then an optimization problem considering a scenarios based approach is solved minimizing the overall energy consumption and a chance-constraint based formulation.

2.2 Thermal comfort representation

Thermal comfort in buildings is conventionally assessed by operative temperature criterion [23] which can be simply elucidated as the average of the air temperature and the Mean Radiant Temperature (MRT). MRT is normally calculated as the mean temperature of the surrounding surfaces multiplied by some area scaling factor [24]. However, the thermal comfort is a more complicated quantity and according to [23] and [25], it can be pointed out that it is a cognitive process influenced by various quantities. Thermal sensation not only depends on the air temperature but also on factors that determine heat gain and loss, namely metabolic rate, clothing insulation, mean radiant temperature, air speed and relative humidity. This process is characterized by the thermal comfort index called predicted mean vote (PMV).

The PMV index as a part of MBPC cost function was presented in [26]. This research appears to validate the view that employing PMV index, leads the HVAC system to higher energy savings. On the other hand, the nonlinear feature of the PMV index complicates the application of this thermal comfort index. Several MBPC problem formulations incorporating the PMV index in the cost function are evaluated in [27] where they compared results, taking advantage of a data abstracted of a real building for solar energy research center.

2.3 Energy peak reduction

Predictive control is not only for energy minimization but also to reduce the energy peaks, which leads to lower the costs of the building operation. A solution to this issue

is presented in [28] which utilizes thermally activated building systems (TABS) in an office building. The simulation results illustrate that the peak loads can be be diminished by activating the thermal mass of the building during the nights when the HVAC system of the unit was off.

Conventional control methodologies were not using building thermal storage in order to reduce the operating costs. An overview of employing building thermal mass is presented in [29], where variable energy prices according to time of use and the cost of the peak hours are contemplated in the formulation of the optimization problem. As it is prominent in the literature, energy peak reduction can significantly lower the costs of the building operation and the initial cost of mechanical parts if considered in the building design.

Evidence for applicability of MBPC in decreasing the energy and demand costs for multi-zone commercial building is borne out by [30], taking advantage of electricity grid with time-of-use pricing and demand charges. All the simulations in this work are done in building controls virtual test bed (BCVTB) as a middleware while the building model is built by Energyplus, which is a whole building energy simulation program. Zone temperature and power are modelled by system identification approach. The results demonstrate cost savings which are brought beneficing from economic objective function in order to pre-cool during the off-peak periods cooling discharging from the building thermal mass during the on-peak periods.

2.4 Thesis contribution

However all these studies focuses on an individual building zone or room. In the case of small commercial buildings, as they typically utilize HVAC systems with a single thermostat controlling a single unit for individual zones, it is easier to develop an intelligent controller. However in large commercial buildings, an external machine serves many zones so the systems are more complex demanding a more specialized control software and extended communication effort between subsystems. This complexity grows exponentially with the number of subsystems. [31] and later in [32] addressed heating of a multi-zone building with a decentralized and distributed MBPC methodologies. The results provide confirmatory evidence that the performance of the decentralized one strongly depends on the level of interactions between subsystems, the distributed one, as each controller knows about control actions of its neighbors, keeps the same performance as the centralized one. The previous version of this study [1] concentrated on the HVAC system control problem pointing to acquire a proper thermal comfort level

whereas to decrease the energy consumption. PMV index is appraised as the optimization constraint criterion to respect thermal comfort conditions. The employed index in this work is an Artificial Neural Network (ANN) model for PMV presented in [33]. The control methodology was a decentralized discrete MBPC algorithm. Indoor and outdoor weather forecasts were done beneficing of predictive models resulted from applying Radial Basis Function (RBF) neural networks [34] exploiting a MOGA implementation ([35], [36] and [37]). There are several technical obstacles to widespread implementation of an efficient control system in large commercial buildings.

First of all, on the basis of the evidence currently available, it seems fair to suggest that to deal with subsystem interactions, an adequate estimation of the energy consumption of the external device which supplies the air with desired temperature to multiple indoor units should be done. This energy highly depends on the number of operating internal machines in each control step. The first goal of this thesis is to address this issue by some dynamic and static modelings. Assessing different occupancy times in different zones of the building, the system should be configured so as to allow communication of different internal machines. This feature is not very common in existing installations. Conversely to the previous work, the objective of this study is to reduce not only the energy consumption but also the energy peak which leads to lower energy costs. In order to fulfill this goal, the taking time-of-use pricing and demand charges are comprised within the objective function leading to have to have a cost-oriented objective function.

The last contribution of this thesis to previous studies ([38], [1], [39], [40] and [41]) is to modify the MBPC algorithm. The first step is to initialize the control at an adequate time with the aim of having thermal comfort in the beginning of pre-scheduled expected occupancy time for controlling zone. Peculiarities of the second and most important task in order to reduce the energy peak, is to modify the optimization algorithm, a discrete branch and bound, employed in the MBPC methodology in order to only bound PMV values within the occupied times, which leads avoiding the energy peaks where it is not required. There is overwhelming evidence corroborating the notion that developed control system has the ability to considerably reduce the energy consumption as well as the corresponding cost while respecting the occupants comfort within all the pre-scheduled expected occupation times.

3

Background

This chapter aims to give a comprehensive account of requisite background material that is relevant for the developments in this thesis. The structure of the chapter is as follows: section (3.1) elucidates the experimental environment and equipments employed in order to examine the control methodology developed for HVAC system in this study. Section (3.2) presents a brief description about Model based predictive control (MBPC) technique. Thermal comfort criterion used to evaluate the comfort conditions is explained in section (3.3). In order to predict the future inside and outside weather conditions, a model structure is introduced in section (3.4) with a brief description about Artificial Neural Networks (ANNs) as well as Radial Basis Functions (RBFs) as a basis to our model structures. Subsequently, site-specific models for our experimental building as well as seasonal predictive model employed in this thesis are introduced in sections (3.5) and (3.6) respectively. Ultimately, the optimization algorithm employed in MBPC in order to choose the best control actions over prediction horizon, Branch-and-Band (BaB) algorithm, is delineated in section (3.7) following with an implementation of BaB utilized in this work.

3.1 Experimental environment

All the control experiments carried out in this thesis benefit from real data of some equipped rooms in building 8 of UAlg. There are 16 equipped locations in total in that building where four of them were used in this work and they are symbolized by the letters A, B, C, and D. Rooms A and B are contiguous with walls positioned to west and north (only A). The HVAC system installed in these rooms are Mitsubishi Variable Refrigerant Flow (VRF) systems (indoor units) sharing an outdoor air compressor unit located on the building roof which is called later on as external machine. The HVAC systems can be centrally controlled by a PC management station. Room C is in the same corridor with A and B and has walls subjected to the north and east. These rooms are located on the second floor. Ultimately, room D is straightly under room C with walls subjected to the north and east. Figure (3.1) demonstrates an overview to floor 2 map.

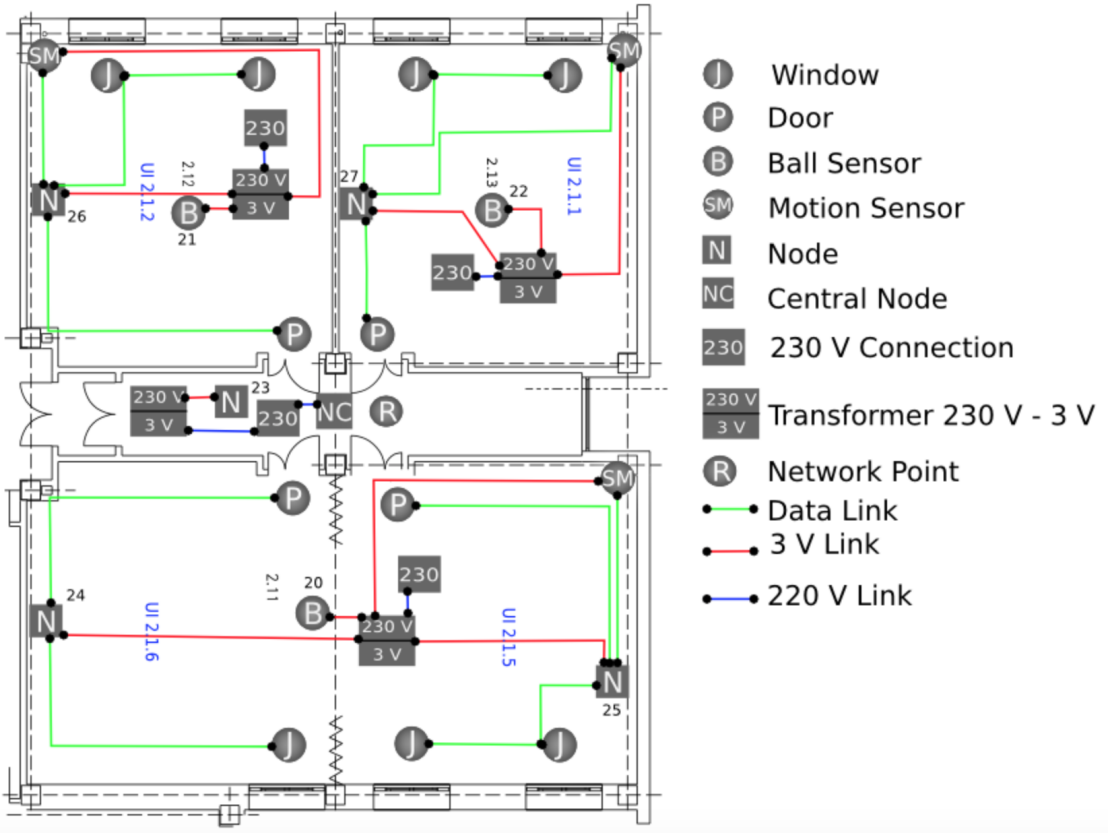

FIGURE 3.1: Overview on the map floor 2.

Each room benefits from one Wireless Sensor Network (WSN) node installed in the wall in order to take the measurements of room air temperature, T_{ai}, and humidity, H_{ai}, from the sensors. Thereabouts in the center of the room, a black globe thermometer is installed in order to estimate the mean temperature of the room. Magnetic switches

in doors and windows are connected to WSN nodes to illustrate the state of each one. As economically it is not plausible to install an energy sensor in for each indoor unit, power transducers were sited in the external machines to provide related data through the LMAP02 interface.

Outside measurements like air temperature, T_{ao}, air humidity, H_{ao}, and global solar radiation, R_{sg}, are obtained through a weather station situated in the campus. The sensors transmit the informations through a Transmission Control Protocol/Internet Protocol (TCP/IP) network to a PC station in the control systems laboratory. Figure (3.2) used from [1] provides an illustration of the system integration.

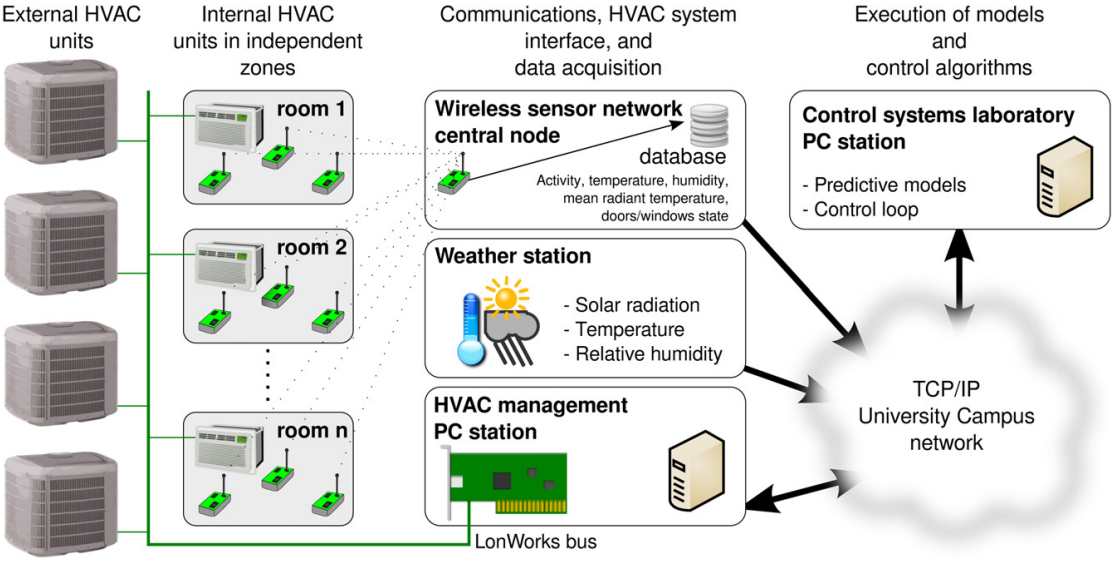

FIGURE 3.2: Overview of the experimental set up used from [1].

3.2 Model based predictive control (MBPC)

Model based predictive control (MBPC) is an congenital technique to constrained control that has been successfully employed in recent years ([42] and [43]). System model is a compulsory material of this control algorithm to derive predictions of the future system behavior. Future control actions are then computed by aid of minimizing a pre-defined objective function. The fundamental preference for widely utilizing MBPC in industry is the capacity to deal easily with multi-variable systems and constraints. The general concept of MBPC is illustrated in figure (3.3) obtained from [2]. Possible control actions are computed by means of past input/output data as well as the predictions of the future system. However the controller choose only the ones that minimizes a specified objective function. Taking advantage of this standard, different methodologies have been proposed where their prominent difference is in predictive models type, the optimization algorithm

in order to find the best future actions as well as the objective function employed and the techniques to deal with the constraints.

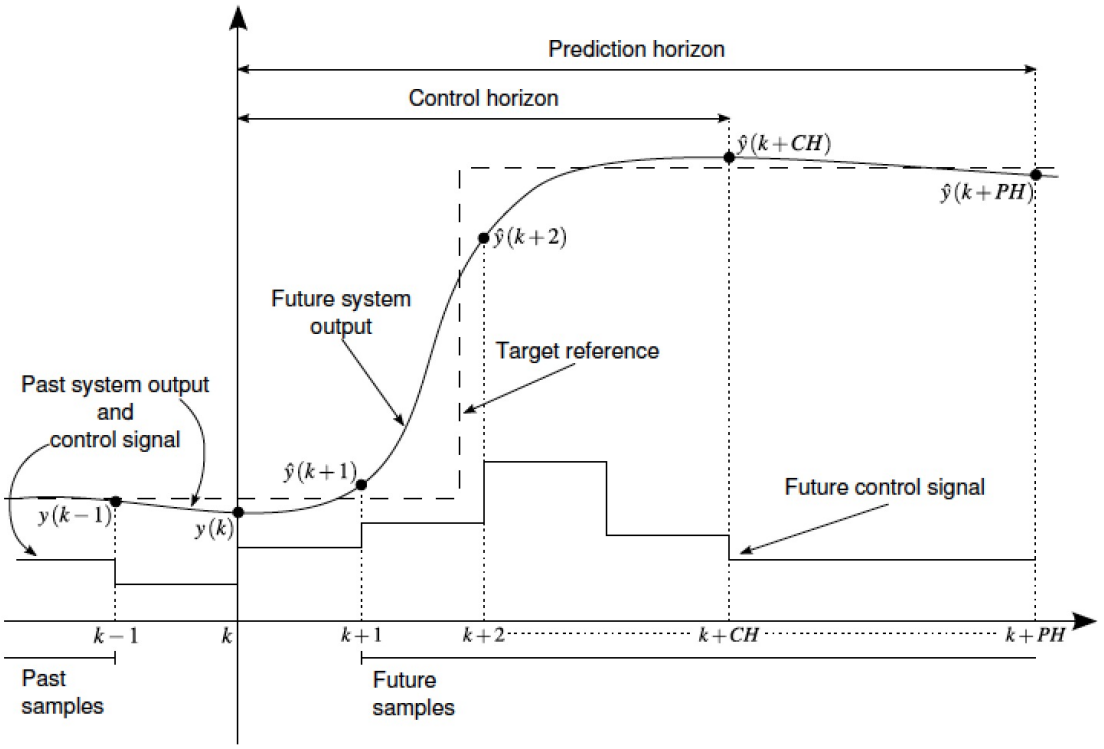

FIGURE 3.3: Model based predictive control strategy obtained from [2].

An efficient and commonly used technique to non-linear MBPC is discrete MBPC which is based on the discretization of the control space into an adequate set of control actions. Next step is to apply an optimization algorithm to search for optimal future control actions within the possible solutions according to dynamics and constraints of the system as well as the predictions commensurate with past system outputs and control signals. The optimization problem is solved by minimizing the prescribed objective function while bounding the specified constraints. However in each control step, only the first control action from input sequence is applied to the system and the rest is discarded.

3.3 Thermal comfort constraint

A thermal sensation scale designated as Predicted Mean Vote (PMV) has been nominated by the American Society of Heating Refrigerating and Air Conditioning Engineers (ASHRAE) [25]. Qualitative thermal sensation has been expounded by numerical coding described in table (3.1).

cold	cool	slightly cool	neutral	slightly warm	warm	hot
-3	-2	-1	0	1	2	3

TABLE 3.1: The ASHRAE thermal sensation scale

This index was first introduced by [6] in order to predict the average vote of a large group of people about the thermal sensation. The index depends on six factors: metabolic rate, clothing insulation, air temperature and humidity, air velocity, and the Mean Radiant Temperature (MRT). It is computed by means of a heat-balance equation [44], [3] given by:

$$\begin{aligned} PMV = {} & (0.303e^{-0.036M} + 0.028)[(M - W) - 3.05 \times 10^{-3}[5733 - 6.99(M - W) - P_a - \\ & - 0.42[(M - W) - 58.15] - 1.7 \times 10^{-5} M(5867 - P_a) - 0.0014M(34 - T_{ai}) - \\ & - 3.96 \times 10^{-8} f_{cl}[(T_{cl} + 273)^4 - (\overline{T}_r + 273)^4 - f_{cl} h_c(T_{cl} - T_{ai}) \end{aligned} \tag{3.1}$$

where M and W are the metabolic rate and work activity, both in $^{W}/_{m^2}$, P_a is the partial water vapor pressure in Pascal, and T_{ai} and $\bar{T}_r$ are the air temperature and MRT, in degrees Celsius. The surface temperature of clothing, T_{cl}, and the convective heat transfer coefficient, h_c, are given by:

$$\begin{aligned} T_{cl} = {} & 35.7 - 0.028(M - W) - I_{cl}[3.96 \times 10^{-8} f_{cl} \times \\ & \times [(T_{cl} + 273)^4 - (\bar{T}_r + 273)^4] + f_{cl} h_c(T_{cl} - T_{ai})] \end{aligned} \tag{3.2}$$

and

$$h_c = \begin{cases} {h_c}^* & \text{if } {h_c}^* > 12.1\sqrt{V_a} \\ 12.1\sqrt{V_a} & \text{if } {h_c}^* < 12.1\sqrt{V_a} \end{cases}$$
$$\left({h_c}^* = 2.38 \times (T_{cl} - T_{ai})^{1/4}\right) \tag{3.3}$$

respectively. V_a is the air velocity in $^{m}/_{s}$ and I_{cl} is the clothing thermal resistance in m^{2C°/W. These two equations are solved iteratively until a determined degree of convergence is fulfilled or a maximum number of iterations is reached. Ultimately, f_{cl}, which is the ratio of body surface area covered by clothes to the naked surface area employed in equations (3.1) and (3.2) is defined as:

$$f_{cl} = \begin{cases} 1.00 + 1.290 \times I_{cl} & \text{if } I_{cl} \leq 0.078 \\ 1.05 + 0.645 \times I_{cl} & \text{if } I_{cl} > 0.078 \end{cases} \tag{3.4}$$

MRT value, $\bar{T_r}$, is a complicated quantity to measure. The device predominantly employed in order to measure this variable is is a black globe thermometer [45]. It comprises of a black painted sphere with a temperature sensor in the middle. Designating the globe temperature by T_g, MRT value may be determined as [25],

$$\bar{T_r} = \left[(T_g + 273)^4 + \frac{1.10 \times 10^8 V_a^{0.6}}{\epsilon D^{0.4}} (T_g - T_{ai}) \right]^{1/4} - 273 \tag{3.5}$$

where D and ϵ are the globe diameter in meters and the globe emissivity coefficient, respectively. P_a, the water vapor pressure in Pascal, is proportional to air relative humidity, H_{ai}, which can be obtained by dint of Antoine's equation [46]:

$$P_a = 10 \times H_{ai} \times e^{(16.6536 - 4030.183/(T_{ai}+235))} \tag{3.6}$$

By virtue of equations (3.1) to (3.6), the PMV comes into view as a function of six variables that can be approximated as:

$$PMV = f(T_{ai}, T_g, H_{ai}, V_a, I_{cl}, M) \tag{3.7}$$

It is plausible that within each type of closed space, people will be performing almost identical activities, thereby for a given space the clothing insulation, I_{cl}, and the metabolic rate, M, can be assumed as constant values. Furthermore the air velocity, V_a, varies little within the space, so vector $C = \{I_{cl}, M, V_a\}$ can be considered constant in PMV model inputs. In our installations, clothing insulation, metabolic rate, and the average air velocity were assumed as $0.65\,clo$, $1.0\,Met$ and $0.1\,{}^{m}/_{c}$ respectively for summer experiments while these values are equal to $1.0\,clo$, $1.0\,Met$ and $0.08\,{}^{m}/_{c}$ for winter experiments.

3.4 Model structure

In order to forecast the weather and all the indoor parameters affecting the thermal comfort , it is essential to develop site-specific models for thermal dynamics of a given building. In the HVAC engineering community, BEPS tools as well as the softwares like as EnergyPlus, TRNSYS and so forth are commonly employed for modeling of the building behavior [47]. However this thesis simulations benefit from predictive models obtained using real data and experiments in building 8 of UAlg.

Levenberg–Marquardt (LM) ([48] and [49]) algorithm was used to train the ANNs minimizing a modified training criterion ([50] and [51]). ANNs have extensively been employed in modeling and identification of non-linear systems acting as function approximators. The most frequent network architectures are undoubtedly the Multi-Layer Perceptron (MLP), RBF and more recently B-Splines (BS). Two main reason that RBF artificial neural networks were employed in the previous version of this work in order to estimate the models were: CSI's interest in contribution with new methods of obtaining and applying RBF neural networks based models to practical real world problems in addition to theoretical properties of this type of neural networks in the context of function approximation, that is the universal approximator and best approximation properties. The following section outline a general overview about ANNs and RBF as well as predictive models structures.

3.4.1 Artificial neural network (ANN)

Artificial Neural networks (ANNs) are a computational paradigm inspired by studies of the brain and nervous system in biological organisms. They are an (very naive) attempt to model the biological leaning mechanism, which consist of highly idealized mathematical models of how we understand the essence of these nervous systems. To achieve good performance, neural networks employ a massive interconnection of simple computing cells referred to as *neurons* or *processing units*. NN are data-driven, self-adaptive, non-parametric, nonlinear methods that do not require specific assumptions about the underlying model. This modeling approach has the ability to learn from experience, which can be very useful for many practical problems since it is often easier to have data than to have good theoretical guesses about the underlying laws governing the systems from which data are generated.

The procedure used to perform the learning process is called a *learning algorithm*, whose function is to modify the synaptic weights of the network in an orderly fashion to attain a desired design objective. A *supervised learning paradigm* is used in this work . This

paradigm considers that the learning is achieved by the help of a *teacher*, which owns *knowledge* about the behavior of the process. This paradigm is illustrated in Figure (3.4).

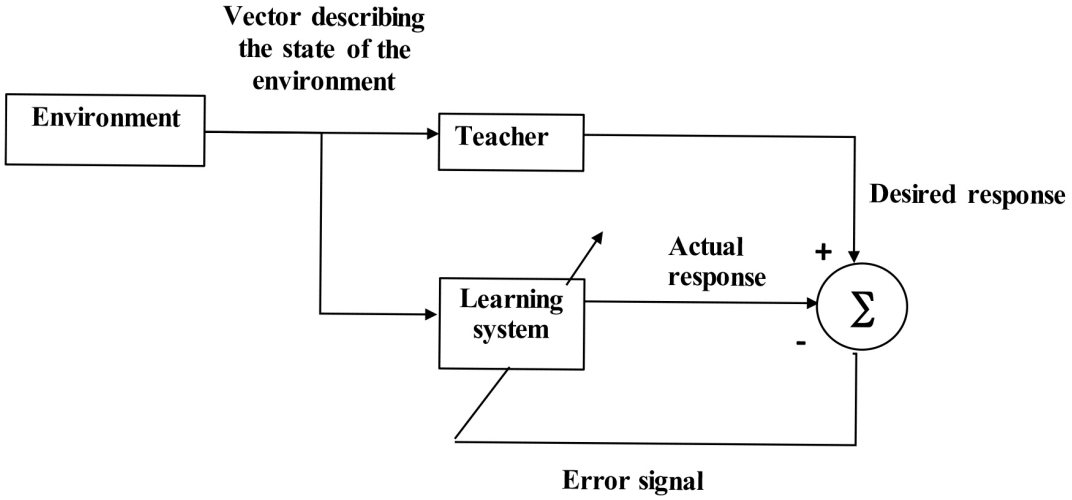

FIGURE 3.4: Block diagram of a learning process with a teacher. Adapted from [3]

The teacher is masked through the available measured data of the process (*environment*), and is used to train the model. The *learning process* allows the network to learn from the environment. Various learning algorithms exist based on [3]. This thesis is interested in a certain type of neural networks, namely Radial Basis Functions (RBFs) introduced in the following section.

3.4.1.1 Radial basis function networks

Designing a supervised neural network can be done using different paradigms. Regarding RBFNs is useful to view the design of a neural network as a *curve fitting* problem in a (possibly) high dimensional space. How do we see *learning* from this perspective? If our problem is to *approximate* a curve then the natural solution would be to find a *surface* in a multi-dimensional space that provides the best fit to a certain training data. Correspondingly, *generalization* in this context refers to the ability to use this multi-dimensional space to interpolate test data. If the *best fit* to the training data is measured in some *statistical* sense, then we reached the motivation behind the method of radial basis functions.

In its most basic form, the construction of a radial basis function network follows a three layered architecture. In this three-layered organization, the second layer, the *hidden* layer, applies a non-linear transformation from the input space to the hidden space. This space is referred as *hidden* because we do not have explicit access to its mathematical expression, like in a traditional analytic model.

The second layer, for RBFNs, is formed by radial basis functions that perform the non-linear transformation. This transformation is followed by a *linear* one, done by the third layer. The motivation for such approach traces back to an early paper (1965) by Cover [52]. This work suggests that a *pattern classification* problem cast in a high dimensional space is more likely to be *linearly separable* than in a low dimensional space. Therefore theoretically we could map an input space into a new space, of high enough dimension, that would turn the problem into a *linearly separable* one.

However, as mentioned, we are viewing the neural network designing from a *curve approximation* (regression) perspective. We can nevertheless infer that, in a similar way, we may use nonlinear mapping to transform a difficult nonlinear regression problem into a easier one.

Lets assume a network that respects the architecture of an AMN, formed by three layers. Without loss of generality we admit the network has a single output. Such a structure would perform a *nonlinear* mapping from the input space to the *hidden* space, followed by a *linear mapping* from the *hidden* space to the output space. Let m_0 denote the dimension of the input space. Then, the network is mapping the m_0 dimensional input space to the single dimensional output space:

$$s: \mathbb{R}^{m_0} \rightarrow \mathbb{R} \tag{3.8}$$

In this way the map s is a *hypersurface* $\Gamma \subset \mathbb{R}^{m_0+1}$. The surface Γ is a multi-dimensional plot of the output as function of the input. As an example consider the following parabola equation:

$$s(x) = x^2$$

Γ is a bi-dimensional plot of the output as function of the input, Figure (3.5). This surface is applying the elementary mapping $s: \mathbb{R}^1 \rightarrow \mathbb{R}^1$

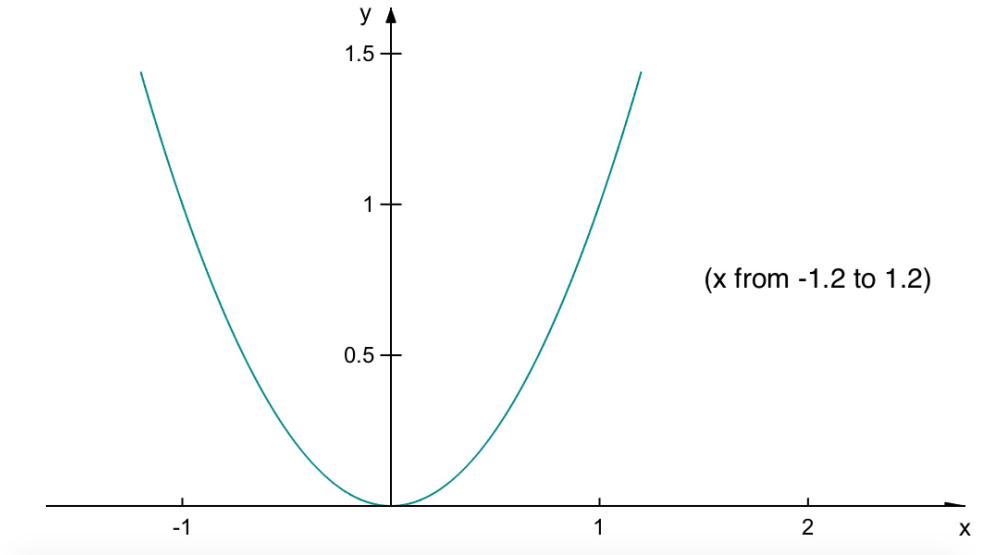

FIGURE 3.5: Plotting of $s(x) = x^2$. In this case Γ is the bi dimensional plot of the output as a function of the input.

Usually we don't know the surface Γ and the training data is contaminated with noise. In its strict sense, the *multivariate interpolation* problem can be stated as:

Given a set of N different points $x_i \in \mathbb{R}^{m_0}$ $i = 1, 2, \ldots, N$ and a corresponding set of N real numbers $d_i \in \mathbb{R}^1$ $i = 1, 2, \ldots, N$, find a function $F : \mathbb{R}^N \to \mathbb{R}$ that satisfies the interpolation condition:

$$F(x_i) = d_i, \quad i = 1, 2, \ldots, N \tag{3.9}$$

In this form, the interpolating surface, i.e. the function F is required to pass through all the training data points. The *radial basis function* method consists of choosing a function F with the following form:

$$F(x) = \sum_{i=1}^{N} \omega_i \vartheta(||x - x_i||) \tag{3.10}$$

Where $\vartheta(||x - x_i|| \; i = 1, 2, \ldots, N$ is a set of N arbitrary (usually nonlinear) functions, known as *radial basis functions*, with $||.||$ denoting the *norm*. The known data points $x_i \in \mathbb{R}^{m_0}$ $i = 1, 2, \ldots, N$ are taken to be the *centers* of the radial functions. Let Φ denote the $N \times N$ matrix with elements $\vartheta_{j,i}$, where:

$$\vartheta_{j,i} = \vartheta(||x_j - x_i||) \quad (j, i) = 1, 2, \ldots, N \tag{3.11}$$

Leading to an *interpolation matrix* Φ of the form:

$$\Phi = \{\vartheta_{j,i} | (j,i) = 1, 2, \ldots, N\} \tag{3.12}$$

Additionally we define:

$$d = [d_1, d_2, \ldots, d_N]^T \tag{3.13}$$

$$w = [\omega_1, \omega_2, \ldots, \omega_N]^T \tag{3.14}$$

The $N \times 1$ vectors d and w represent the *desired response vector* and the *linear weight vector*, respectively. Respecting the interpolation conditions of equation (3.9), we obtain the following set of linear equations for the unknown *coefficient vector* w, in matrix form:

$$\Phi w = x \tag{3.15}$$

Equation (3.15) can be solved for the weight vector w:

$$w = \Phi^{-1} x \tag{3.16}$$

However this last equation is only solvable if the interpolation matrix Φ is nonsingular, i.e. the inverse matrix Φ^{-1} exists. *Michelli's Theroem* [53] covers a large class of radial basis functions that can be used under certain conditions. The theorem can be stated as:

Let $\{x_i\}_{i=1}^N$ *be a set of distinct points in* $\mathbb{R}^{m_0}$*. Then the* $N \times N$ *interpolation matrix* Φ*, whose ji-th element is* $\vartheta_{j,i} = \vartheta(||x_j - x_i||)$*, is nonsingular.*

In this work we particularly have interest in Gaussian functions that are covered in Micchelli's theorem:

$$\vartheta(r) = exp\left(-\frac{r^2}{2\sigma^2}\right), \quad for\ some\ \sigma > 0\ and\ r \in \mathbb{R} \tag{3.17}$$

Now we know that for the solution of equation (3.16) to exist, i.e. for the interpolation matrix Φ to be nonsingular, the input points that form the training set $\{x_i\}_{i=1}^N$ must

be all distinct. This results is independent of the input dimensionality m_0. Gaussian functions are highly used because they are *localized* functions, meaning that these functions will vanish $\vartheta(r) \to 0$ as $r \to \infty$, a property that provides Gaussian functions a desirable bounding and stability. This covers the basis of RBFNs. For a more detailed reference we suggest [54]. However specifically for this work, radial basis functions take the following form:

$$\hat{y}(x, w, C, \sigma) = \sum_{i=1}^{n} w_i \varphi_i(x, c_i, \sigma_i) \tag{3.18}$$

Where w_i is the weight associated with the *i-th* RBF. c_i is the center of the RBF and σ_i the spread of the function. φ_i is the Gaussian function:

$$\varphi_i(x, c_i, \sigma_i) = e^{-(1/2{\sigma_i}^2)\|(x-c_i)\|^2}, \varphi_0 = 1 \tag{3.19}$$

For a designated number of neurons, n, and for a determined set of inputs, X^t, off-line training a RBFN corresponds to stipulating the values of w, C, and σ so that (3.20) is minimized:

$$\Phi(X^t, w, C, \sigma) = \frac{1}{2}\|y - \hat{y}(X^t, w, C, \sigma)\|^2 \tag{3.20}$$

Where y is the desired output and $\hat{y}(X^t, w, C, \sigma)$ is the network output. Take into account that (3.20) is then applied to a set of training input patterns, X^t, and not to a single input pattern, x. As the model output is a linear combination of the neuron activation functions output (3.18), (3.20) can be given as:

$$\Phi(X^t, w, C, \sigma) = \frac{1}{2}\|y - \phi(X^t, C, \sigma)w\|^2 \tag{3.21}$$

where excluding the dependence of φ on C and σ,

$$\phi(X^t, C, \sigma) = [\varphi(x(1))\varphi(x(1)) \dots \varphi(x(N))]^T \tag{3.22}$$

By computing the overall optimal value (w^*) of the linear parameters w, with respect to the nonlinear parameters C and σ, as a least-squares solution:

$$w^* = \phi^+(X^t, C, \sigma)y \tag{3.23}$$

where "$+''$ outlines a pseudo-inverse operation, and superseding equation (3.23) in (3.21), the training criterion to estimate the nonlinear parameters C and σ is:

$$\Psi(X^t, C, \sigma) = \frac{1}{2}\|y - \phi(X^t, C, \sigma)\phi^+(X^t, C, \sigma)y\|^2 \tag{3.24}$$

The initial values for the neuron center locations are haphazardly chosen from the training data, and the spreads of the neuron activation functions are initialized employing the straightforward rule in [54], p. 299. The training procedure proceeds iteratively exerting the LM algorithm minimizing criterion (3.24), until a termination rule is satisfied. This termination rule is based on early-stopping approach [54] within a maximum number of iterations. Further details in this area may be studied through [51], [55] and [33].

Subsequent to designating combinations of input variables (and their lags) in addition to the number of neurons, Multi-Objective Genetic Algorithm (MOGA) is employed in order to develop RBF artificial neural networks that optimize pre-particularized model functioning norm. Developing models by mean of MOGA is an iterative process which entitles the user to fine tune the further experiments. There are several parameters taken into account in MOGA while developing the models that are employed in this thesis including: the number of neurons in the hidden layer, number of input terms in each neuron, number of randomly initialized training trials for RBFNs as well as the maximum number of training iterations. The model selection criterion in MOGA contain the Root Mean Squared Error (RMSE) obtained in the training and validation datasets, as well as the model complexity. Details on the MOGA application for model development can be found in [35].

3.5 PMV model

Assuming $X^t = [T_{ai}\ T_r\ H_{ai}]$ [1] as the input matrix for training the RBFNs, T_{ai} and H_{ai} were created using random values having picked up from the range $[16, 32]$ and $[20, 70]$

respectively. Then a correlated T_{g_k} in T_g for each T_{ai_k} in T_{ai} is computed by mean of equation (3.5).

$$T_{g_k} = T_{ai_k} + \rho(-3.0, 3.0) \tag{3.25}$$

where $\rho(a, b)$ is randomly chosen from uniform distribution in the range $[a, b]$ thereby $T_{ai} - 3 < T_g < T_{ai} + 3$. Then by dint of $V_a = 0.08$, $D = 0.125$, and $\epsilon = 0.95$, T_r is derived employing equation (3.5). Subsequently PMV index values are computed considering $C = \{0.85, 1.2, 0.08\}$. Y_t is created by virtue of equation (3.1) utilizing each triplet X_k^t in X^t along with the values in C. Finally a fresh validation dataset of $23,100$, D^v, training pairs is employed to test the models trained by training set $\{X^t, Y^t\}$.

Having been acquainted with the input–output structure of the model, number of neurons and the number of training patterns were chosen by an extensive search in range of $[2, 32]$. Taking into account the RBF in equation (3.18) each neuron accounts for 5 parameters, thus the total number of parameters is stated by $n \times 5$ where n is the number of neurons utilized.

By particularizing the number of patterns (p) for each model parameter, N for the training dataset would be $N = n \times 5 \times p$. In this circumstance, p was evaluated by a search over $\{20, 40, 60, 80, 100, 120\}$. Taking into account the the random initialization of RBF, 20 try-outs were carried out for each (n, p) pair where in each try-out, 200 iterations of the modified training criterion LM algorithm were applied. The number of training patterns are thus chosen by the maximum absolute error on the validation dataset. By and large, the best result for PMV model was 80 training patterns for each model parameter.

3.6 Predictive models

In order to implement the MBPC methodology, several predictive models are required. This section presents the various models that were obtained in CSI research center using the techniques described in the previous section. The models to be presented may be classified considering the nature of the modeled quantities. The first category comprises process models, namely the room air temperature and relative humidity ones, which are the variables to be controlled. The building climate is strongly influenced by the external weather, which may be viewed as a disturbance to the control system. External disturbance models are another category to be addressed as these will be inputs to the building climate models.

All the required predictive models for MBPC methodology were implemented by RBFNs utilizing the approach explained in (3.4.1.1). A comprehensive explanation of the model structure identification procedure is on the far side of this thesis and can be referenced to ([36],[37], [35] and [56]) for further studies.

Three Auto-Regressive (AR) predictive models were designated by MOGA for outside air temperature, T_{ao}, outside air humidity H_{ao}, and solar radiation R_{sg}. These models are essential in order to predict the room air temperature and humidity within forthcoming hours.

The first step in order to attain site-specific air temperature and humidity models is to randomly control the zone by applying different temperature setpoints, particularly [18, 27] in case for our HVAC systems, as well as turning off the indoor machine for differing time periods. This function was generated by dint of Pseudo Random Binary Signals (PRBS) ([2] and [57]). Two groups of seasonal predictive models were developed in order to be applied in summer and winter circumstances [1]. The effect of outside variables to room climate models has clearly some delay as objected to indoor parameters and HVAC setpoint temperature. Table (3.2) and (3.3) outline these delays for both summer and winter models.

Variable	**Delays in T_{ai} model**	**Delays in H_{ai} model**
T_{ai}	0,1,6,7,8,10,11	1,6,8
H_{ai}	0,1,2,7,9	0,1,4,6,7,8,9,10
T_{ao}	2,3,4,5,8	-
H_{ao}	-	3,5,6,8,11
R_{sg}	7	6,8,11
T_{sp}	0,1,4	0,1,2,3,6,9,10,11

TABLE 3.2: Input–output structure for room climate summer models.

Variable	**Delays in T_{ai} model**	**Delays in H_{ai} model**
T_{ai}	0,6,7,8,11	1,5,8
H_{ai}	0,1,5,6,9,10,11	0,1,3,6,8,10
T_{ao}	1,4	-
H_{ao}	-	3,6,9,11
R_{sg}	0,3,4,8,9	6,9,10
T_{sp}	0,1,3,10,11	0,1,2,5,8,9,10,11

TABLE 3.3: Input–output structure for room climate winter models.

3.7 Optimization algorithm: Branch-and-Band (BaB)

In a discrete MBPC strategy, the exhaustive problem is to find the optimal sequence of control actions over the prediction horizon within a very short time. BaB methods [58] are structured search methods categorized as enumerative schemes, that are regularly

utilized to solve complex discrete optimization problems by dividing them into smaller subproblems using a tree structure; therefore they have been widely employed in practice to this type of discrete (or discretized) non-linear MBPC problems ([59] and [60]). Figure (3.6) obtained from [2] illustrates the tree structure imposed by the BaB method when applied to a discrete MBPC problem having a prediction horizon of PH and a control horizon CH.

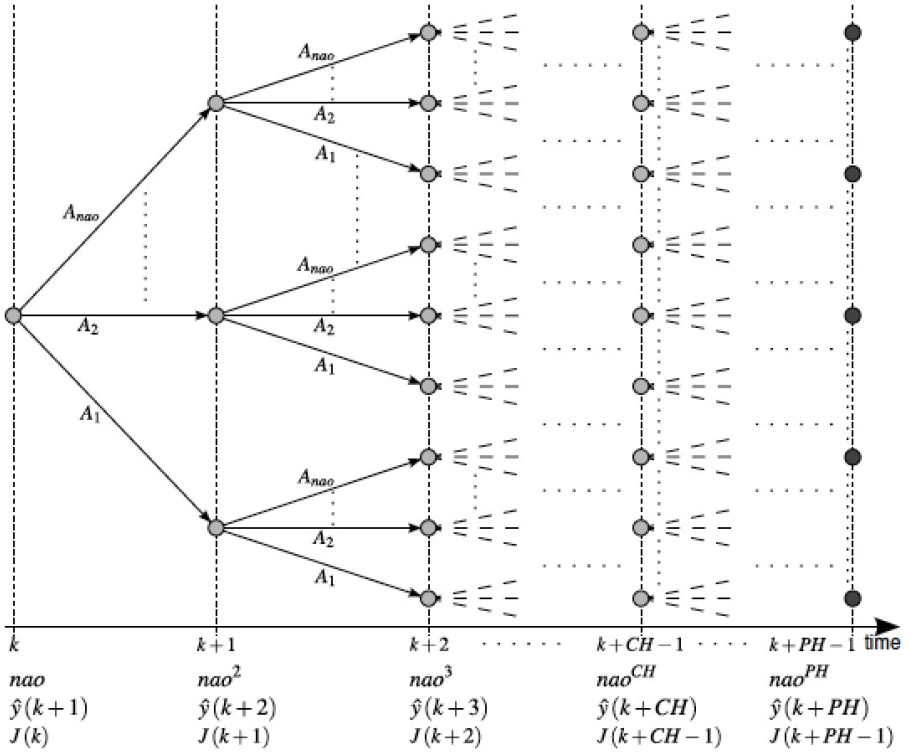

FIGURE 3.6: Branch and bound tree structure for MBPC obtained from [2].

Taking into consideration NA actuators for the studying HVAC system, PA is a $(nao \times NA)$ matrix of nao possible combinations of control actions. PA_i outlines the i^{th} possible combination of actions and corresponds to row i in matrix PA. At the initialization point, in time instant k, a primary tree node is built by BaB according to the required control action at that time step. As nao control combinations are available, the corresponding number of branches is created by computing the predicted system output, $\hat{y}(k+1)$, and for each branch the objective function, $J(k+1)$, is estimated. Subsequently in the next prediction step, $k+1$, nao^2 new branches are generated from the nodes created in each branch resulting from the previous step. This procedure is repeated until the algorithm reaches to time instant $k+PH-1$. The number of generated branches is equal to nao^{PH} in this step. As it can be clearly figured out from the algorithm procedure, the number of searchable solutions swiftly becomes prohibitively large even if the number of control options are low. The optimal solution is chosen by selecting

the control trajectory, $[u(k) \quad u(k+1) \cdots u(k+PH-1)]$, that minimizes the estimated accumulated cost from time instant $k+1$ to $k+PH$:

$$J_{1:PH}(k) = \sum_{i=k+1}^{K+PH} J(i) \tag{3.26}$$

As described before, this type of search simply becomes computationally prohibitive. Thus in order to decrease the number of solutions enumerated, two approaches are taken: the use of bounds to restrict branching and performing the search over the control horizon, CH. As formulated in [59], two bounds are employed: an upper bound on the total cost from instant $k+1$ to $k+PH$, and a lower bound on the cost from instant $k+i$ to $k+PH$. At time step i of the optimization, a branch is followed only if the cumulative cost from step 1 to step $i-1$, $J_{1:i-1}(k)$, plus the lower bound on the cost from i to PH, $\hat{J}_{i:PH}(k)$, is smaller than the upper bound on the total cost, $\hat{J}_{1:PH}(k)$. Thus the branching rule is given by:

$$J_{1:i-1}(k) + \hat{J}_{i:PH}(k) \leq \hat{J}_{1:PH}(k) \tag{3.27}$$

This rule may be further decomposed by noting that its second term on the left hand side of the condition equals the cost of using a control profile AP_j at step i, $J(k+i)|_{u(k+i-1)=AP_j}$, plus the estimated cost from step $i+1$ to PH:

$$J_{1:i-1}(k) + J(k+i)|_{u(k+i-1)=AP_j} + \hat{J}_{i+1:PH}(k) \leq \hat{J}_{1:PH}(k) \tag{3.28}$$

When the rule does not hold, the branch is not followed because it does not contain an optimal solution, thus pruning all the tree nodes that would be created from the current node. In the typical formulation, branching is only performed until the control horizon is reached and it is suggested that the last control combination, $u(k+CH-1)$, should be applied successively to the system model until the prediction horizon is reached [59] and [61]. The global efficiency of the BaB method depends on the accuracy of the bounds used. $\hat{J}_{1:PH}(k)$ should be as close as possible to the optimum value and $\hat{J}_{i+1:PH}(k)$ should be as large as possible in order to reduce the number branching operations. The bounds estimation method and availability are problem dependent, although a basic approach is suggested by [59]: at each instant k, before the optimization starts, a first search on the tree of possible solutions is done by successively choosing the control action giving the smallest values of $J(k+i)_{i=1}^{PH}$, a search usually called "greedy". The total cost found is the initial estimated upper bound, $\hat{J}_{1:PH}(k)$. If at a later stage in the optimization a smaller value is found, it replaces the previous one. Regarding the lower bound, $\hat{J}_{i+1:PH}(k)$, if an

adequate estimate may not be computed, it is suggested that it is set to 0 for all steps i of the optimization. Even when this worst-case estimate is employed, according to some authors [59] and [60], the algorithm is prevented from exploring a significant portion of the search space. The same authors also outline strong points of BaB compared to other non-linear optimization techniques in MBPC applications. First, they not only insure the existence of a solution but it is also guaranteed that the controller is optimal in the discrete space without any pre-assumption requirement. Second point is that not only the constraints do not influence on the algorithm performance but also they enhance the proficiency of bounding by eliminating those control actions that precipitate to constraint violation. The last is that the algorithm result is not affected by a deficient initialization, nevertheless that may cause a lager process time.

The implementation of BaB method to solve the MBPC optimization problem is outlined and discussed in the following.

3.7.1 Branch-and-Band algorithm implementation

While the system is in operation, at every iteration k, a new optimization problem is solved and actually only the first component of $U(k)$, $u(k)$, is used to control the actuators, following the receding horizon principle, while boundaries are employed as restrictions to the optimization problem. In order to estimate the quantities involved in the calculus of $\hat{J}(i), i = K+1 \ldots k+PH$, predictive models are required. As discussed in the previous section, at each time instant k, before the minimization problem is solved by the BaB method, the upper bound on the cumulative cost is computed by minimizing $\hat{J}(i)$ from $i = 1$ to $i = PH$:

$$\jmath^{U}_{1:PH}(k) = \sum_{i=k+1}^{K+PH} \min_{u(i-1)=AP_j} \{\hat{J}(i)\}_{i=1}^{nao} \tag{3.29}$$

This value, also called the *incumbent value* [58], is the initial estimate of the minimum of $\jmath^{U}_{1:PH}(k)$. Taking into account that no branching will be performed beyond the control horizon CH, equation (3.29) may be decomposed as:

$$\jmath^{U}_{1:PH}(k) = \jmath^{U}_{1:CH}(k) + \jmath^{U}_{CH+1:PH}(k) \tag{3.30}$$

hence,

$$\jmath^{U}_{CH+1:PH}(k) = \jmath^{U}_{1:PH}(k) - \jmath^{U}_{1:CH}(k) \tag{3.31}$$

where $\jmath^U_{CH+1:PH}(k)$ is the initial estimate of the optimal cumulative cost from step $CH+1$ to PH. When the BaB algorithm is in one node at level $i < CH$ and it must decide if a particular branch j should be searched in more depth or not, the estimate of the lower bound on the cumulative cost from step i to PH, $\jmath^L_{i:PH}(k)$, must be computed. Using the result from equation (3.31) this estimate may be given by:

$$\jmath^L_{i:PH}(k) = \hat{J}(k+i)\Big|_{u(k+i-1)=AP_j} + \jmath^U_{CH+1:PH}(k) \tag{3.32}$$

This formulation presents the cost of creating a new branch corresponding to the control action AP_j , plus the current estimate of the cumulative cost from step $CH+1$ to PH. It is very complicated to estimate an accurate lower bound from step $i+1$ to CH thereby it is preferable to make it implicitly zero in equation (3.31) in order to prevent the search from not exploring parts of the tree, which may contain the optimal solution, due to a bad estimate. With the aim of saving some additional computing time when evaluating the branching rule, the first term in the right hand side of equation (3.32) may be further decomposed as,

$$\hat{J}(k+i)\Big|_{u(k+i-1)=AP_j} = \left(\hat{J^e}(k+i) + \hat{J^m}(k+i)\right)\Big| \, u(k+i-1) = AP_j \tag{3.33}$$

$\hat{J^e}(k+i)$ accounts for the actuator wear-off and energy consumption terms in the cost functions. $\hat{J^m}(k+i)$ accounts for those terms that need the process models to be evaluated, which is the relevant time consuming task. Using this decomposition the branching rule at step i due to the control action AP_j may be done in two steps by first computing the lower bound estimate of the cumulative cost from step $i = 1$ to step $i = PH$ as,

$$\jmath^L_{i:PH}(k) = \jmath_{1:i-1}(k) + \hat{J^e}(k+i)\Big|_{u(k+i-1)=AP_j} + \jmath^U_{CH+1:PH}(k) \tag{3.34}$$

and then evaluating the following conditions in the order presented:

$$\jmath^L_{i:PH}(k) < \jmath^U_{i:PH}(k) \tag{3.35}$$

$$\jmath^L_{i:PH}(k) + \hat{J^m}(k+i)\Big|_{u(k+i-1)=AP_j} < \jmath^U_{i:PH}(k) \tag{3.36}$$

In the first condition only the contribution of $\hat{J}^e(k+i)$ is accounted in $\jmath^L_{i:PH}(k)$. If the result of the evaluation of (3.35) is not true then the optimization over branch j is stopped because this branch will not lead to a better solution than the current best. In this case the computing time needed to evaluate $\hat{J^m}(k+i)$ is spared, thus contributing to a faster traversal of the tree of solutions. If condition (3.35) evaluates to true then the second condition, given in (3.36), which adds the contribution of $\hat{J^m}(k+i)$, is evaluated in order to decide if the solution search will follow this particular branch.

When the BaB method is in one node at level $i = CH$, in order to choose the best control input $u(k+CH-1)$ and a particular control alternative, AP_j , is being tested, if the two branching conditions, (3.35) and (3.36), evaluate to true it means that a better solution than the current one has been found. Denoting the control trajectory corresponding to the particular path followed from $i = 1$ to $i = CH$ by $U^*_{1:CH}(k)$, the new value of the best solution is recomputed using,

$$\jmath^U_{i:PH}(k) = \jmath_{i:CH}(k)|_{U^*_{1:CH}(k)} + \jmath^U_{CH+1:PH}(k) \tag{3.37}$$

where the second term in the sum is recomputed in a similar way as the initial estimate of $\jmath^U_{i:PH}(k)$ in equation (3.29), but starting from step $i = CH + 1$ and assuming the newly found control solution, $U^*_{1:CH}(k)$:

$$\jmath^U_{CH+1:PH}(k) = \left(\sum_{i=k+CH+1}^{K+PH} min_{u(i-1)=AP_j} \{\hat{J}(i)^{nao}_{j=1}\} \right) \Bigg|_{U^*_{1:CH}(k)} \tag{3.38}$$

At this stage the values of the best solution found (the incumbent), $\jmath^U_{i:PH}(k)$, and the upper bound on the cumulative cost from $i = CH + 1$ to $i = PH$, $\jmath^U_{CH+1:PH}(k)$, are stored and the algorithm resumes its operation on the remaining branches of the current node and then on other nodes still unexplored. As better solutions are found by the BaB method the branching operation becomes more restrictive, thus having a higher probability of eliminating more branches from the search. When there are no branches to explore in the current node and no unexplored node remains, the optimization stops and the best solution stored is the optimal one.

During algorithm initialization, when computing the upper bound of the optimum solution, and when a new best solution is found and $\jmath^U_{CH+1:PH}(k)$ needs to be recomputed, violations to the restrictions should be checked and predefined control alternatives should be enforced when the restriction is predicted to be violated irregardless of the control alternative applied.

Algorithm 3.2. Branch-and-Band Algorithm

1: $(\jmath^U_{1:PH}, U) \Leftarrow \sum_{i=1}^{PH} min_{u(i-1)=AP_j}\{\hat{J}(i)\}_{i=1}^{nao}$
2: $\jmath^U_{CH+1:PH} \Leftarrow \jmath^U_{1:PH} - \jmath^U_{1:CH}$
3: $BestNode.\jmath \Leftarrow \jmath^U_{1:PH}$
4: $BestNode.U \Leftarrow U$
5: $(node.i, node.U, node.\jmath) \Leftarrow (0, [], 0)$
6: $NodeList \Leftarrow \{node\}$
7: **while do**$len(NodeList) \neq 0$
8: $\quad node \Leftarrow NodeList.PopFirst$s
9: $\quad node.i \Leftarrow node.i + 1$
10: $\quad$ **for** $j = 1$ to nao **do**
11: $\quad\quad NewNode \Leftarrow node$
12: $\quad\quad NewNode.U \Leftarrow [NewNode.U\ A_i^T]$
13: $\quad\quad NewNode.\jmath \Leftarrow NewNode.\jmath + \hat{J}^e$
14: $\quad\quad$ **if** $\mid NewNode.\hat{\Theta} \mid \leq \Theta_T$ **then**
15: $\quad\quad\quad$ **if** $(NewNode.\jmath + \jmath^U_{CH+1:PH}) < \jmath^U_{1:PH}$ **then**
16: $\quad\quad\quad\quad NewNode.\jmath \Leftarrow NewNode.\jmath + \hat{J}^m$
17: $\quad\quad\quad\quad$ **if** $(NewNode.\jmath + \jmath^U_{CH+1:PH}) < \jmath^U_{1:PH}$ **then**
18: $\quad\quad\quad\quad\quad$ **if** $NewNode.i = CH$ **then**
19: $\quad\quad\quad\quad\quad\quad BestNode \Leftarrow NewNode$
20: $\quad\quad\quad\quad\quad\quad \jmath^U_{1:PH} \Leftarrow BestNode.\jmath$
21: $\quad\quad\quad\quad\quad\quad \jmath^U_{CH+1:PH} \Leftarrow \left(\sum_{i=1}^{PH} min_{u(i-1)=AP_j}\{\hat{J}(i)\}_{i=1}^{nao}\right)\Big|_{BestNode.U}$
22: $\quad\quad\quad\quad\quad\quad \jmath^U_{1:PH} \Leftarrow \jmath^U_{1:PH} + \jmath^U_{CH+1:PH}$
23: $\quad\quad\quad\quad\quad$ **else**
24: $\quad\quad\quad\quad\quad\quad NodeList \Leftarrow \{NodeListNewNode\}$
25: $\quad\quad\quad\quad\quad$ **end if**
26: $\quad\quad\quad\quad$ **end if**
27: $\quad\quad\quad$ **end if**
28: $\quad\quad$ **end if**
29: $\quad$ **end for**
30: **end while**

An implementation of the procedures described above is listed in algorithm (3.2) which was presented in [2]. The listing assumes the cost function which is subject to restrictions. The operations performed in lines 8, 10 and 24 of the algorithm define the way the tree is traversed. In the example given, the instruction *NodeList.PopFirst* removes the first node from the list and in the following lines the algorithm starts branching from this node. Line 10 cycles through the available control actions in matrix A and if the bounding conditions are true, new nodes are appended to the end of list. This results in a tree traversal illustrated in figure (3.6), from [2], which visits all nodes in one level before starting branching in the next tree level.

As it can be seen from the algorithm, when some of the control options do not violate restrictions, then the one that minimizes the cost function is chosen as the optimal

control action. Figure (3.7) illustrates the implementation of BaB used in the simulations in this work.

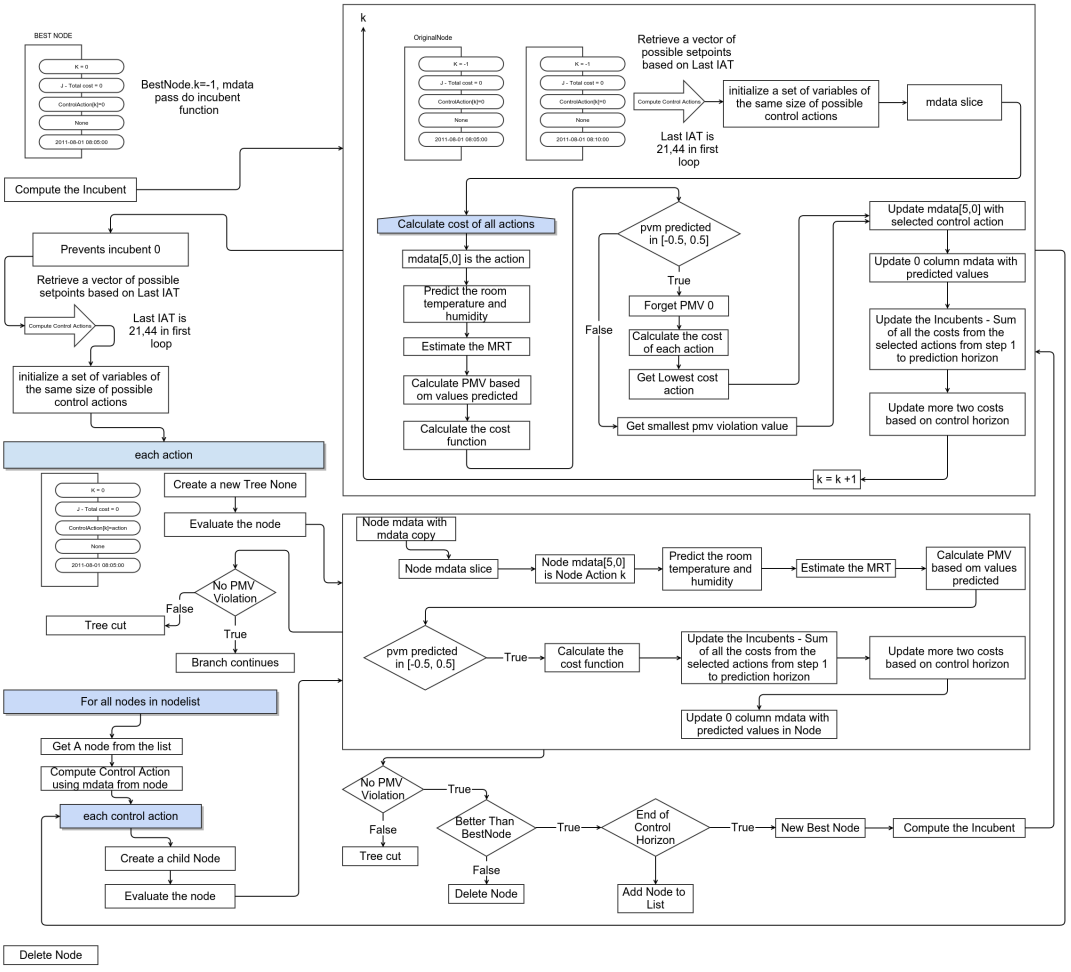

FIGURE 3.7: Branch and band implementation diagram.

4

Energy Estimation Methodology

In the present chapter, the issue under scrutiny is an adequate estimation of the external energy consumption of the external device which supplies the air with desired temperature to multiple indoor units connected to the correspondent outside machine. Naturally this rate can be affected by different criteria. However this is considered as an limitation which requires a vast study for an adequate energy consumption estimation method which is practically function of each type of machine.

This chapter is organized with an introduction to the previously used method for this estimation in section (4.1). Nevertheless, there are some interesting and relevant problems to be addressed. As an alternative, section (4.2) introduces some dynamic models designed to estimate the energy consumption in the external machine according to the number of indoor units connected to that outdoor unit which work in parallel at the same time. *Autoregressive exogenous models (ARX)* are considered as an energy estimation paradigm and are implemented using the system identification toolbox in Matlab. Another approach is proposed in section (4.3) which has a close look to HVAC power consumption profile that seems to have a steady state feature whenever one of the indoor units turns on. This static rate is varying according to the number of indoor units that are working simultaneously. Simulation results are presented and compared in section 4.4 in order to demonstrate the performance of each method. Conclusions are drawn in section (4.5).

4.1 Previous energy estimation method

The previously used energy estimation is based on the deviation of the average inside air temperature over the integration period to its setpoints [1]:

$$\hat{E(k)} = 1 + \frac{|T_{sp}(k) - T_{ai}(k)|}{\lambda} \tag{4.1}$$

where T_{sp} is the HVAC's setpoint temperature and T_{ai} is the room average temperature over the integration period. The scaling factor, λ, is considered as an estimate of the maximum value of $|T_{sp} - T_{ai}|$. The term itself reflects the notion that the higher the difference $|T_{sp} - T_{ai}|$, the bigger is the energy required to achieve T_{sp}. Considering a temperature integration period of TIP days and a data sampling interval such that there are PPD data points per day, the number of data points within the integration period is defined as $NP_{TI} = TIP \times PPD$. The average temperature over the integration period, at time instant k, $\bar{T}_{ai}(k)$, is given by:

$$\bar{T}_{ai}(k) = \frac{1}{NP_{TI}} \times \sum_{i=k-NP_{TI}+1}^{k} T_{ai}(i) \tag{4.2}$$

where T_{ai} is inside air temperature. At time instant k the error, $\bar{T}_{\varepsilon}(k)$, is the difference between the average temperature and its reference value, $T_{sp}(k)$:

$$\bar{T}_{\varepsilon}(k) = \bar{T}_{ai}(k) - T_{sp}(k) \tag{4.3}$$

Further studies of analysis of this method can be reached in [1]. However in order to analyze the estimation methods, the values of the external machine energy consumption connected to 4 internal machines while only one indoor unit is working at a time is plotted in figure (4.1). Inside room temperature deviation from the HVAC setpoint as well as air-conditioner on/off bits is also added in order to examine the dependency of these parameters to the outdoor machine consumption. All the values are scaled to 1 in order to have a explicit plot to analyze.

Looking closely to the energy profile shows that external unit acts independently from the temperature difference of the control action and inside room air temperature. However one point is clear and it is that the energy consumption behavior changes more according to the on/off status of the HVAC system so that whenever the AC is off, the energy consumptions is zero except an amount of 10 W each 15 minutes which has to be spent by external machine for its regular operation. Therefore a novel approach should

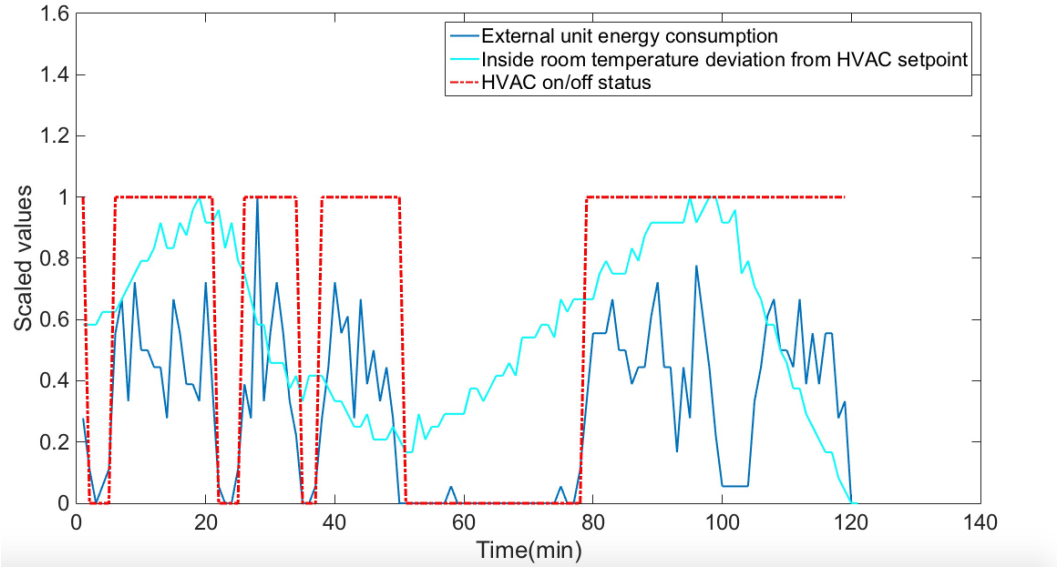

FIGURE 4.1: External unit energy consumption trend profile while switching on/off the HVAC system.

be considered to have a better estimation of the energy consumption in the objective function function. The next sections will discuss two methods developed in this work to replace the previous estimation of the energy.

4.2 Dynamics energy estimation modeling

In order to estimate the actual characteristics of the HVAC system's energy consumption, an approach is to estimate a model of a system based on observed input-output data. Several ways to describe a system and to estimate such descriptions exist. The procedure to determine a model of a dynamical system from observed input-output data involves three basic ingredients [62]:

- The input-output data.
- A set of candidate models (the model structure).
- A criterion to select a particular model in the set, based on the information in the data (the identification method).

Matlab system identification toolbox is therefore used in oder to obtain dynamic models that will be used to estimate the energy consumption rate. The identification process amounts to repeatedly selecting a model structure, computing the best model in that

specific structure, and evaluating this model's properties to see if they are satisfactory. The cycle can be itemized as Figure (4.2):

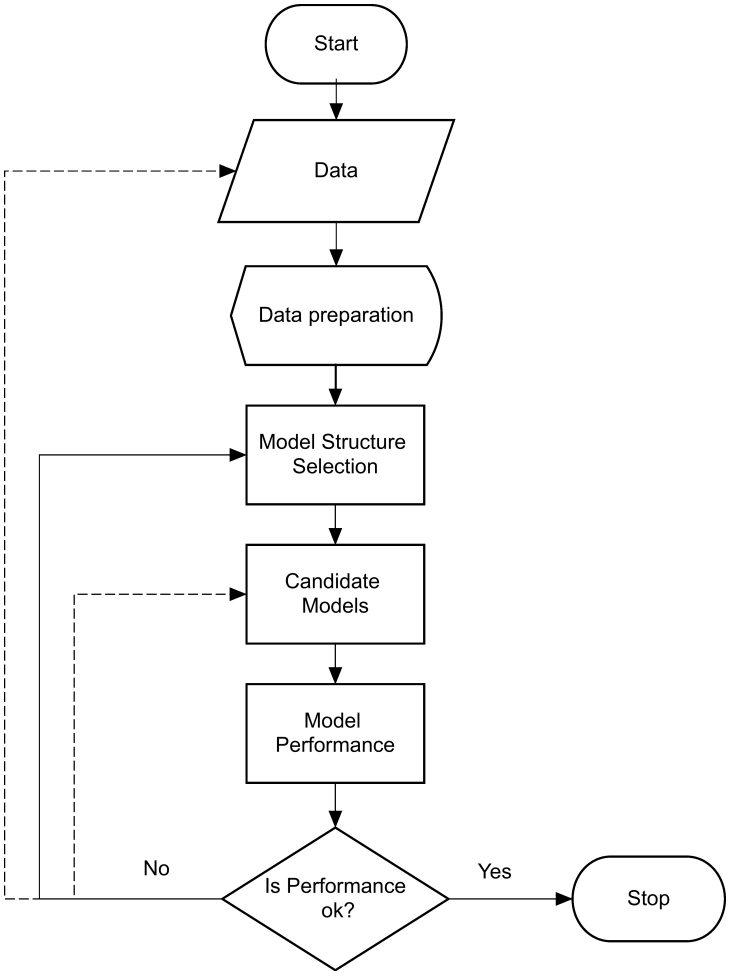

FIGURE 4.2: Model identification process.

In order to perform this task, single-input single-output (SISO) Auto-regressive Exogenous (ARX) models are used where the inputs are the on/off state of all the indoor units connected to the external machine and the output is the actual power measurements. The task of model identification is challenging due to intermittent HVAC operations and disturbances [63]. In order to identify the models, an experiment is designed to inspect the system behavior while it is operating under normal conditions. In order to develop the models, linear, discrete time, single-input single output ARX models are discussed in the following.

4.2.1 Autoregressive exogenous models (ARX)

A suitable model class for linear control implementation is an ARX model. ARXs are AutoRegressive models with eXogenous inputs. Exogenous variables are determined

completely uncorrelated to the process that is considered to be modeled. The ARX model is written as a state space system and optimal predictions of future output is given by the stationary Kalman filter. This method has an important privilege of hypothesizing the additivity of the signals with noise despite other Kalman filter based methods that require some preliminary assumption about the characteristics of the noise superimposed to the signal. [64] presents a complete review and discussion of these methods. A typical linear, discrete time SISO ARX model is represented by:

$$\hat{E(k)} = -\sum_{i=1}^{n_a} a_i E(k-i) + \sum_{j=d}^{d+n_b-1} b_j \times U(k-j) + \varepsilon_i(k) \tag{4.4}$$

Which relates the current energy consumption value, $\hat{E(k)}$, to a finite number of the past outputs $E(k-i)$ as well as the input $U(k-j)$. $\varepsilon_i(k)$ is the white-noise disturbance value. The noise is coupled to the dynamics model as ARX does not allow to model the noise and dynamics independently thereby the model posses a good signal-to-noise ratio. n_a and n_b are the orders of the autoregressive and the moving average part of the model respectively. In other words, n_a outlines the order of polynomial $A(q^{-1})$ while n_b depicts the order of polynomial $B(q^{-1})$ minus one. A temporal delay d with respect to the driving signal $U(k)$ (dead-time) is introduced to take into account the differences in latency of the signal responses. Number of poles and zeros of the model equivalent transfer function is equal to n_a and $n_b - 1$ respectively. A more compact way to write the difference equation is:

$$A(q^{-1})E(k) = B(q^{-1}) \times U(k-d) + \delta(k) \tag{4.5}$$

where q^{-1} is the delay operator and A and B are the polynomials of the model defining the orders of an ARX model in the backwards shift operator q^{-1} and $\delta(k)$ is the matrix of white-noise disturbance values. The dimensions of n_a, n_b and d, in the general case, are $[N_y \times N_y]$, $[N_u \times N_u]$ and $[N_y \times N_u]$ respectively in which N_u and N_y are the numbers of inputs and outputs. Specifically,

$$\begin{aligned} A(q^{-1}) &= 1 + a_1\, q^{-1} + \ldots + a_{n_a}\, q^{-n_a} \\ B(q^{-1}) &= 1 + b_1\, q^{-1} + \ldots + b_{n_b-1}\, q^{-(n_b-1)} \end{aligned} \tag{4.6}$$

This gives the z-domain transfer function:

$$G(z) = \frac{b_0 + b_1\, z^{-1} + \ldots + b_{n_b-1}\, z^{-(n_b-1)}}{1 + a_1\, z^{-1} + \ldots + a_{n_a}\, z^{-n_a}} \tag{4.7}$$

Multi-variable regression models are based on the use of the least mean square algorithm to estimate the coefficients of the model parameters. This procedure is accomplished by minimizing the mean squared error (MSE):

$$MSE = \frac{1}{N}\sum_{i=1}^{N} e_i(k)^T e_i(k) \tag{4.8}$$

where N is the number of samples and $e_i(k)$ is the difference between the real output, $E_i(k)$ rand the one estimated by the model $\hat{E}_i(k)$:

$$e_i(k) = E_i(k) - \hat{E}_i(k) \tag{4.9}$$

4.2.2 Model structure

Assuming that the energy profile is the measured energy by the power transducers installed in the outdoor unit and that the all the outdoor units in the university are connected to the maximum of 4 indoor units, 4 models of energy consumption are considered for every external unit:

A. Only one indoor unit is working in a time.

B. Only two indoors units are working in each time.

C. Three indoors units are working in a time.

D. All the indoor units are working.

Choosing a structure i.e. the orders of ARX model as well as the delay is usually the first step towards the model estimation after data preparation. However before choosing a model structure, data preprocessing is accomplished. In this study, a length of $^1/_3$ and $^2/_3$ of total data length is considered for the estimation and validation datasets respectively.

After generating different model-order combinations and possible delays for multi-input ARX models, the next step is to estimate the models for each defined model structure. The estimated models are then simulated using the inputs from the validation data set. Finally the normalized *quadratic fit* between the model output and the measured output in the validation data set is formed and the best model structure that minimizes the normalized quadratic fit criterion is chosen.

4.2.3 One-at-a-time running internal machine

In this 69 hours scenario, there is always a single internal machine working in each time and all the other indoor units connected to the correspondent external machine are off. The prepared data is then divided to estimation and validation datasets as described in the previous section. Several models were developed with different structures within them the best model will be used as the energy consumption. Figure (4.3) shows the step responses of each of the developed models having a fresh input from the validation dataset.

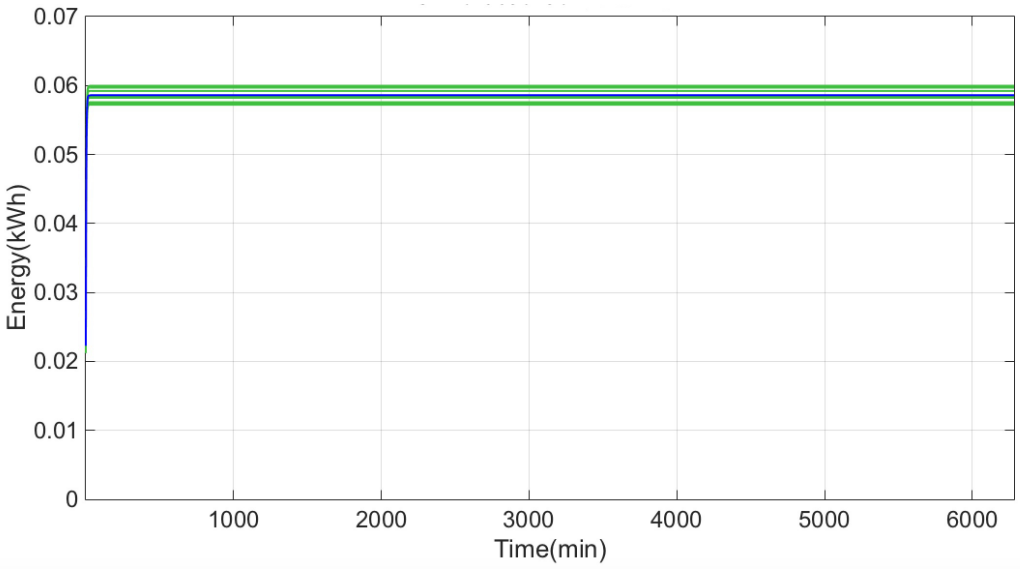

FIGURE 4.3: Response of each developed model for one working internal machine.

The best model structure achieved considers the energy profile as a second order polynomial with the order vector $[2 \quad 2 \quad 1]^T$. Note that polynomial order vector has the structure of $[n_a \quad n_b \quad d]^T$ explained earlier. The fit percentage for this model is 16.73% and MSE is equal to 6.97 e^{-4}. The polynomials of the model are as:

$$\begin{aligned} A(q) &= 1 - 0.4262\ q^{-1} - 0.1938\ q^{-2} \\ B(q) &= 0.02227\ q^{-1} \end{aligned} \tag{4.10}$$

Which leads to the transfer function, $G(z)$ in which the output the external unit energy consumption and input is considered as the only working indoor machine that is to be controlled.

$$G(z) = \frac{0.02227\ z^{-1}}{1 - 0.4262\ z^{-1} - 0.1938\ z^{-2}} \tag{4.11}$$

Model prediction efficiency is evaluated using the *Akaike's Final Prediction Error (FPE)* method which is defined by:

$$FPE = V\left(\frac{1+S/\iota}{1-S/\iota}\right) \tag{4.12}$$

Where V is the loss function, S is the number of estimated parameters, and ι is the length of the estimation dataset. Assuming that the final prediction error is asymptotic for $S \ll \iota$, the following approximation is used in order to compute FPE:

$$FPE = V\left(1+2S/\iota\right) \tag{4.13}$$

The loss function V is thus defined by:

$$V = |\frac{1}{\iota}\sum_{1}^{\iota}\varepsilon(n,\hat{\theta}_\iota(\varepsilon(n,\hat{\theta}_\iota)^T)| \tag{4.14}$$

where θ_ι represents the estimated parameters. Regarding the equation (4.13), FPE for this model is equal to 6.98 e^{-4}. However in the light of evaluating the efficacy of the model encountering the new circumstances, a new fresh dataset (validation dataset) is required. The selected data set for validation purpose is 105 hours during which only one HVAC system is working. Figure (4.4) illustrates the performance of the model output to follow the measured output.

Note that only the first 200 steps are shown in this figure for clarity purposes. However *Normalized mean square error (NRMSE)* fitness is a common evaluation that is used in Matlab to compare the measured and model output values and it is calculated as equation (4.15). Considering our validation data set of 105 hours, this error is 0.2066.

$$NRMSE = 100(1 - \frac{e_i(k)}{\parallel E_i(k) - mean(\hat{E}_i(k)) \parallel}) \tag{4.15}$$

Formerly obtained the best model fitting the data, a univariate and causal transfer function mapping from the input $U(k)$ to the output $E(k)$ can be represented by:

$$\hat{E(k)} = 0.02227\,U(k-1) + 0.4262\,E(k-1) + 0.1938\,E(k-2) \tag{4.16}$$

where $\hat{E(k)}$ is the energy estimation value at instant k.

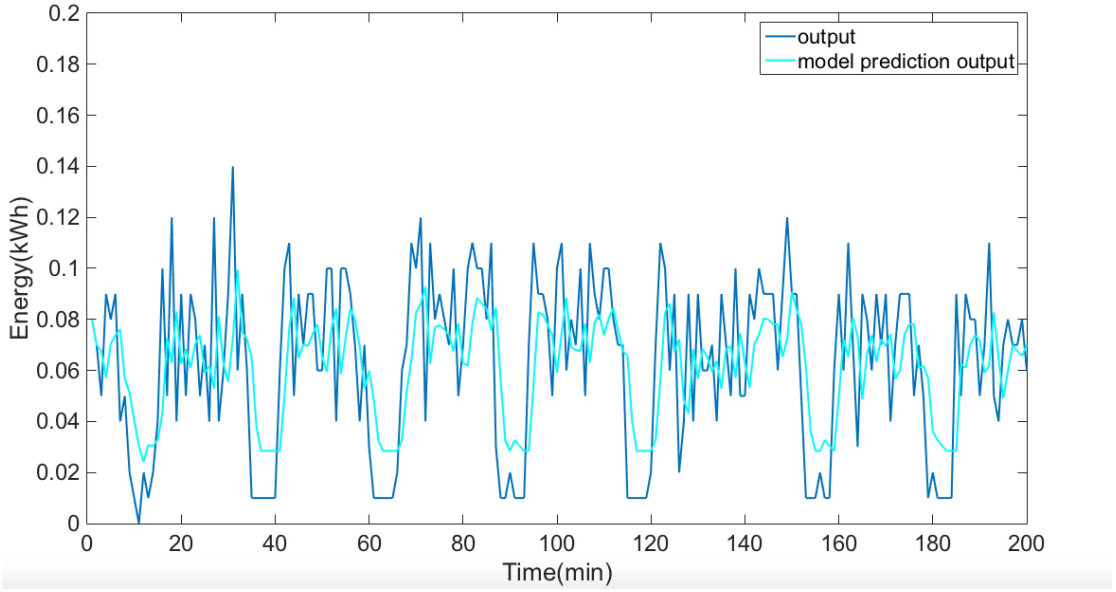

FIGURE 4.4: Model estimated output compared with the energy consumption trend in one-at-a-time running internal machine case.

4.2.4 Two-at-a-time running internal machine

The second scenario is designed in a way that only two internal machines are working in a same time. Using an estimation dataset of 22 hours, the step responses of each of the developed models having a fresh input from the validation dataset is compared to the best fitted model in figure (4.5).

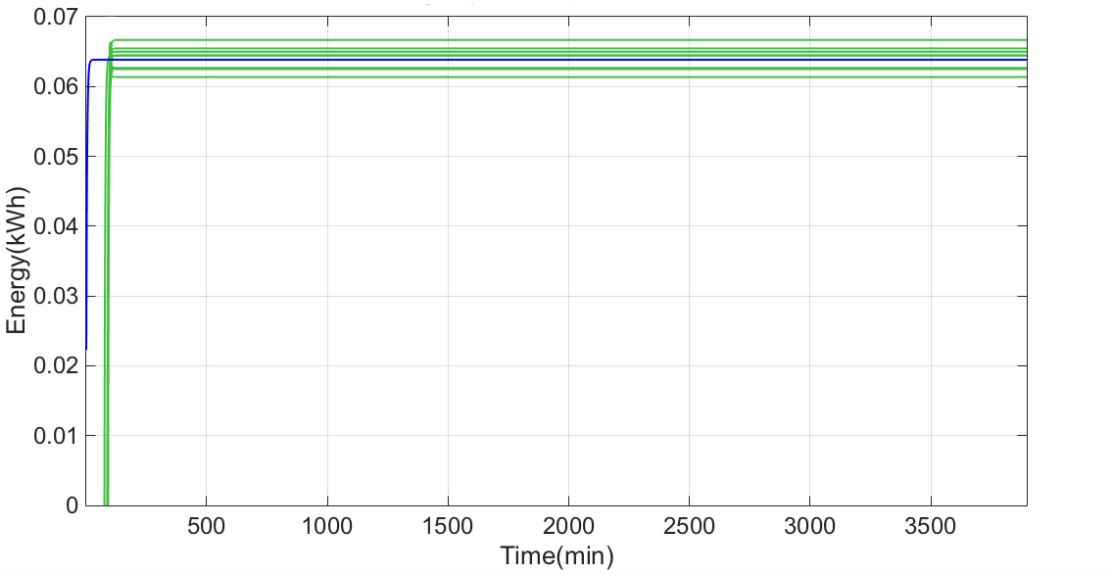

FIGURE 4.5: Response of each developed model for two working internal machines.

These results provide confirmatory evidence that best model polynomial coefficients values are as:

$$\begin{aligned} A(q) &= 1 - 0.3968\ q^{-1} - 0.2544\ q^{-2} \\ B(q) &= 0.02226\ q^{-1} \end{aligned} \tag{4.17}$$

Which leads to the transfer function:

$$G(z) = \frac{0.02226\ z^{-1}}{1 - 0.3968\ z^{-1} - 0.2544\ z^{-2}} \tag{4.18}$$

Polynomial orders of the best model are $[2 \quad 2 \quad 1]^T$ respectively, where having a delay of step. What is more, the fit percentage for this model is equal to 18.31% and MSE value is 8.19 e^{-4}. Equally important, FPE of this model is 8.24 e^{-4} that by and large proves an adequate estimation. As an evidence, figure (4.6) illustrates the proficiency of the model to to pursue the measured value. By the same token, the NRMSE error of model using a validation data set of 65 hours is calculated as 0.1727 for this model while considering that like as the previous case, only the first 200 steps are depicted in this figure for better visibility purpose.

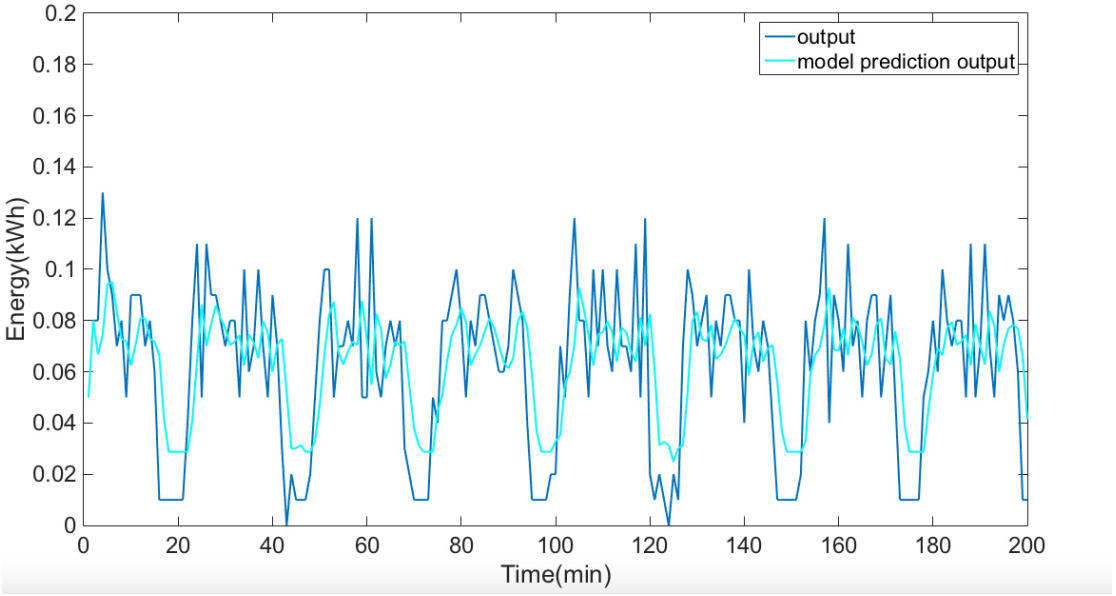

FIGURE 4.6: Model estimated output compared with the energy consumption trend in two-at-a-time running internal machine case.

Considering that one of the internal machines is already working, even so by turning on the second one the energy consumption by the external unit augments, though the increase is not as the same rate as for the first internal unit. The following difference equation describes how old values of energy affect current output:

$$\hat{E(k)} = 0.02226\, U(k-1) + 0.3968\, E(k-1) + 0.2544\, E(k-2) \tag{4.19}$$

4.2.5 Three-at-a-time running internal machine

The data yielded by this scenario provides a circumstance in which three indoor unites are working simultaneously. The ARX model beneficing an estimation data set of 26 hours suggest some possible models plotted in figure (4.7) so that to be compared to the measured external machine energy consumption thereby the best fitted model is chosen.

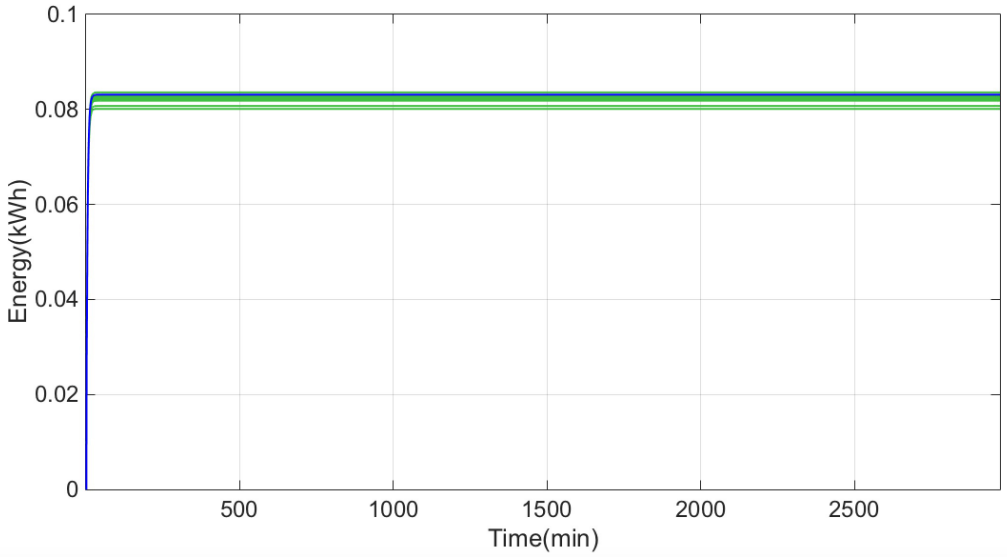

FIGURE 4.7: Response of each developed model for three working internal machines.

All things considered, the most suitable model structure suggests the polynomial coefficients as:

$$\begin{aligned} A(q) &= 1 - 0.3589\, q^{-1} - 0.3145\, q^{-2} \\ B(q) &= 0.02715\, q^{-1} \end{aligned} \tag{4.20}$$

That is to say, the transfer function can be written as:

$$G(z) = \frac{0.02715\, z^{-1}}{1 - 0.3589\, z^{-1} - 0.3145\, z^{-2}} \tag{4.21}$$

The selected model structure considers $[2 \quad 2 \quad 1]^T$ as polynomial orders and 1 steps before is the required delay to compensate the dead time in the system under the circumstance that three internal machines are working at a time. so long as the estimation

dataset, the fit percentage of the model is calculated 19.28% while MSE is equal to $1.09^{e^{-4}}$ shows a considerably decrease compared to the condition that only one or two indoor machines are working in the same time. In the final analysis, the FPE value of $1.1^{e}-4$ as well as the NRMSE error of 0.0945 are calculated within 50 hours of the validation data. Correspondingly, figure (4.8) illustrates the model performance to follow the measured output using the presented model. Noting that only the first 200 steps are shown for better analyses of the response behavior.

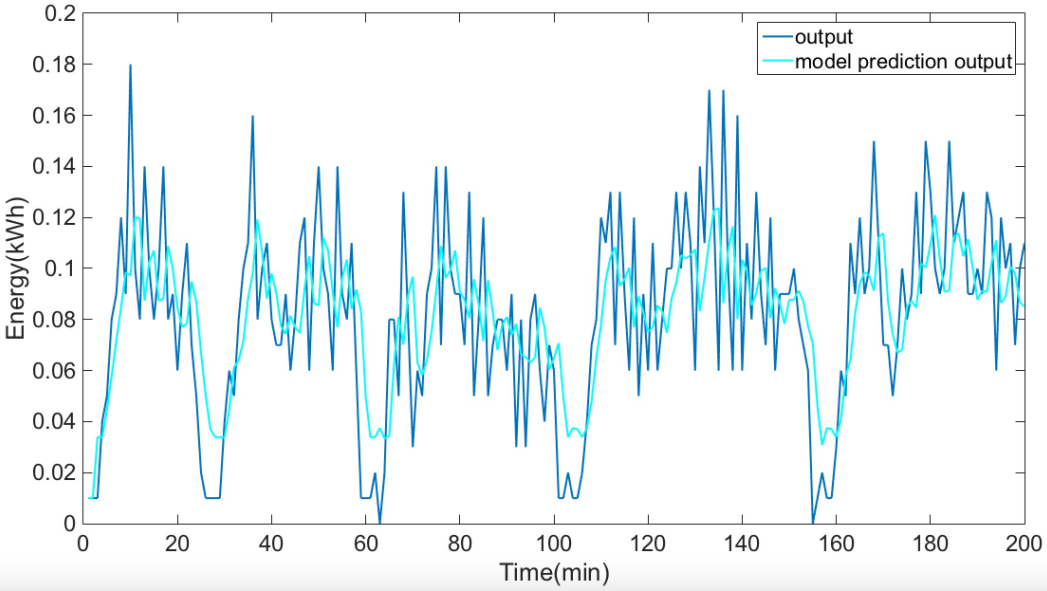

FIGURE 4.8: Model estimated output compared with the energy consumption trend in three-at-a-time running internal machine case.

Describing the model in discrete time, the estimation of energy can be found as:

$$\hat{E(k)} = 0.02715\, U(k-1) + 0.3589\, E(k-1) + 0.3145\, E(k-2) \tag{4.22}$$

4.2.6 Four-at-a-time running internal machine

Employing a dataset of 11 hours to model the circumstance in which all the four internal machines connected to the external machine are running at a time, a set of ARX models achieved are presented in figure (4.9).

The resulted model polynomial coefficients values can be represented as:

$$\begin{aligned} A(q) &= 1 - 0.2987\, q^{-1} - 0.4476\, q^{-2} \\ B(q) &= 0.02419 \end{aligned} \tag{4.23}$$

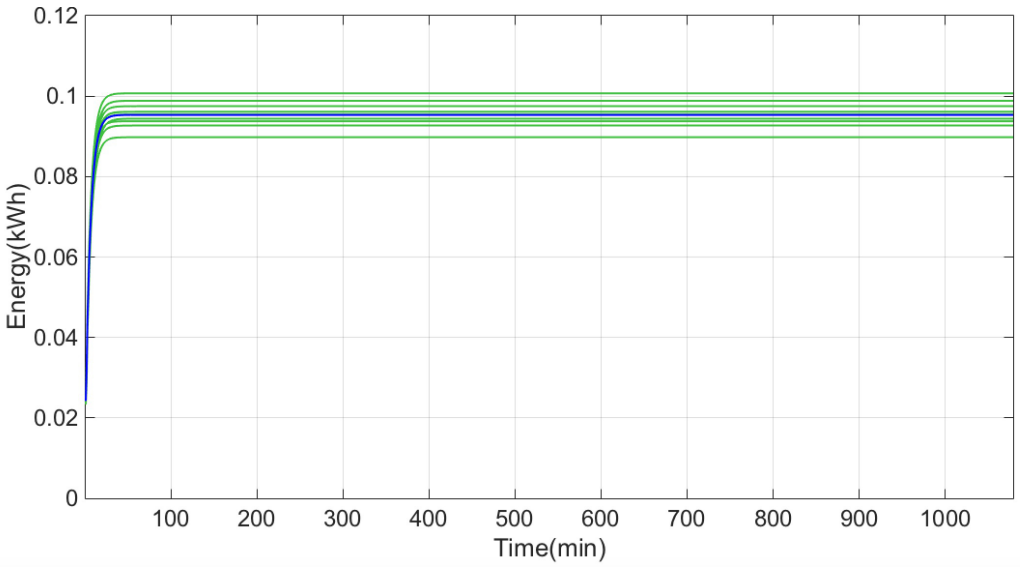

FIGURE 4.9: Response of each developed model for four working internal machines.

Resulting to the transfer function:

$$G(z) = \frac{0.02419}{1 - 0.2987\ z^{-1} - 0.4476\ z^{-2}} \tag{4.24}$$

Polynomial orders of the selected model are $[2 \quad 1 \quad 0]^T$. In the same way, the fit percentage and MSE are calculated as 24.47% and 1.32 e^{-4} respectively. Moreover, final prediction error of the model is measured as 1.32 e^{-4} and the normalized mean square error is determined to an amount of 0.1934. The model output along with the measured energy consumption values over validation dataset of 18 hours are demonstrated in figure (4.10). Like as the previous cases, only the first 200 steps are outlined in this figure.

According to the model transfer function, the energy estimation of the external machine in instant k can be calculated as:

$$\hat{E(k)} = 0.02419\ U(k) + 0.2987\ E(k-1) + 0.4476\ E(k-2) \tag{4.25}$$

4.3 Static energy estimation modeling

Taking a middle-ground position, external unit power consumption profile seems to have a steady state feature during the periods of time in which the number of working indoor units are constant. That means there are specific static values of energy consumption while only one, two , three or four internal machines are running at a time. Although this

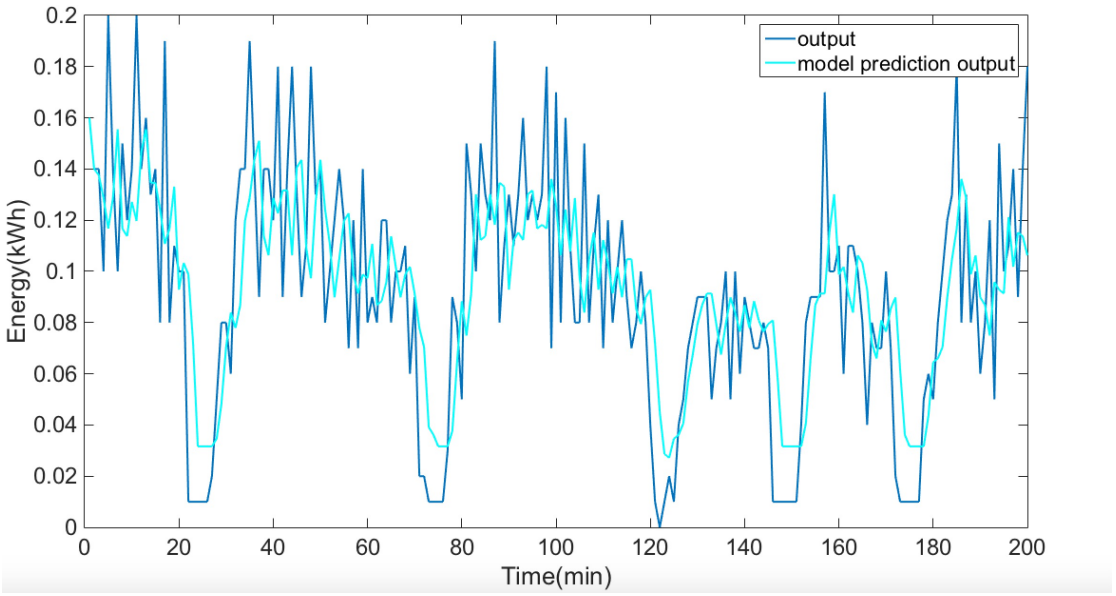

FIGURE 4.10: Model estimated output compared with the energy consumption trend in four-at-a-time running internal machine case.

value falls down to zero or around zero as explained in section (5.2). However the static rate is varying according to the number of indoor units that are working simultaneously. Given the centrality of considering the electrical energy consumption as a constant rate, figure (4.11) provides confirmatory evidence for this assumption.

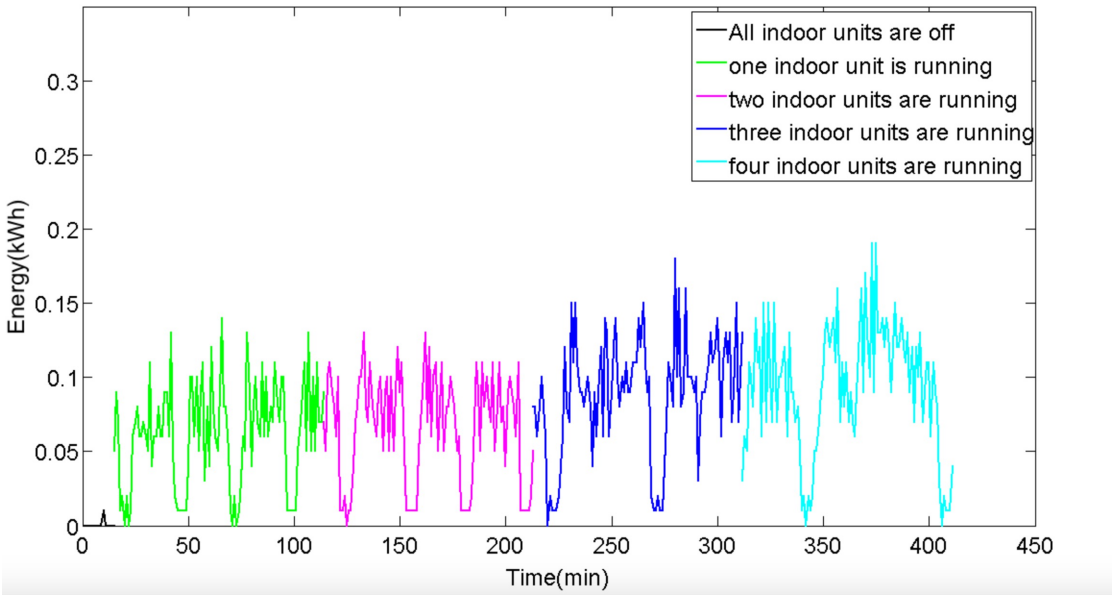

FIGURE 4.11: Energy consumption trend profile distinguished by the number of indoor units that are working simultaneously.

In order to calculate the steady-state energy consumption, 4 months of real data was extracted from the database. This data was classified to four categories of the conditions

where only 1, 2, 3 and 4 internal machines were operating at the same time. The static rates in each case was calculated by:

$$\zeta(i) = \frac{1}{\ell_i - 1} \sum_{k=1}^{\ell_i - 1} E_i(k+1) - E_i(k), \quad i = 1, 2, 3, 4 \tag{4.26}$$

where ζ is the static rate of energy consumption according to the number of simultaneously running internal machines, i, while ℓ_i is the length of each period of data where i indoor units are working at the same time. Furthermore, E_i is noted as the energy consumption vector of each case in kWh. The overall measurement results are summarized in table (4.1).

Number of internal machines	**Constant rate (ζ)**
$i = 1$	0.0603
$i = 2$	0.0650
$i = 3$	0.0805
$i = 4$	0.1041

TABLE 4.1: Static rates of the energy consumption for the experimental external units.

Employing the static rates for the external unit energy consumption while the number of working indoor units are varying, demonstrates a valid estimation and explicitly with low calculation cost to be used in real-time control. The result of this method compared to the real energy profile is represented in figure (4.12).

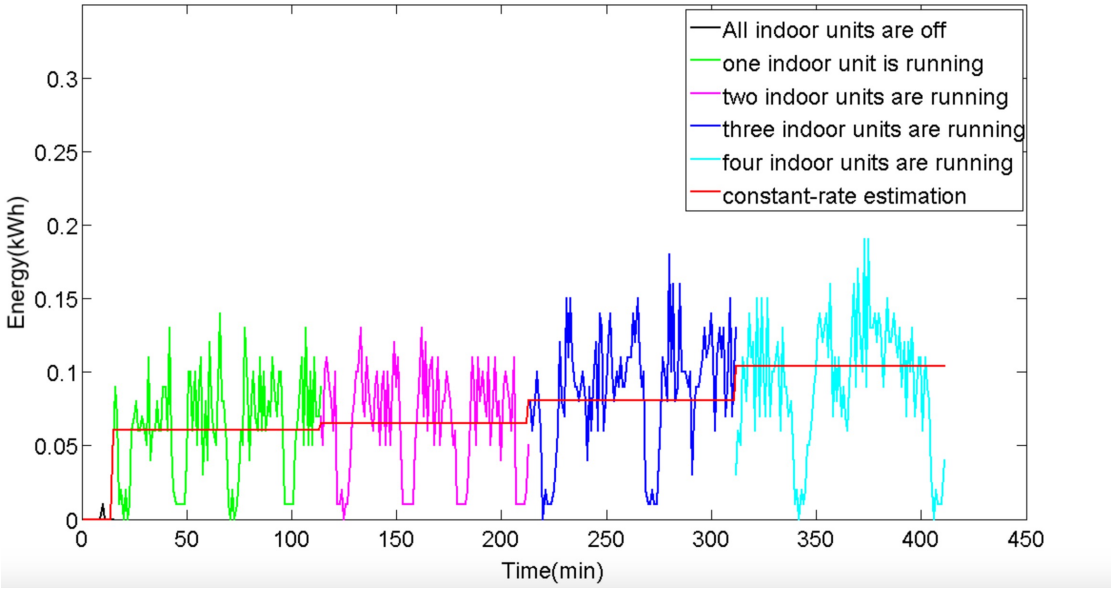

FIGURE 4.12: Static energy estimation modeling.

4.4 Simulation results

In order to verify the validity of the developed approach, several experiments were conducted. These experiments were carried out to find out which of the energy estimation methods best suits our system with a higher precision degree.

The first scenario considers a situation in which only one of the indoor units connected to the external machine is working at a time. Three different experiments are conducted for different times of the day and varying duration. Energy is estimated using the real data in the database. Such cases named as 'experiment 1', 'experiment 2' as well as 'experiment 3' are depicted in the following figures.

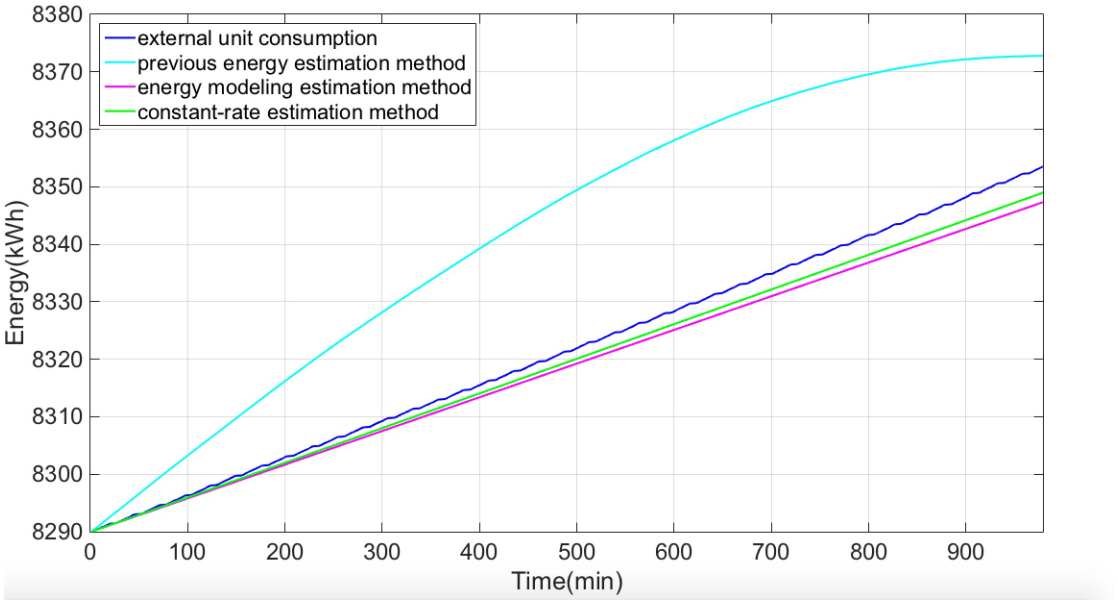

FIGURE 4.13: A comparison on energy consumption estimation methods within 'experiment 1' while there is only one internal machine working.

For visual representation of the total energy estimated by each method as well as the correspondent error, the reader is referred to table (4.2).

Exp	Duration (min)	Actual consumption (kWh)	Consumption estimation (kWh)			MAE (kWh)		
			Previous method	Dynamic model	Static model	Previous method	Dynamic model	Static model
1	981	63.56	82.93	57.38	59.03	21.28	2.82	2.00
2	961	59.39	118.40	56.21	57.83	26.57	1.55	0.76
3	525	31.54	39.67	30.68	31.54	4.05	0.66	0.25

TABLE 4.2: Energy estimation method evaluation within 3 different experiments in case that only one internal unit connected to the external machine is running.

where MAE refers to Mean Absolute Error which is a measure in order to evaluate how close the predictions are to the eventual outcomes. This value is given by:

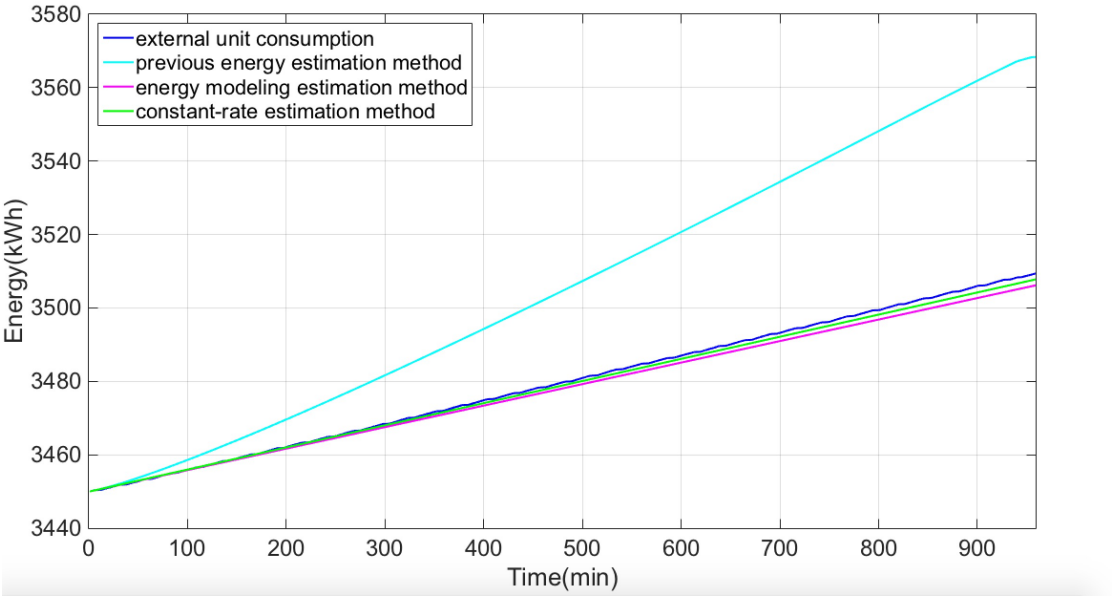

FIGURE 4.14: A comparison on energy consumption estimation methods within 'experiment 2' while there is only one internal machine working.

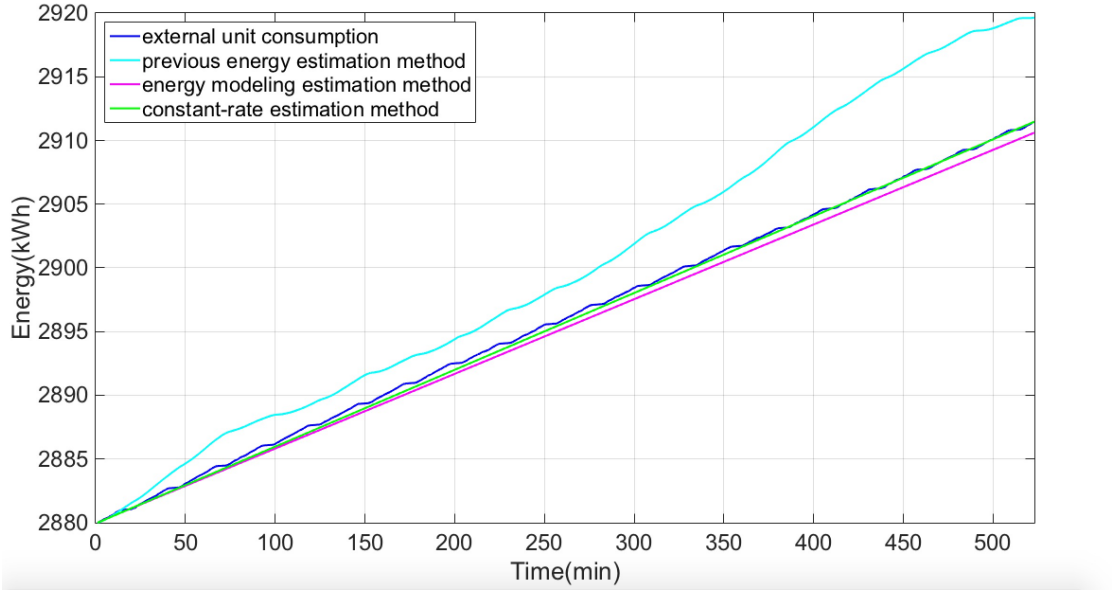

FIGURE 4.15: A comparison on energy consumption estimation methods within 'experiment 3' while there is only one internal machine working.

$$MAE(i,j) = \frac{1}{\ell_i}\sum_{k=1}^{\ell_i}\left|E_{i,j}(k) - \hat{E}_{i,j}(k)\right| \qquad i = 1,\ldots,n, \quad j = 1,2,3 \tag{4.27}$$

where $MAE(i,j)$ is the mean absolute error of experiment i applying energy estimation method j. As the name suggests, the mean absolute error is an average of the absolute

errors $|e(i,j)| = |E_{i,j}(k) - \hat{E}_{i,j}(k)|$, where $\hat{E}_{i,j}(k)$ is the estimation and $E_{i,j}(k)$ the external machine real calculated energy of each instant $k \in [1, \ell_i]$ while ℓ_i notes the length of each experiment over n total experiments. Table (4.3) summarize the accuracy percentage of each method, $\Upsilon(i,j)$ calculated according to Mean Absolute Percentage Error (MAPE) to estimate the precision of each approach that is calculated by:

$$\Upsilon(i,j) = \left(1 - \frac{1}{\ell_i}\sum_{k=1}^{\ell_i}\left|\frac{E_{i,j}(k) - \hat{E}_{i,j}(k)}{E_{i,j}(k)}\right|\right) \times 100 \qquad i = 1,\ldots,n, \quad j = 1,2,3 \tag{4.28}$$

The results show that static modeling estimation method has the best accuracy among the all ranging from 96.85% to almost 99.21% in three experiments notwithstanding that the dynamic model approach has a slightly less accuracy compared to the static model. However previous estimation approach does not exceed 87.15% and for experiment 2 it only introduce 55.26% of accuracy. The results thus obtained for this condition outline the efficiency of the static model compared to the other methodologies.

Exp	**Duration (min)**	**Accuracy (%)**		
		Previous method	**Dynamic model**	**Static model**
1	981	66.52	95.56	96.85
2	961	55.26	97.39	98.71
3	525	87.15	97.91	99.21

TABLE 4.3: Energy estimation method accuracy for 3 different experiments while only one internal unit is working.

We can now process analogously the case that only two of indoor units are working simultaneously. Three experiments of this scenario named as 'experiment 4', 'experiment 5' and 'experiment 6' are depicted in the following. The overall measurement results are outlined in table (4.4).

Exp	**Duration (min)**	**Actual consumption (kWh)**	**Consumption estimation (kWh)**			**MAE (kWh)**		
			Previous method	**Dynamic model**	**Static model**	**Previous method**	**Dynamic model**	**Static model**
4	148	11.47	13.27	9.26	9.49	0.72	1.65	1.52
5	184	11.51	18.15	11.49	11.83	2.36	0.08	0.22
6	174	10.51	9.36	10.78	11.11	1.88	0.12	0.27

TABLE 4.4: Energy estimation method evaluation within 3 different experiments in case that only two internal units connected to the external machine are running.

The analysis of the simulations are summarized in table (4.5). The results indicate that be that as it may the previous method has a slightly better accuracy of 93.72% compared to the other methods in 'experiment 4', however still the dynamic model seems to estimate with higher precision according to the results achieved in 'experiments 5' and 'experiments 6' while the static model energy estimation method lies in after that with a marginally lower accuracy.

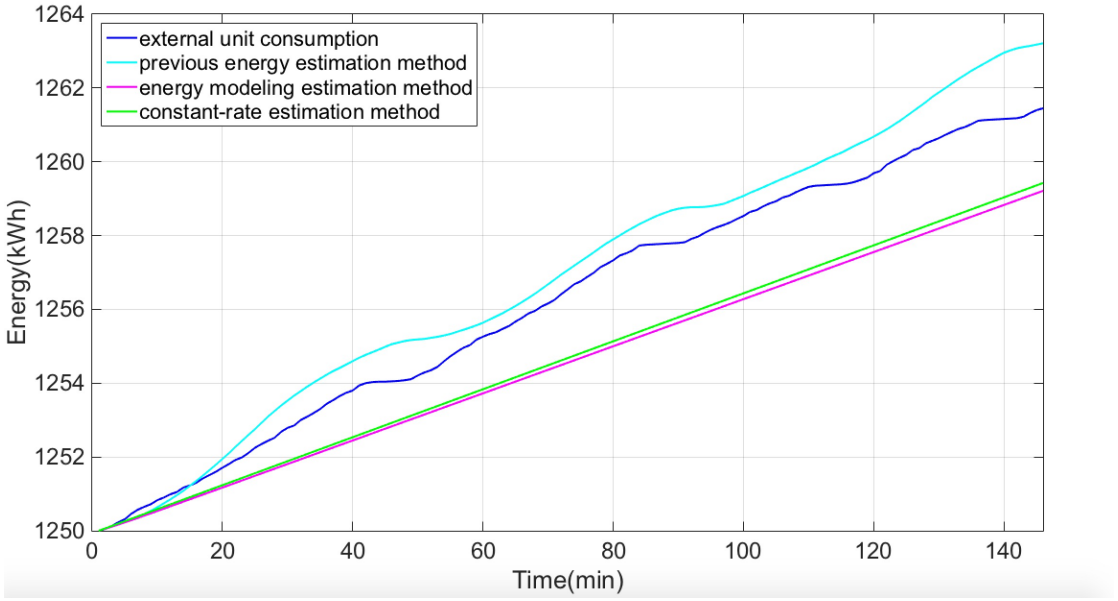

FIGURE 4.16: A comparison on energy consumption estimation methods within 'experiment 4' while there are only two internal machines working.

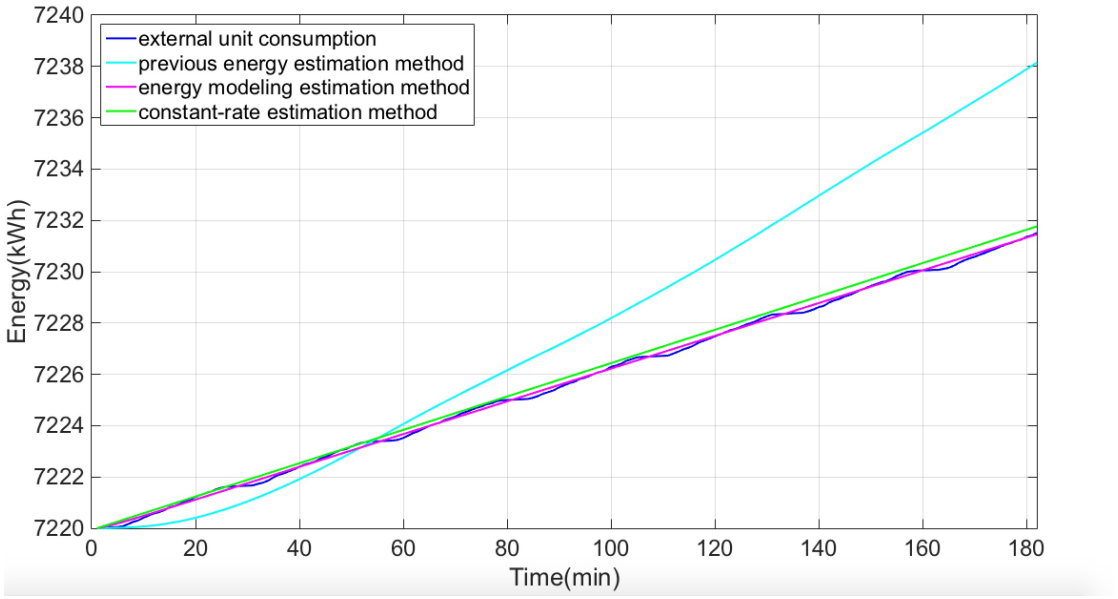

FIGURE 4.17: A comparison on energy consumption estimation methods within 'experiment 5' while there are only two internal machines working.

Exp	Duration (min)	Accuracy (%)		
		Previous method	Dynamic model	Static model
4	148	93.72	85.64	86.73
5	184	79.53	99.28	98.10
6	174	82.10	98.82	97.39

TABLE 4.5: Energy estimation method accuracy for 3 different experiments while only two internal units are working.

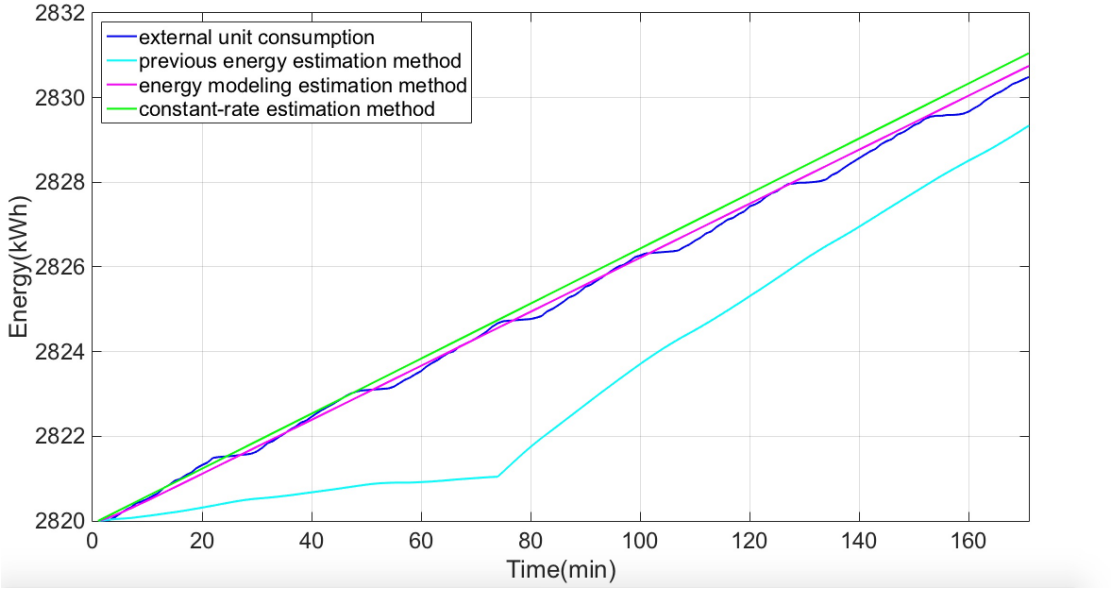

FIGURE 4.18: A comparison on energy consumption estimation methods within 'experiment 6' while there are only two internal machines working.

To examine a circumstance that only three of the indoor units connected to the external machine are working simultaneously, a scenario with three experiments named as 'experiment 7', 'experiment 8' and 'experiment 9' are defined as can be seen from figures (4.19) to (4.21).

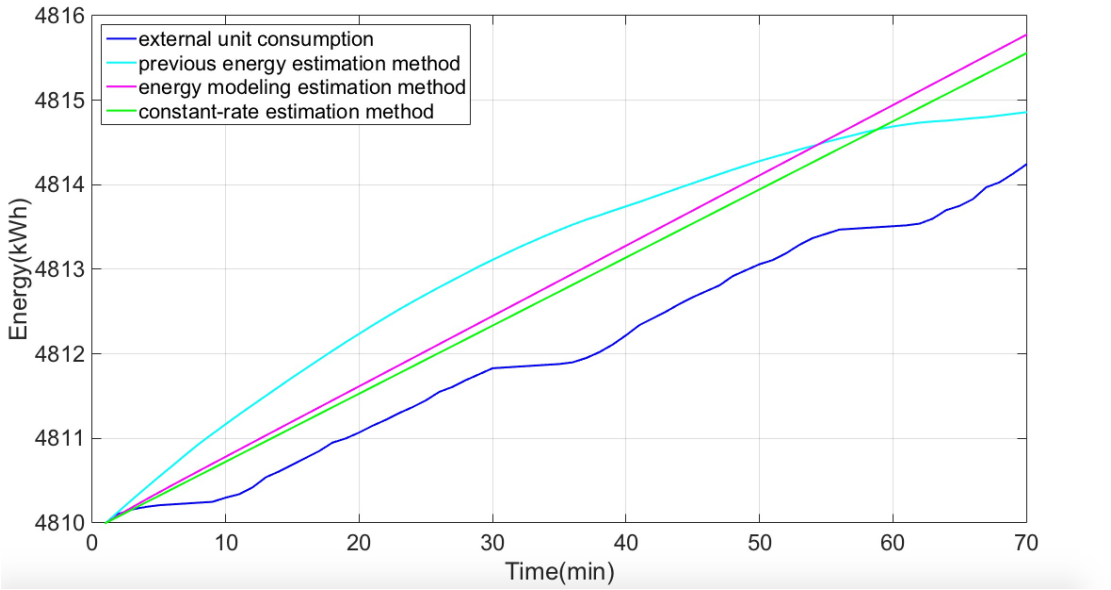

FIGURE 4.19: A comparison on energy consumption estimation methods within 'experiment 7' while there are three internal machines working simultaneously.

Conversely to the previous scenarios, in this scenario the best estimation for 'experiment

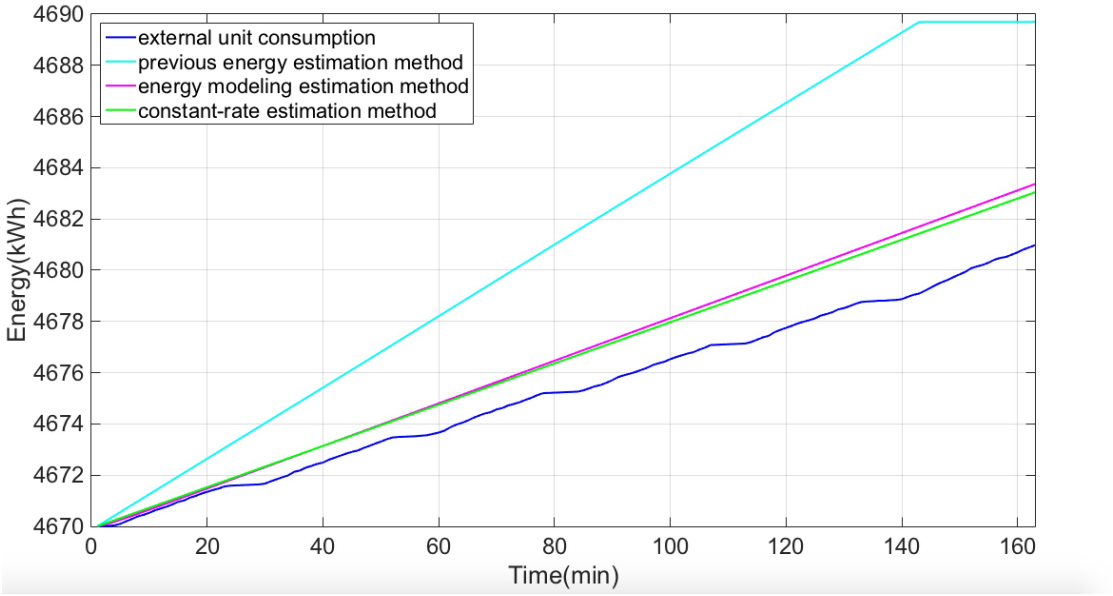

FIGURE 4.20: A comparison on energy consumption estimation methods within 'experiment 8' while there are three internal machines working simultaneously.

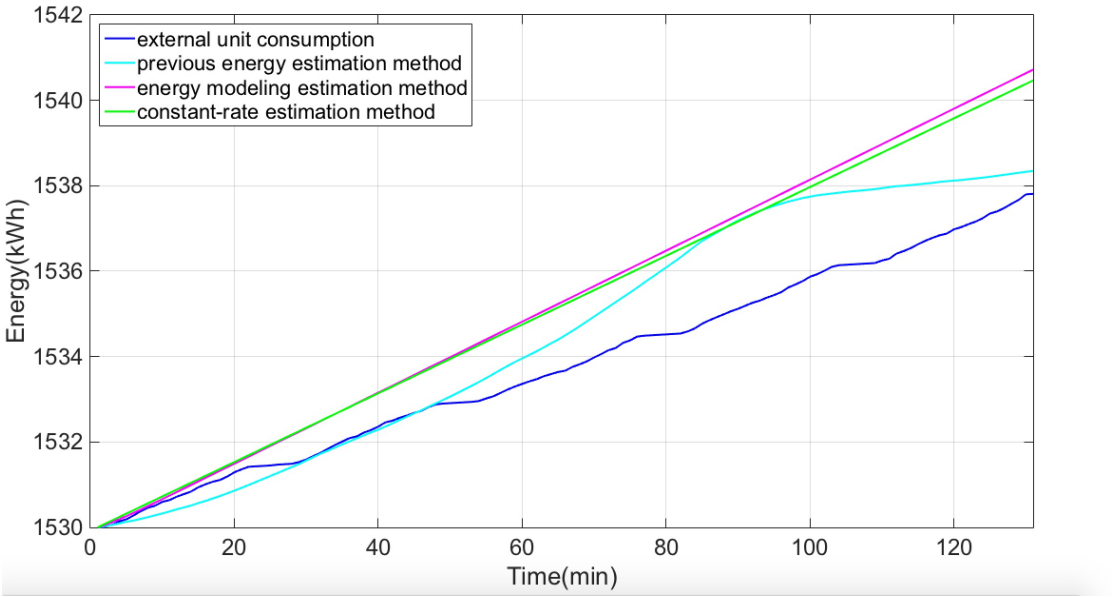

FIGURE 4.21: A comparison on energy consumption estimation methods within 'experiment 9' while there are three internal machines working simultaneously.

7' and 'experiment 8' is achieved through the static model while in the case for 'experiment 9' the best accuracy belongs to the old estimation method nonetheless the static and dynamic models lie in the next with a vaguely lower precision. In order to deal with this contradiction, an average of the total performance is taken into consideration. This value is calculated as 70.33%, 82.77% and 84.46% for the previous approach, dynamic and static models respectively thereby the static model leads to the best estimation

Exp	Duration (min)	Actual consumption (kWh)	Consumption estimation (kWh)			MAE (kWh)		
			Previous method	Dynamic model	Static model	Previous method	Dynamic model	Static model
7	72	4.30	5.00	5.87	5.63	1.09	0.86	0.74
8	164	10.99	19.84	13.40	13.12	5.78	1.34	1.22
9	132	7.82	8.37	10.76	10.55	0.86	1.52	1.43

TABLE 4.6: Energy estimation method evaluation within 3 different experiments in case that three internal units connected to the external machine are running.

accuracy in general.

Exp	Duration (min)	Accuracy (%)		
		Previous method	Dynamic model	Static model
7	72	74.55	79.89	82.82
8	164	47.41	87.82	88.85
9	132	89.04	80.61	81.70

TABLE 4.7: Energy estimation method accuracy for 3 different experiments while three internal units are working.

In the final analysis, a scenario is considered for the case that all the four indoor units connected to the external machine are working at the same time so that external machine needs to work in full capacity. Like as the previous scenarios, three experiments with different durations and different times of the day are designed named as 'experiment 10', 'experiment 11' and 'experiment 12'. Figures (4.22) to (4.24) represent the energy estimation methods performance for each of these experiments. Total energy consumption estimation as well as correspondent MAE of each approach can be found in table (4.8)

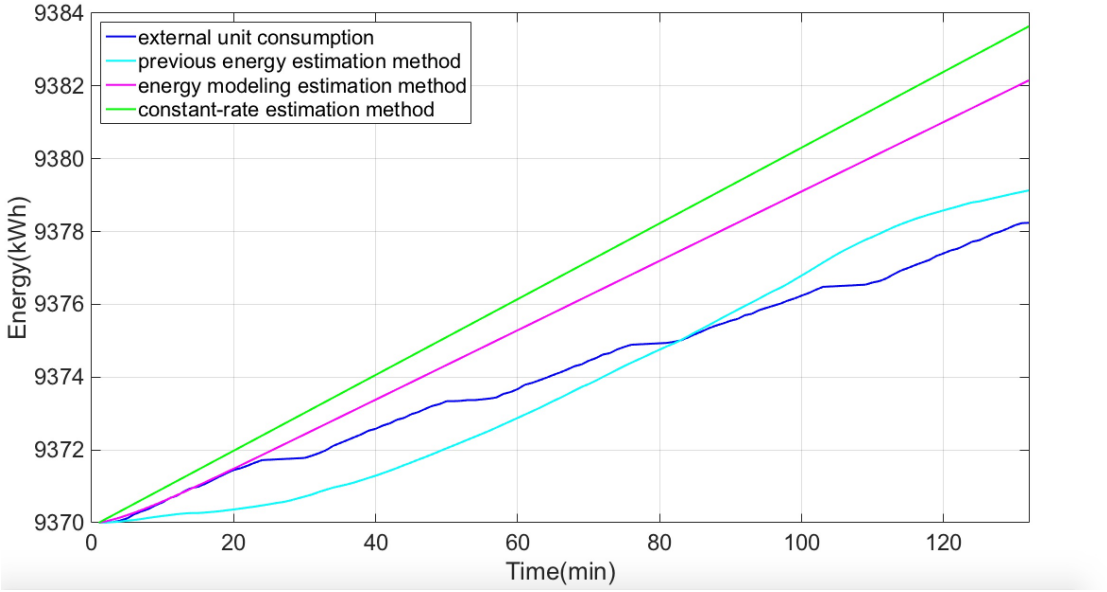

FIGURE 4.22: A comparison on energy consumption estimation methods within 'experiment 10' while all the four internal machines are working simultaneously.

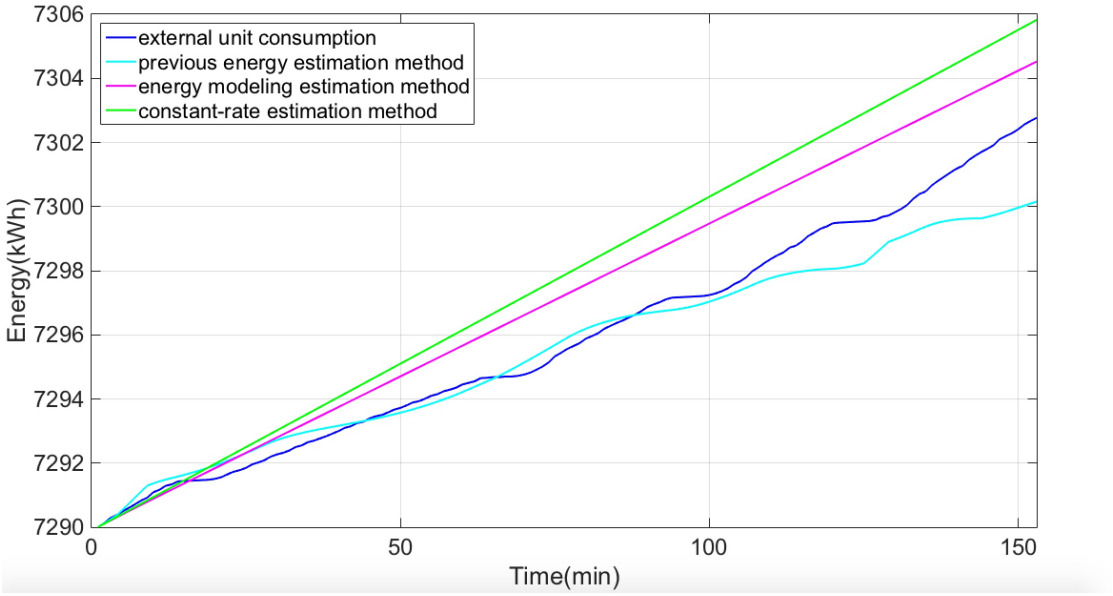

FIGURE 4.23: A comparison on energy consumption estimation methods within 'experiment 11' while all the four internal machines are working simultaneously.

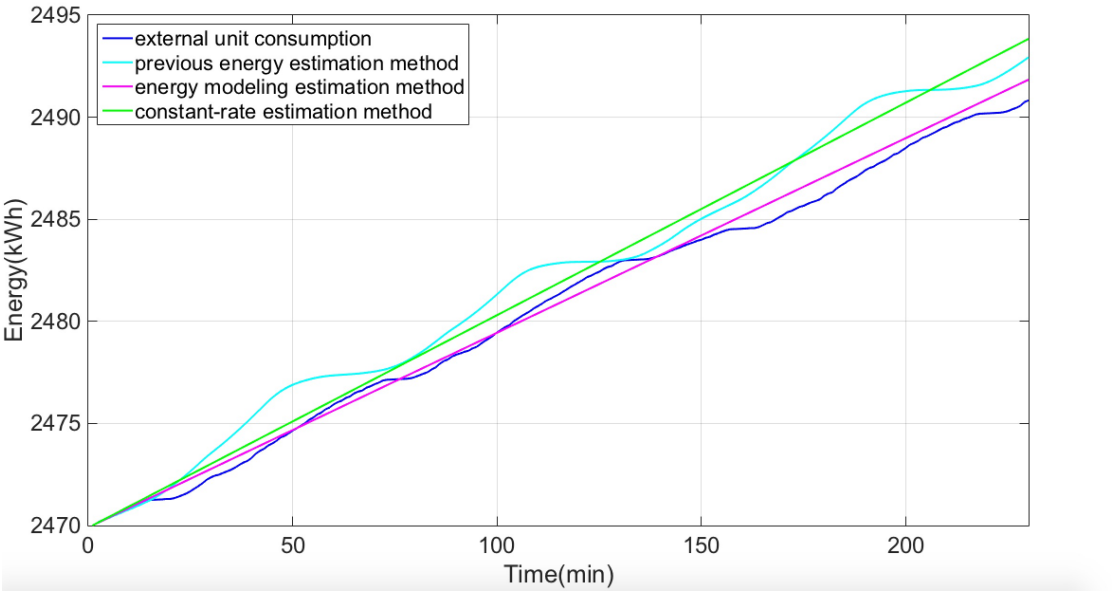

FIGURE 4.24: A comparison on energy consumption estimation methods within 'experiment 12' while all the four internal machines are working simultaneously.

Exp	Duration (min)	Actual consumption (kWh)	Consumption estimation (kWh)			MAE (kWh)		
			Previous method	Dynamic model	Static model	Previous method	Dynamic model	Static model
10	134	8.25	9.14	12.18	13.74	0.80	1.78	2.68
11	155	12.84	10.27	14.62	15.93	0.60	1.40	2.03
12	232	20.92	23.04	21.93	23.94	1.48	0.41	1.22

TABLE 4.8: Energy estimation method evaluation within 3 different experiments in case that all the four internal units connected to the external machine are running.

Considering table (4.8) which depicts the values of energy estimation and the related error for each method, the accuracy percentage can be found in table (4.9). The analysis and simulations illustrate that the previous method leads to the best precision in the case of experiment 10 and 11 notwithstanding the dynamic model stands in the next with a moderately lower precision. However in the case for experiment 12, the dynamic model energy consumption is more accurate than the other methods. In order to sum up the results and evaluate the performance, the average accuracy percentage for previous approach, dynamic and static models are calculated as 92.85%, 88.50% and 81.97% respectively.

Exp	**Duration (min)**	**Accuracy (%)**		
		Previous method	**Dynamic model**	**Static model**
10	134	90.30	78.40	67.55
11	155	95.35	89.07	84.19
12	232	92.90	98.03	94.16

TABLE 4.9: Energy estimation method accuracy for 3 different experiments while all the four internal units are working.

4.5 Concluding remarks

Summing up the results, it can be concluded that according to the number of simultaneously operating indoor units connected to the same external machine, the energy consumption behavior of the outdoor unit is varied. From the comparisons between two developed methods in this work along with the energy estimation method that was used in the previous work, it is possible to conclude that: The data obtained from the database for the energy consumption of the external unit is more broadly consistent with the major trends from static and dynamic models respectively whereas in a circumstance that all the four internal machines are working simultaneously, the previous approach provides us a better estimation of energy although the dynamic model has a moderately lower precious regard to the earlier.

5

Objective Function Study

Based on the energy estimation approaches presented earlier, the purpose of this chapter is to formulate a more effective objective function in order to reach the control goal which is minimizing the energy costs while maintaining the thermal comfort within the controlling zone.

The structure of this chapter is as follows: section (5.1) serves as an introduction to objective function definition. The objective function used in the previous work is shortly described in (5.2). Sections (5.3) and (5.4) represent two new developed energy-oriented objective functions based on two energy estimation methodologies, model and constant rate energy consumption, presented in the previous chapter. The second phase of improving the objective function of the control algorithm is to employ economical terms in order to minimize the energy expenses inside the building. In order to formulate the cost-oriented objective function the electricity rate structure of University of Algarve is considered and the new formulation is presented in section (5.5). Simulation results are covered in section (5.6). Section (5.7) summarizes the results of this chapter and draws conclusions.

5.1 Objective function definition

In order to control HVAC systems of public buildings, there are two possibly conflicting goals: the first one is the fact that each environmental factor is affecting the various processes simultaneously and the second one is the balance between costs and thermal comfort that must be taken into account. Thereby designing an efficient cost function has a significant influence on characterizing the optimization problem as mathematical terms for use in control. This is executed in a systematic way by choosing the proper values of setpoints within an allowed set of temperatures. Considering $U(k)$ as a sequence of control actions over the prediction horizon PH [2]:

$$\begin{gathered} U(k) = [u(k), u(k+1), \ldots, u(k+PH-1)], U(k) \in \upsilon_{PH} \\ u(k+i)_{i=0}^{PH-1} = PA_j^T, j \in [1, nao] \end{gathered} \tag{5.1}$$

in which, υ_{PH} is the space of all sequences of size PH that can be formed as combinations of all the possible control actions nao. PA is the $(nao \times NA)$ matrix of nao possible control combinations for the NA actuators. Choosing a particular set of $U(k)$, the accumulated cost from the time instant k to $k+PH-1$ is given by:

$$\jmath_{1:PH}(k) = \left(\sum_{i=k+1}^{K+PH} \hat{J}(i) \right) \Bigg|_{U(k)} \tag{5.2}$$

The notation $\jmath_{i:j}(k)$ denotes the sum of expressions over the iterations $k+i$ to $k+j$. The optimization problem may now be formulated as the search for a particular sequence $U(k)$ that minimizes the objective function $\jmath_{1:PH}(k)$:

$$\min_{U(k) \in \upsilon_{PH}} \jmath_{1:PH}(k) \tag{5.3}$$

Using the above definition, the HVAC control problem can be solved as described in (5.2) and the constraint (5.4) in order to ensure the thermal comfort:

$$|\hat{\Theta}(i)| < \Theta_T \tag{5.4}$$

where $\hat{\Theta}(i)$ is the estimated PMV index resulting from selecting the setpoint T_{sp} at time instant i. Θ_T is a threshold value for the PMV index which should guarantee acceptable thermal comfort for the occupants of the space. The ASHRAE standard [8] recommends a value of 0.5 which predicts that less than 10% of the occupants will

be dissatisfied [1]. However according to the energy estimation study in chapter (4), alternative objective functions are developed and discussed in the following sections. Note that in order to provide thermal comfort, the constraint (5.4) applies for all the object functions developed in this work.

5.2 Previous objective function

In the previously used objective function, optimal control was achieved by minimizing a cost function that reflects energy consumption criteria based on the deviation of the average inside air temperature over the integration period to its setpoints [1] and can be formulated as:

$$\hat{J}_e(i) = \begin{cases} 1 + \frac{|T_{sp} - T_{ai}|}{\lambda} & T_{sp} > 0 \\ 0 & T_{sp} = 0 \end{cases} \tag{5.5}$$

In which $\hat{J}_e(i)$ is the cost of selecting one control action, T_{sp} at instant i. $T_{sp} = 0$ encodes the action of switching off the HVAC unit. The scaling factor, λ, is used to make the deviation term small compared to 1. In practice this factor is considered as an estimate of the maximum value of $|T_{sp} - T_{ai}|$. The term itself reflects the notion that the higher the difference $|T_{sp} - T_{ai}|$, the bigger is the energy required to achieve T_{sp}.

5.3 Dynamic model objective function

Dynamic energy models presented in the previous chapter, suggest adequate estimations of the energy at each time instant k regarding the number of simultaneously working indoor units connected to the same external machine. These models are employed in order to formulate the objective function to be used in the control algorithm. Considering that this method highly depends on the number of indoor units that are operating in each time instant, distinct formulations are taken into account in each individual circumstance.

First case considers a condition in which there is only one internal machine operating at a time while other indoor units connected to the corresponding external machine are off. The commensurate object function according to energy estimation model presented in (4.15) is as:

$$\hat{J}_e(k) = \begin{cases} 0.02227\, U(k-1) + 0.4262\, \hat{J}_e(k-1) + 0.1938\, \hat{J}_e(k-2) & U_c(k) = 1 \\ 0 & U_c(k) = 0 \end{cases} \tag{5.6}$$

Where U_c is the HVAC's on/off state of controlling unit at instant k. The above equation illustrates that the previous control action affects the current cost value thereby the cost of turning on the controlling unit, highly depends on the last past state of HVAC system as well as the energy values of 2 steps before. It may be true that keeping the system off costs zero however the first objective of the control system is to provide thermal comfort. Thereby in case of existence of any violation, cost does not take into consideration and the HVAC system starts operating.

Second situation considers a case in which there is already one running internal machine, turning on the controlling unit will add operating internal machines by one and so according to the two-at-a-time dynamic model presented in the previous chapter, the objective function can be formulated as:

$$\hat{J}_e(k) = \begin{cases} 1/2 \times \Big(0.02226\, U(k-1) + 0.3968\, \hat{J}_e(k-1) + 0.2544\, \hat{J}_e(k-2)\Big) & U_c(k) = 1 \\ 0 & U_c(k) = 0 \end{cases} \tag{5.7}$$

where multiplying the term by 1/2 illustrates the fact the estimated models are the external machine energy consumption, thereby while calculating the cost of taking a control action for an internal machine, the overall cost should be divided by 2. By the same token, in a circumstance that there are already two internal machines operating, turning on the third unit increases the energy consumption as outlined in (4.21) which leads to an objective function given by:

$$\hat{J}_e(k) = \begin{cases} 1/3 \times \Big(0.02715\, U(k-1) + 0.3589\, \hat{J}_e(k-1) + 0.3145\, \hat{J}_e(k-2)\Big) & U_c(k) = 1 \\ 0 & U_c(k) = 0 \end{cases} \tag{5.8}$$

Ultimately, in the condition that three of four indoor units are operating at the same time, turning on the last unit means that the external machine will need to work in full power and so the corresponding objective function according to dynamic model formulated in the previous chapter can be defined as:

$$\hat{J}_e(k) = \begin{cases} 1/4 \times \Big(0.02419\ U(k) + 0.2987\ \hat{J}_e(k-1) + 0.4476\ \hat{J}_e(k-2)\Big) & U_c(k) = 1 \\ 0 & U_c(k) = 0 \end{cases} \tag{5.9}$$

As it can be seen in all the dynamic model objective functions, the past values of energy consumption as well as the control action of one step before, influence on the current cost value.

5.4 Static model objective function

Recalling static model energy estimation method presented in the previous chapter, steady rates of energy consumption can be employed in the objective function according to the number of concomitantly operating internal machines. Having calculated the static rates earlier, algorithm (5.1) summarizes the procedure of computing the objective function. In the trend of algorithm, $N_{IM}(k)$, represents the number of internal machines that are operating simultaneously considering the controlling unit as well. Furthermore, as the static rates calculated in the previous chapter are the steady state energy consumption rate of the external machine, thereby the model values should be divided by $N_{IM}(k)$ in order to calculate the cost of each control action for each of the controlling internal machines.

Algorithm 5.1. static model objective function

1: **if** $N_{IM}(k) \Leftarrow 0$ **then**
2: $\quad \hat{J}_e(k) \Leftarrow 0.0$
3: **else if** $N_{IM}(k) \Leftarrow 1$ **then**
4: $\quad \hat{J}_e(k) \Leftarrow 0.0603$
5: **else if** $N_{IM}(k) \Leftarrow 2$ **then**
6: $\quad \hat{J}_e(k) \Leftarrow 1/2 \times 0.0650$
7: **else if** $N_{IM}(k) \Leftarrow 3$ **then**
8: $\quad \hat{J}_e(k) \Leftarrow 1/3 \times 0.0805$
9: **else if** $N_{IM}(k) \Leftarrow 4$ **then**
10: $\quad \hat{J}_e(k) \Leftarrow 1/4 \times 0.1041$
11: **end if**

5.5 Cost-oriented objective function

In the light of considering the electricity price structure of the building, a cost-oriented objective function can be designed in order to not only consider the energy consumption

but also taking into account the terms that affects the prices, while maintaining thermal comfort, the consumer is billed for.

5.5.1 Real-Time Pricing

Nowadays electrical utility companies provide a service in which the electric rate structure depends on the climate and clients demand that varies hourly and seasonally known as real-time pricing (RTP). Benefiting from time-of-use rates plane, end users can save in their electric bills if they are able to use a majority of energy during, or shift a significant amount of energy consumption to the lower rate hours of the day.

EDP[1] *universal service* electric rate structure is used in this work as they provide electrical service to University of Algarve so that the real bills can be analyzed. The used electric rate structure of this work is medium voltage, long-term operation, tetra-hourly and daily cycle service. Medium-sized commercial and industrial customers may benefit from choosing this plan in which the energy price is dependent on the time-of-use. Tetra-hourly means that it consists of on-Peak, mid-peak, mildly-off-peak and off-peak hours demonstrating varying pricing for different hours of a day. Tetra-hourly plan applicable in this work is shown in table (5.1) while the daily range of real-time pricing structure at summer and winter peaks are outlined in figure (5.1).

Term	**Schedules**	
	Fall and winter	**Spring and summer**
on-peak	9:30-11:30 & 19-21	10:30-12:30 & 20-22
mid-peak	8-9:30 & 11:30-19 & 21-22	9-10:30 & 12:30-20 & 22-23
Mildly-off-peak	22-2 & 6-8	23-2 & 6-9
off-peak	2-6	2-6

TABLE 5.1: Tariff timetable specified in UAlg contract with EDP.

Furthermore, the electricity price is comprised of energy charge, demand charge and customer charge. The energy charge is depicted in table (5.2). The demand charge is fixed per monthly maximum kW which is 0.3155 €/kW according to the university current contract tariffs. However since customer charge is fixed, it is not included in the optimization scheme in this work.

5.5.2 Formulation

Considering the electricity price structure discussed in previous topic, an economic objective function is designed as follows:

[1]Energias de Portugal

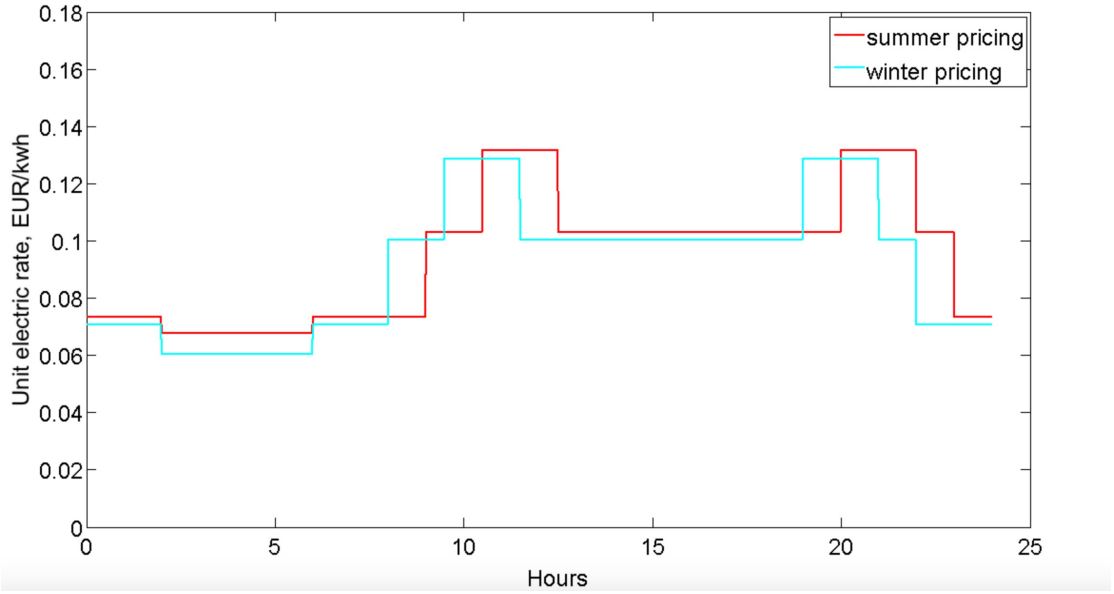

FIGURE 5.1: Real-time pricing unit electric rate daily range at summer and winter peaks.

Term	T_e**: rate (€/**kWh**)**	
	Fall and winter	**Spring and summer**
On-Peak (Highest Cost)	0.1287	0.1316
Mid-Peak (Mid-range Cost)	0.1004	0.1030
Mildly-Off-Peak (Low Cost)	0.0708	0.0735
Off-Peak (Lowest Cost)	0.0604	0.0677

TABLE 5.2: UAlg electricity active power rate charges specified in UAlg contract with EDP.

$$\min J = C_e + C_d \tag{5.10}$$

Where J denotes the total daily electricity expenses, which is a combination of energy and demand costs, defined by Equation (5.11) and (5.12) respectively:

$$C_e(k) = T_e(i,j) \times E(k) \tag{5.11}$$

$$C_d(k) = \begin{cases} T'_p \times E(k) & k \in Hours_{on-peak} \\ 0 & k \notin Hours_{on-peak} \end{cases} \tag{5.12}$$

Where $T_e(i,j)$ is the rate shown in table (5.2) corresponding to the time-of-use, i, and season j. $E(k)$ is the active energy consumption in the time instant k and T'_p is a coefficient it is needed to be determined. As everyday consists of a 4 hours interval

of on-peak, the demand energy during each minute within on-peak hours, (in terms of KW), can be calculated as:

$$E_d = \frac{\sum_{d=1}^{ND}\sum_{k=1}^{24} E(k,d)}{ND \times 4}, k \in Hours_{on-peak} \tag{5.13}$$

Where ND is the number of days of the invoice. Therefore the economic cost, applicable for the entire billing period, and the peak hours (i.e., $j = 1$, $k \in Hours_{on-peak}$), is given by:

$$\begin{aligned}\sum_{d=1}^{ND}\sum_{k=1}^{24} T_e(i,1)E(k,d) + ND \times T_p \times \frac{\sum_{d=1}^{ND}\sum_{k=1}^{24} E(k,d)}{ND \times 4} = \\ = \sum_{d=1}^{ND}\sum_{k=1}^{24}\left(T_e(i,1) + \frac{T_p}{4}\right)E(k,d)\end{aligned} \tag{5.14}$$

Where $E(k,d)$ is the active energy that is consumed in the time k of day d. Thus the ratio of in (5.11) is given by $T_p/4$ and (5.10) can be formulated as:

$$J(k) = \begin{cases}\left(T_e(i,1) + \frac{T_p}{4}\right) \times E(k) & k \in Hours_{on-peak} \\ T_e(i,j) \times E(k), j \neq 1 & k \notin Hours_{on-peak}\end{cases} \tag{5.15}$$

Thus, for the calculation of the objective function, we can use equation (5.16), where coefficients $\varkappa(i,j)$ shown in table (5.3) are calculated after some adjustment of the power-related coefficient in rush hour.

$$J(k) = \varkappa(i,j) \times E(k) \tag{5.16}$$

Term	$\varkappa(i,j)$ **(€**/kWh**)**	
	Fall and winter(i=1)	**Spring and summer(i=2)**
On-Peak (j=1)	0.2076	0.2105
Mid-Peak (j=2)	0.1004	0.1030
Mildly-Off-Peak (j=3)	0.0708	0.0735
Off-Peak (j=4)	0.0604	0.0677

TABLE 5.3: Coefficient values calculated for the objective function in (5.16)

5.6 Simulation results

In order to analyze the possible benefits of the developed objective functions, a number of simulations were carried out. The simulations were run over different length of data in order to analyze the system behavior applying each of the cost functions in our MBPC algorithm in order to find the best control action in each sampling instant. The room climate was simulated using the models and additive noise taken from normal distributions that approximate fairly well the existent error distributions. In this way the error that the control system is exposed to in the real operating environment is also simulated to a certain extent. A 24 hours of outside weather data employed in order to initialize the predictive models, was that measured by the sensors. In these simulations the actuator control signals are those obtained in the control experiment. In each time instant, the predictive models are applied in order to predict the room's climate over the prediction horizon. The optimal solution is then chosen by selecting the control trajectory that minimizes the estimated accumulated cost, while maintaining thermal comfort.

The simulations to be presented further on, were executed through 3 experiments within varied time durations and circumstances. The first scenario considers a 140 minutes period before which the internal machine of controlling room is off thereby the room is not in thermal comfort. The MBPC initializes in the beginning of this period. The outside weather data considered was the data acquired for that period, and the other values were obtained by means of the models. Employing different objective functions presented in this chapter, the control actions chosen by BaB are varied. Figure (5.2) illustrates the inside, outside and setpoint temperatures associated with each sampling instant, using the old, dynamic and static models objective functions while the outside air temperature (OAT) is around $9°C$ as shown in the plot. As can be seen in the plot, the HVAC system is operating for all the duration of the experiment applying each of the discussed methods.

In Figure (5.3) the evolution of the PMV index using three cost functions is presented. As it can be seen, non of the rooms enter the comfort zone, i.e., the PMV index within the $[0.5 - 0.5]$ threshold. That happens because the MBPC starts only in the beginning of this period in a condition that outside air temperature is $9°C$ and room temperature is equal to $12°C$. The plot represents that although the HVAC system has been operating for whole the period, but cause of the weather and inside air temperature conditions, the system fails to reach to thermal comfort using each of these methods within this period.

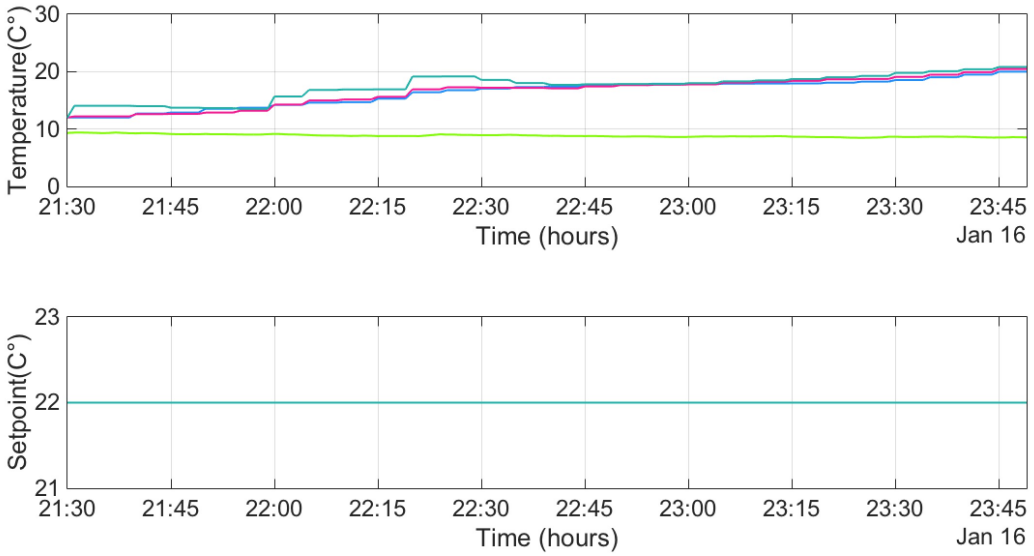

FIGURE 5.2: Upper plot: OAT (in green) and IAT evolution using the old cost function (in blue), dynamic model (in pink) and static model (in sea green) objective functions. Lower plot: setpoint temperature evolution using the old, dynamic and static objective functions with same specified colors for experiment 1.

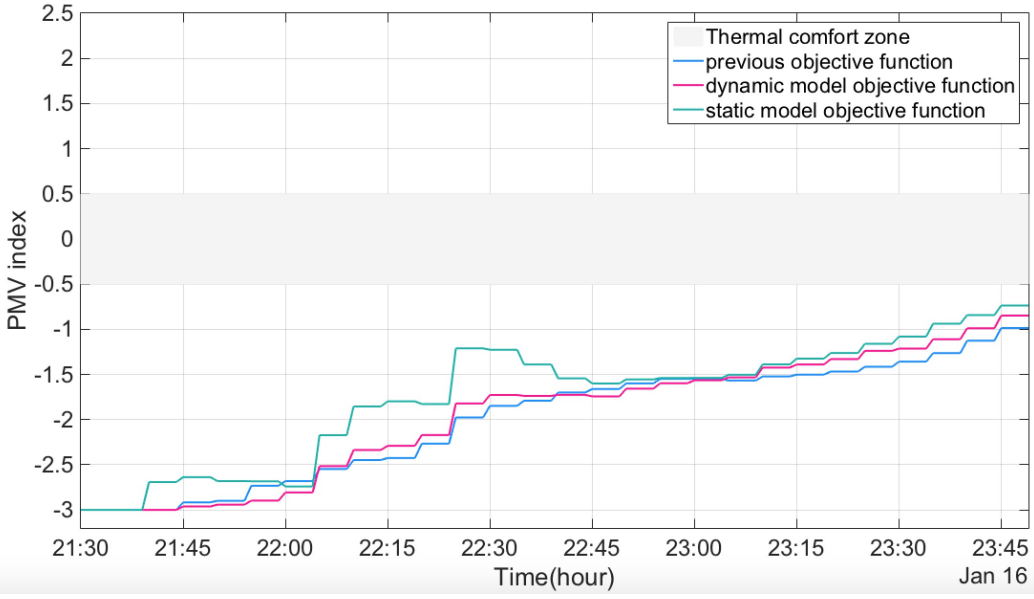

FIGURE 5.3: PMV evolution of experiment 1 using specified objective functions.

To compute an estimate of the real energy consumption, a procedure suggested by Mitsubishi [65], was followed to give a first, a crude approximation to the electric energy consumption of the indoor unit using each cost function:

$$E_i(k) = E_o(k)\frac{T_{th_i}}{\sum_i T_{th_i}} + 220\, T_{on_i} + \frac{32}{N} \tag{5.17}$$

where $E_i(T)$ is the energy assigned to the i^{th} indoor unit, out of N units connected to the external machine. $E_o(T)$ denotes the energy consumed by the outdoor unit, at the period k where T_{on_i} stands for the periods of time (hours) where the fan of i^{th} indoor unit is working. Moreover, T_{th_i} indicates the periods where the unit is cooling or heating. As the result, the corresponding energy consumption and price according to EDP pricing table presented earlier, is equal to 3.75 kWh and 0.75 € for each of the three approaches.

Second experiment simulates a 390 minutes scenario in which the controlling room is not in thermal comfort previously. The best control actions chosen by BaB accompanied with the room inside and outside air temperatures are outlined in figure (5.4). As it is shown in the plots, the control starts in a condition that the inside and outside air temperatures are 14.1°C and 8.3°C respectively.

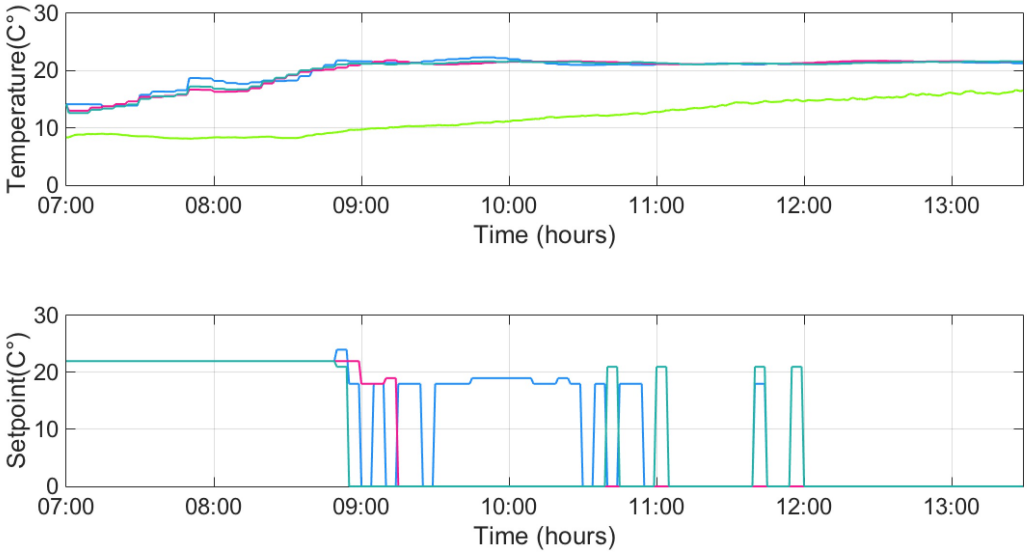

FIGURE 5.4: Upper plot: OAT (in green) and IAT evolution using the old cost function (in blue), dynamic model (in pink) and static model (in sea green) objective functions. Lower plot: setpoint temperature evolution using the old, dynamic and static objective functions with same specified colors for experiment 2.

As it can be found from thermal comfort evolution outlined in figure (5.5), employing both old and static model objective functions in MBPC algorithm, the room enters the comfort zone after 116 minutes of starting control notwithstanding this happens for dynamic model objective function 10 minutes later than the others.

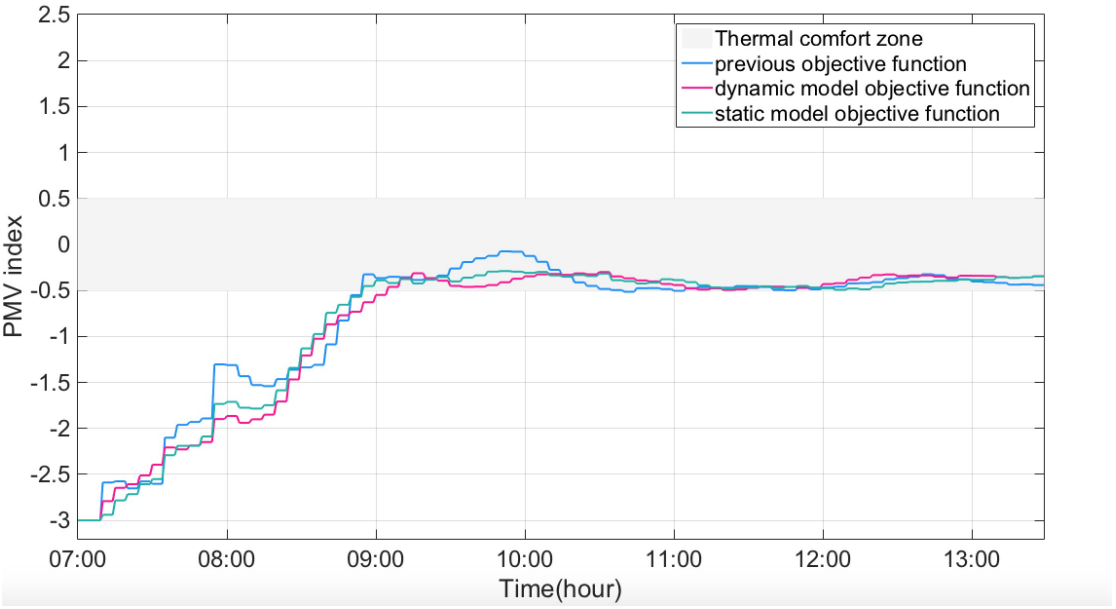

FIGURE 5.5: PMV evolution of experiment 2 using specified objective functions.

However as follows from the table (5.4) that represents the energy consumption and its corresponding costs for this experiment, previous objective function has the best saving in energy as well as expenses among the three considered approaches nevertheless both old and dynamic model objective functions have 32.05% of violations within this period. However this value is equal to 29.49% for static model that makes this approach preferable among the considered methods.

Approach	**Energy (kWh)**	**Price (€)**
old objective function	2.81	0.49
dynamic model objective function	3.75	0.75
static model objective function	7.92	1.27

TABLE 5.4: Energy consumption and expense of different objective functions related to experiment 2.

The last scenario considers a 11 hours experiment while the outside and inside temperatures are considerably higher in the beginning compared to the previous experiments. Figure (5.6) depicts the inside and outside air temperatures as well as best control actions sequence applying each objective function.

Regarding the PMV evolution plot corresponding to this experiment outlined in figure (5.7), utilizing static model, the controlling room reaches to thermal comfort after 56 minutes while this delay is equal to 61 and 126 minutes for dynamic model and previous objective functions respectively. In other words, evaluating the possible control actions using static model objective function leads the system to reach the thermal comfort 5 and 70 minutes earlier than dynamic model and old objective functions respectively.

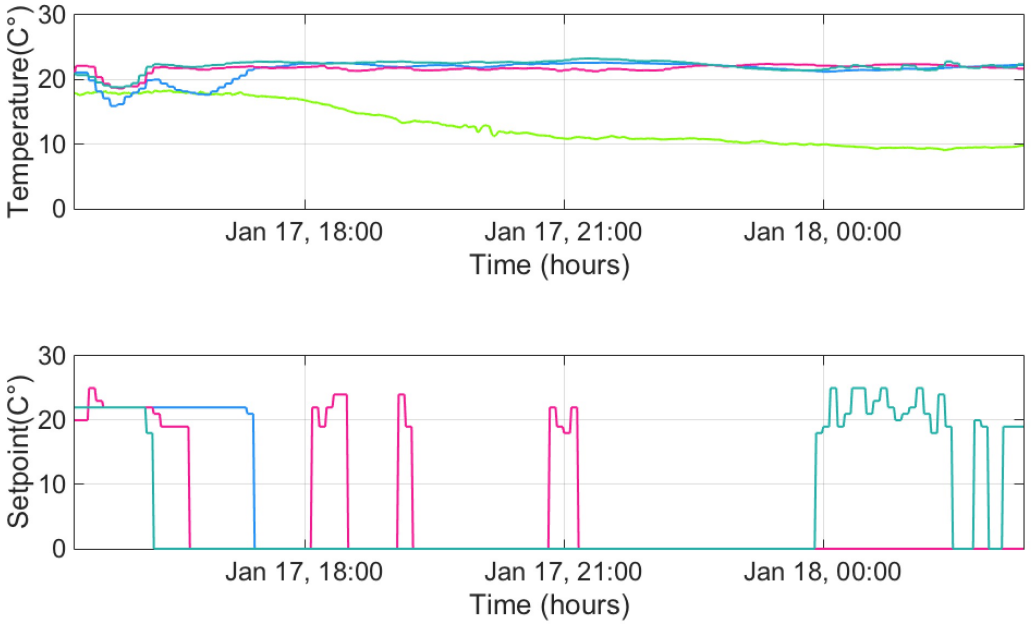

FIGURE 5.6: Upper plot: OAT (in green) and IAT evolution using the old cost function (in blue), dynamic model (in pink) and static model (in sea green) objective functions. Lower plot: setpoint temperature evolution using the old, dynamic and static objective functions with same specified colors for experiment 3.

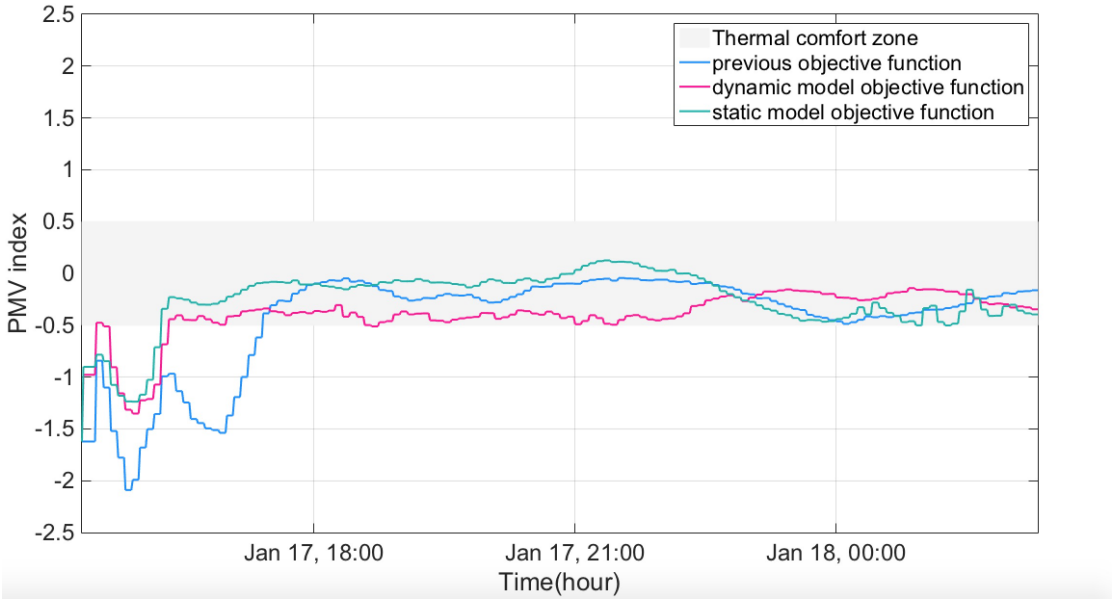

FIGURE 5.7: PMV evolution of experiment 3 using specified objective functions.

The analysis of the energy consumption as well as the costs depicted in table (5.5), suggest that the dynamic model objective function can be used in order to decrease the energy prices while maintaining the room in thermal comfort which is the first goal of the control system.

Approach	Energy (kWh)	Price (€)
old objective function	2.98	0.60
dynamic model objective function	4.16	0.48
static model objective function	6.99	0.82

TABLE 5.5: Energy consumption and expense of different objective functions related to experiment 3.

To sum up the results, as it can be seen from the numerical values, except in the experiment 3 where dynamic model objective function operates better, the static model objective function seems to better result considering both thermal comfort as well as energy consumption and corresponding expenses.

In the second phase of experiments, the cost-oriented objective function is simulated in order to figure out the possible benefits of applying this objective function in the control methodology. For this purpose, the three experiments carried out in the first phase of simulations are repeated in order to compare the best objective function from energy-oriented simulations, static model objective function, to cost-oriented form of the same objective function. Simulating MBPC algorithm using both objective functions, figure (5.8) depicts the corresponding inside and setpoint temperatures associated with each sampling instant for each method.

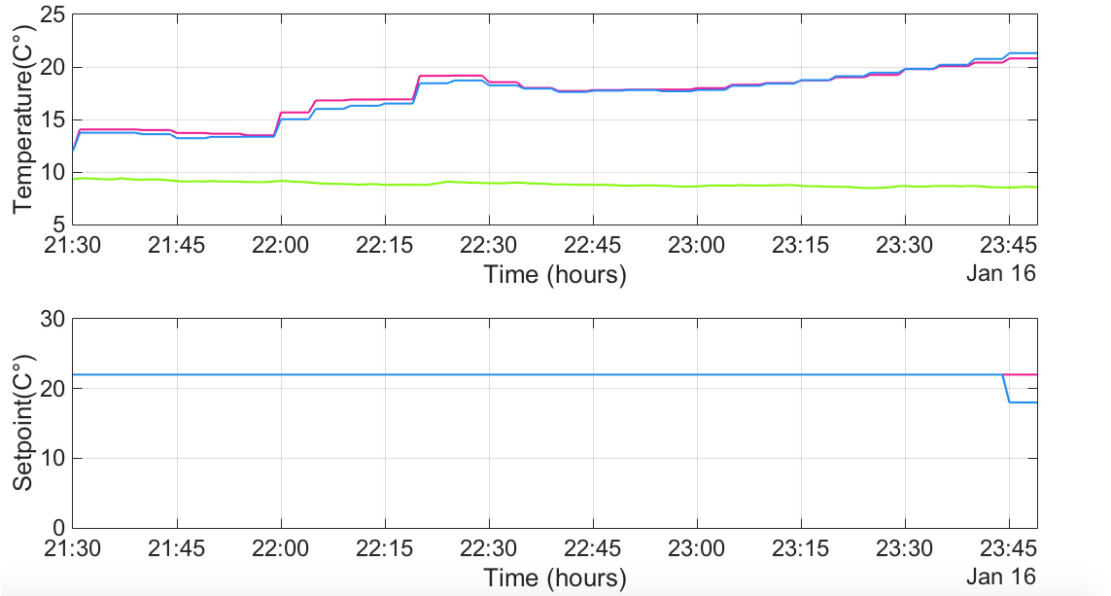

FIGURE 5.8: Upper plot: OAT (in green) and IAT evolution using the energy-oriented (in pink) and cost-oriented (in blue) objective functions. Lower plot: setpoint temperature evolution using the energy-oriented (in pink) and cost-oriented (in blue) objective functions for experiment 1.

As follows from figures (5.9) showing the PMV evolution of each formulation, employing cost-oriented objective function in control algorithm does not help to reach to thermal

comfort considering the outside and inside air temperatures within this experiment nevertheless employing the cost-oriented objective function, the HVAC system is off for the last 5 minutes.

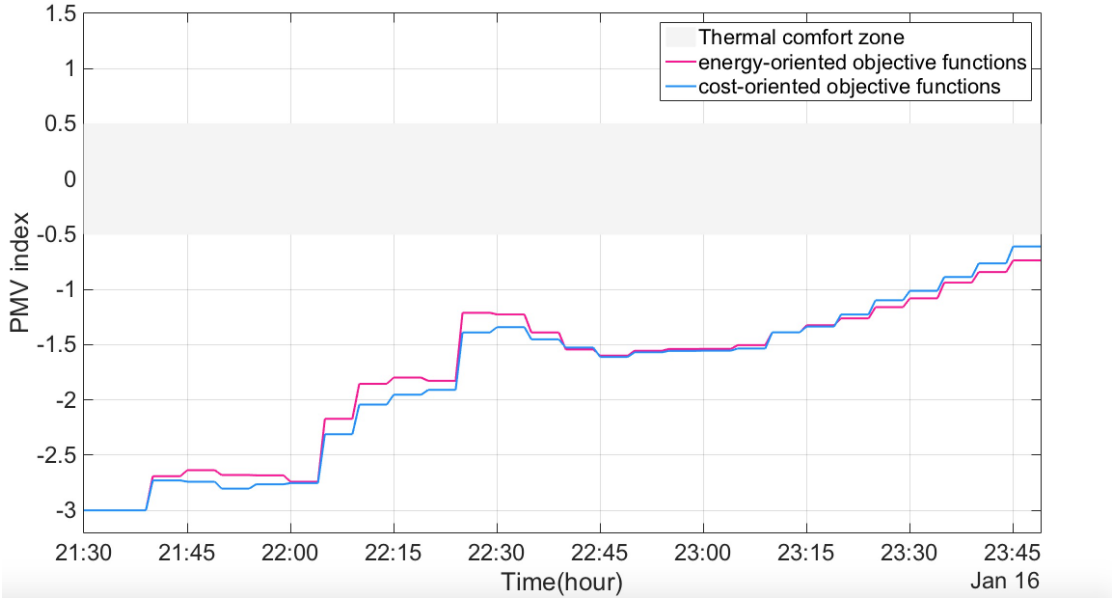

FIGURE 5.9: A comparison between PMV evolution of energy-oriented and cost-oriented objective function for experiment 1.

Simultaneously for experiment 2, air temperature and HVAC's setpoint evolution of each sampling instant is plotted in figure (5.10). The plot shows that by using the cost-oriented objective function, setpoint fall down to zero more times than the energy-oriented as the rooms is in thermal comfort due to the setpoint provided to the HVAC system despite the fact that the outside air temperature is $9°C$. However the room enters the thermal comfort at the same time using each of the objective functions as outlined in figure (5.11).

The results obtained in table (5.6), shows 19% and 30% of saving of energy consumption and energy prices respectively in this experiment proving the effectiveness of the cost-oriented objective function to achieve the control goal.

Approach	**Energy (kWh)**	**Price (€)**
energy-oriented objective function	7.92	1.27
cost-oriented objective function	6.44	0.89

TABLE 5.6: Energy consumption and expense of energy-oriented and cost-oriented objective functions related to experiment 2.

The air temperature and setpoint evolution for the last experiment with the length of 11 hours is plotted in figure (5.12). The results thus obtained represent that employing energy-oriented objective function, the room reaches to comfort condition 35 minutes

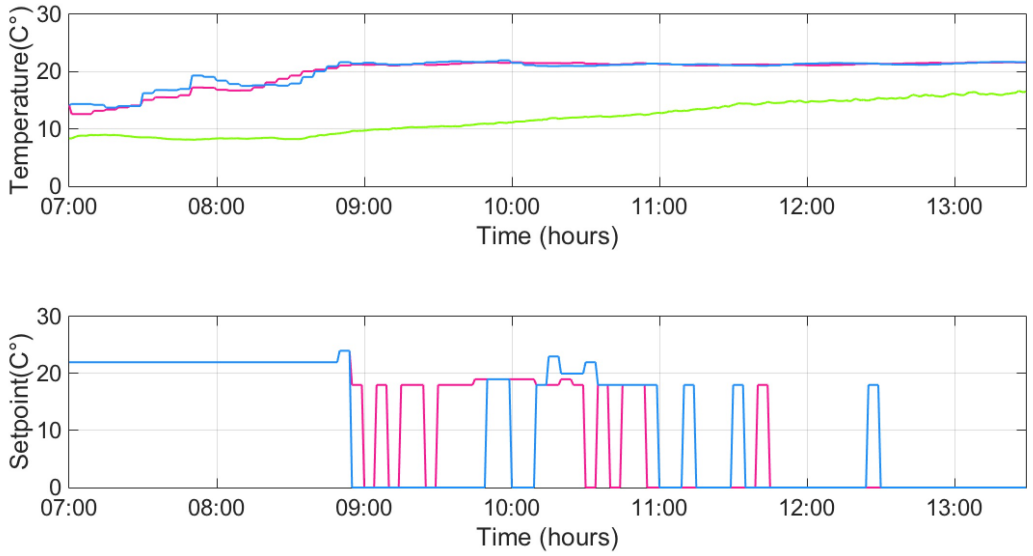

FIGURE 5.10: Upper plot: OAT (in green) and IAT evolution using the energy-oriented (in pink) and cost-oriented (in blue) objective functions. Lower plot: setpoint temperature evolution using the energy-oriented (in pink) and cost-oriented (in blue) objective functions for experiment 2.

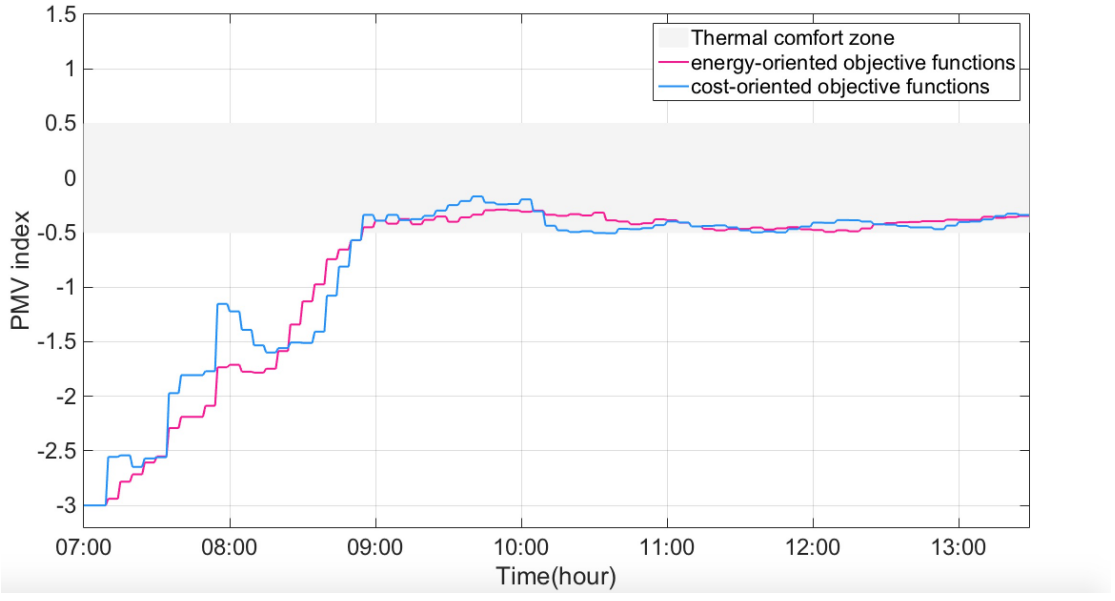

FIGURE 5.11: A comparison between PMV evolution of energy-oriented and cost-oriented objective function for experiment 2.

earlier than cost-oriented objective function which makes a significant difference for the occupants.

Table (5.7) outlines the energy consumption as well as related energy prices for this experiment. Analyzing the numerical values, cost-oriented objective function saves 95%

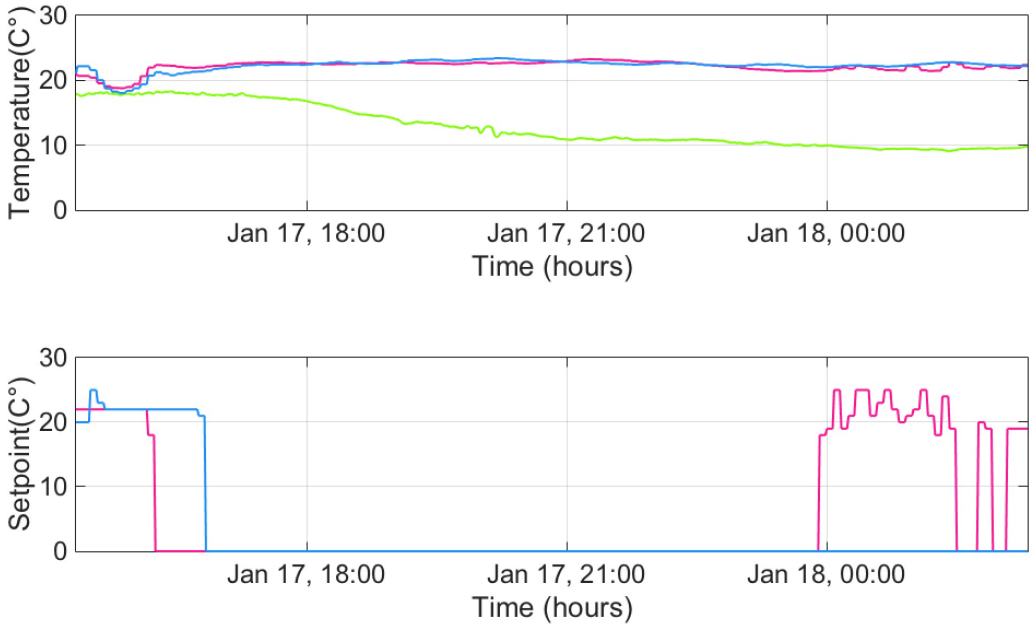

FIGURE 5.12: Upper plot: OAT (in green) and IAT evolution using the energy-oriented (in pink) and cost-oriented (in blue) objective functions. Lower plot: setpoint temperature evolution using the energy-oriented (in pink) and cost-oriented (in blue) objective functions for experiment 3.

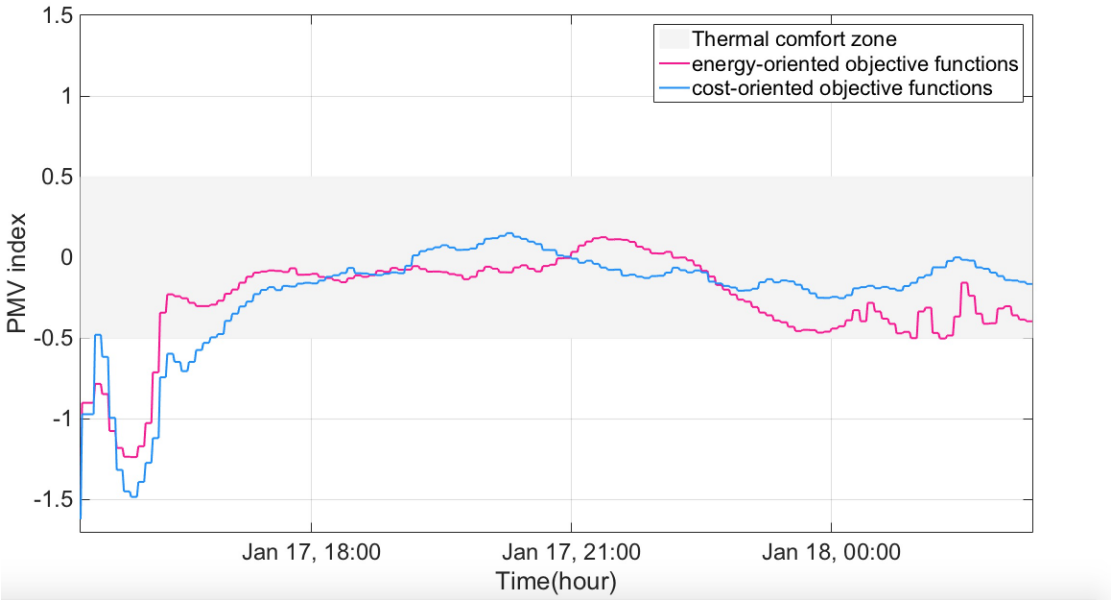

FIGURE 5.13: A comparison between PMV evolution of energy-oriented and cost-oriented objective function for experiment 3.

of energy as well as 94% of the expenses compared to the energy-oriented objective function.

Approach	Energy (kWh)	Price (€)
energy-oriented objective function	6.99	0.82
cost-oriented objective function	0.36	0.05

TABLE 5.7: Energy consumption and expense of energy-oriented and cost-oriented objective functions related to experiment 3.

5.7 Concluding remarks

This chapter has clearly shown that the new developed objective functions have apparent advantages over the old cost function. The analysis and simulations indicate that not only employing static model objective function in most of the cases lead the system to reach the thermal comfort conditions earlier than the other approaches, but also it reduces the energy consumption and the related cost of each control action so that energy expenses will be lower. Although this may be true that dynamic model objective function in overall is acting more efficient in case for experiment 3.

formulating the cost function used by the MBPC algorithm in economic terms, instead of just energy estimations, we were able to decrease the costs of operating the HVAC equipment, while maintaining thermal comfort. In the given context, the dynamic tariff provides an economic incentive for the building controller to adjust control actions in case of high spot market electricity prices and high grid load levels, respectively. The results from the price evaluation concur in good agreement with the energy estimation simulations which proves the fact that considering the economical terms along with a well defined energy estimated objective function can considerably decrease the energy consumption as well as the prices.

6

Modified Model-based Predictive Control

A model-based predictive control approach regarding the control of HVAC systems has been presented in [2] which was earlier discussed in chapter (3). However, several practical questions arise when dealing with buildings which are not occupied for all the time instants but only within the pre-defined schedules. It is important to consider that thermal comfort only matters within the occupation times and it is the key point to reduce energy consumption and its correspondent expenses for such huge consumers.

The structure of this chapter is as follows: section (6.1) depicts the necessity of introducing a scheduling plan for buildings. Later, three original approaches considering this issue are developed. Section (6.2) presents a method that initializes the scheduled MBPC 4 hours approach to the expected occupied time. However in order to avoid overly conservative scheduling, section (6.3) describes the control approach to be started only 2 hours before that occupants arrive to the building. Section (6.4) is devoted to our last method that is a scheduled MBPC with some modifications applied to the search methodology of BaB algorithm. The efficiency of our approaches compared to the previous work is outlined in section (6.5). Section (6.6) concludes this chapter.

6.1 Occupation period scheduling plan

As discussed in the previous chapters, the concept of thermal comfort only matters within the times that the rooms are occupied. A lot of times, the HVAC systems are being left working even though there are no occupancies in the rooms which is definitely very costly to the building. Figure (6.1) plots the HVAC on/off status of 4 indoor units connected to an external machine located in the second floor of building 8 in UAlg. The collected data are for a period of 6 hours and 30 minutes in which only 2 hours has been occupied. As it can be found in the correspondent plot, ACs are working even within the times that there is no occupancy in the rooms.

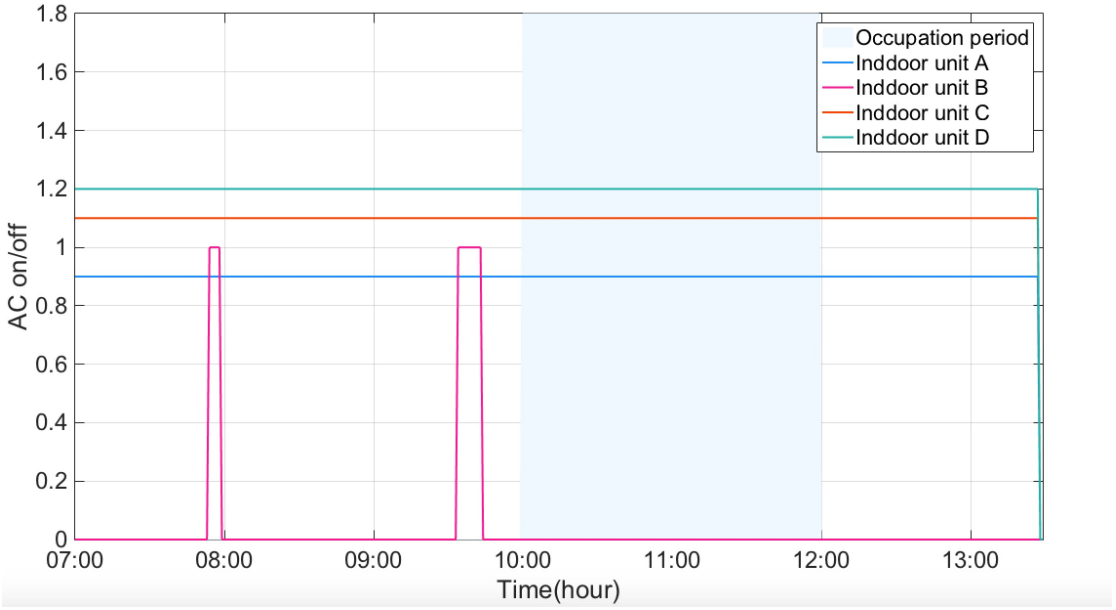

FIGURE 6.1: Sample trend data of HVACs on/off status of 4 indoor units without occupation scheduling plan consideration. In order the plot to be discernible, indoor units A, B, C and D on/off states are distinguished in different levels of 0.9, 1, 1.1 and 1.2 respectively.

Thermal comfort level evaluated according to ASHARE standard is plotted versus the hours of day for the scenario that can be found in figure (6.2). The plot indicates that despite the HVAC systems have been working for most of this period, the rooms are not providing thermal comfort for the occupants which is the most compelling evidence of the need to have an occupation scheduling plan. By and large, occupation period scheduling plan aims to give a comprehensive account of using an efficient scheduling plan so that the rooms are already in thermal comfort by the time the people enter the building and notwithstanding this is ignored while there is no occupancy in the rooms. In energy consumption analysis of mentioned case, the energy usage patterns of the rooms are depicted in figure (6.3).

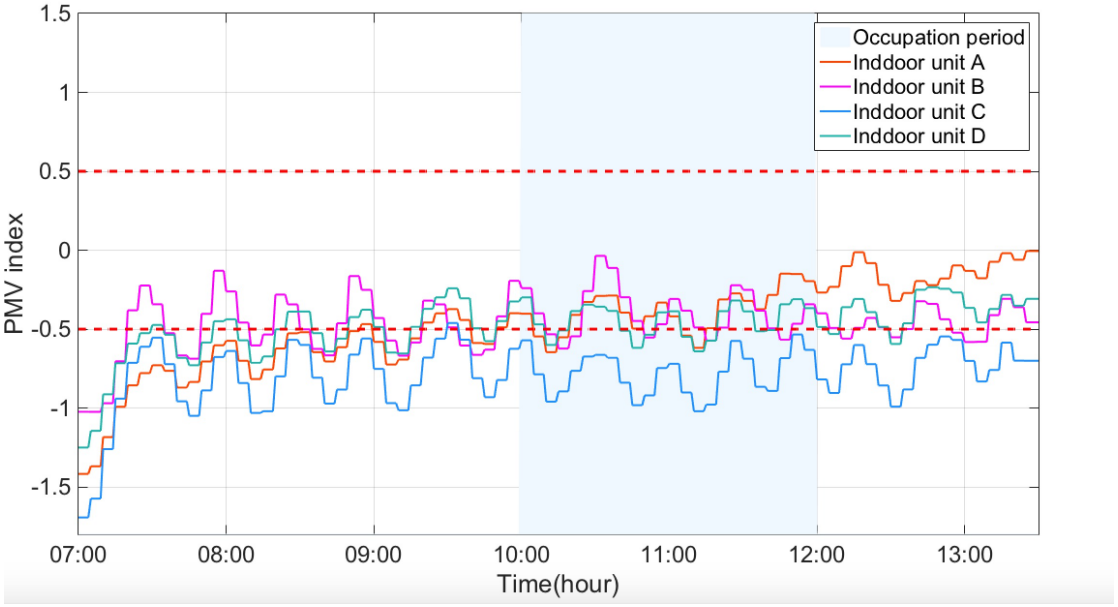

FIGURE 6.2: Sample trend data of thermal comfort without 4 indoor units without occupation scheduling plan consideration.

The previous implementation of branch and band used in this work benefits from a 4 hour prediction horizon. However having the occupation timetable of the rooms, there is no need to have 24 hour of control in the rooms. Three solution approaches to this problem are developed in this work which will be discussed in the following sections.

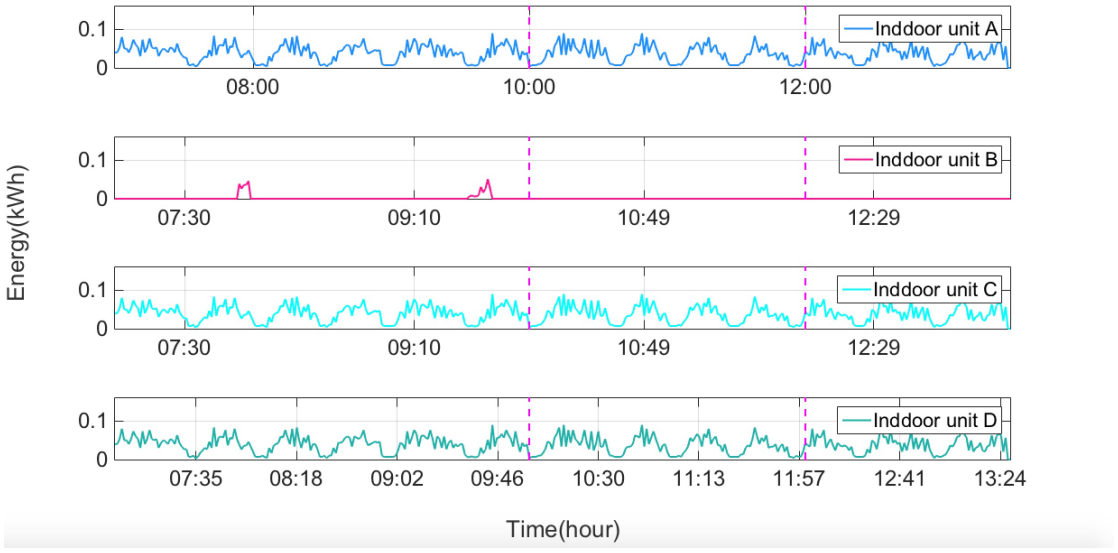

FIGURE 6.3: Sample trend data of the energy consumption and its related cost without 4 indoor units without occupation scheduling plan consideration.

6.2 Scheduled MBPC 4 hours

In order to have thermal comfort by people's arrival, the HVAC system must start prior to occupation time and has to operate long enough for the room to reach the desired occupied comfort. Employing a conservative approach in the first step, the schedules are programmed in order to start the predictive control four hours prior to rooms occupancy. The first condition checked by the algorithm is to examine whether the current time of starting the control is within any pre-scheduled occupation period or four hours prior to that. In the first place, the predictions are calculated using the predictive models for 48 steps ahead. However the thermal comfort only matters within the occupation periods that is to say the limitations are only applied for the steps in the occupation interval. In the circumstance that the predictions depict thermal comfort within occupied periods, the HVAC system can be shut down thereby the control system sends a off-state command signal to the HVAC system until the time that it detects any violation. Conversely if it is not the case, ignore control parameter turns to false and the control algorithm is activated in order to compensate the violations. At the end of the scheduled occupied period, the HVAC system setpoint is set to zero and the room is allowed to drift away from the occupied comfort zone.

Algorithm 6.1. Scheduled MBPC 4 hours

```
1: for l = 1 to N_I do
2:     if (t_os.l − 4 [h] ≤ CurrentTime < t_oe.l) then
3:         for i = 0 to Ω_pr.l do
4:             if | node_i.Θ̂ | > Θ_T then
5:                 call algorithm 3.2 ⇐ C_ign ⇐ False
6:             end if
7:         end for
8:     end if
9: end for
```

Algorithm (6.1) summarizes the implementation procedure discussed above in which N_I is the number of existing occupation time intervals within the time that is being considered. Let t_{os} be given as the start and t_{oe} the end of the occupation interval, D_{os} and D_{oe} can be defined as the time durations to start and end of occupation periods respectively while Ω_{pr} depicts the number of steps in occupation period.
In order to analyze the possible benefits of starting up MBPC four hours prior to occupation time, the simulations are carried out in section (6.5).

6.3 Scheduled MBPC 2 hours

Avoiding overly conservative scheduling through the use of timed override buttons, determining the times to start and stop the HVAC system is a very sensitive issue and typically is based on the assumptions regarding the the building and the HVAC characteristics as well as the number of expected occupancy in each interval. Purposely low for the sake of caution, many consider an early start and late stopping for the system which is not interesting from an energy perspective. Consequently in order to minimize comfort complaints as well as not going through wasting energy, the optimal start time is required for the control algorithm in such a way that the control system waits as long as possible before starting the occupation so that all the zones reach to thermal comfort in time for occupancy.

According to the historical performance of how quickly the zone has been able to warm up or cool down for our HVAC systems, the best time to start the control is estimated as 2 hours prior to the occupation time. This strategy reduces the number of system operating hours and saves energy by avoiding the need to maintain the PMV index at thermal comfort level prior to the beginning of the scheduled occupied period. The procedure of this method is similar to scheduled MBPC 4 hours and it is summarized in algorithm (6.2).

Algorithm 6.2. Scheduled MBPC 2 hours

```
1: for l = 1 to N_I do
2:     if (t_os.l ≤ CurrentTime ≤ t_oe.l) or                then
          (t_os.l − 100 [min] ≤ CurrentTime < t_os.l)
3:         for i = 0 to Ω_pr.l do
4:             if | node.i.Θ̂ |> Θ_T then
5:                 call algorithm 3.2 ⇐ C_ign ⇐ False
6:             end if
7:         end for
8:     end if
9: end for
```

6.4 Modified MBPC Algorithm

In the typical implementation of the BaB, branching operation becomes more restrictive by applying the thermal comfort constraint in every step of the prediction horizon which results to have a higher probability of eliminating more branches from the search. When the BaB algorithm is in one node of the tree of solutions, no branching is performed for those control alternatives that lead to the violation of at least one restriction, thus pruning the sub-tree that would originate from the candidate branch. Looking from

energy consumption perspective and its correspondent prices, this method imposes extra costs as BaB is only limited to those control actions having PMV values in the thermal comfort range which is quiet unnecessary within rooms unoccupied periods. This study propose some modifications to BaB search algorithm strategy in order to restrict the branching only for those nodes of the prediction horizon that are within the occupation times. For the rest of the nodes, the constraints are not applied as the result of the fact that the thermal comfort that is the primary objective of the control can be ignored within those times and the second objective which is the energy prices are considered as our first goal.

In Modified BaB algorithm, MBPC initialize 4 hours prior to the pre-scheduled occupation time. At each time instant k, the predictive models provide the predictions for 4 hours ahead. The scheduling trend is as followed in algorithm (6.1). In the first place, the PMV values of the nodes of the prediction horizon within the occupation period are calculated using the models , assuming no control. In case that there is any predicted violation for desired nodes, then modified BaB algorithm is activated. Taking into account that the restrictions are only applied to the nodes within occupation period, the upper bound on the cumulative cost, incumbent value, is decomposed in two terms:

$$\jmath^{U}_{1:PH}(k) = \sum_{i=k+1}^{K+\Omega_{pr}} \min_{u(i-1)=AP_j} \{\hat{J}(i)\}_{i=1}^{nao} + \sum_{i=k+\Omega_{pr}+1}^{K+PH} \min_{u(i-1)=AP_j} \{\hat{J}(i)\}_{i=1}^{nao} \tag{6.1}$$

when BaB is in the time instant k within 4 hour prior to start of occupancy, considering that only steps $i = K + PH - \Omega_{pr}$ to $i = K + PH$ are within the occupation, the constraints are only applied to the second term of right hand of equation (6.1). Hence the cumulative cost from step $i = k + 1$ to $i = K + \Omega_{pr}$ are computed experiencing no restrictions. This approach allows the algorithm to be able to choose the best nodes minimizing the energy term inasmuch as the thermal comfort criterion is out of interest in these periods. Important to realize that if the time instant k is within occupation period, conversely this time the steps $i = k + 1$ to $i = K + \Omega_{pr}$ should be bounded by restrictions and so the constraints are applied to the objective function so as to calculate the cumulative cost within these periods. Overall cost over steps $i = k + PH - \Omega_{pr}$ to $i = K + PH$ are computed with no restrictions. Taking into account that no branching will be performed beyond the control horizon CH, equation (6.1) may be decomposed as,

$$\jmath^{U}_{1:PH}(k) = \begin{cases} \jmath^{U}_{1:CH}(k) + \jmath^{U}_{CH+1:PH}(k) & \Omega_{pr} \leq CH \\ \jmath^{U}_{1:CH}(k) + \jmath^{U}_{CH+1:\Omega_{pr}}(k) + \jmath^{U}_{\Omega_{pr}+1:PH}(k) & \Omega_{pr} > CH \end{cases} \tag{6.2}$$

BaB is faced to two circumstances in this phase. First if the algorithm is in the time instant k within 4 hour prior to start of occupancy, in this case the cumulative cost from step $i = K+PH-\Omega_{pr}$ to $i = K+PH$, $\jmath^{U}_{\Omega_{pr}+1:PH}(k)$ is bounded within thermal comfort criterion; however as the nodes within steps $i = k+1$ to $i = K+\Omega_{pr}$ are outside of occupation period the restriction is not applied in calculation of overall cost of $\jmath^{U}_{1:CH}(k)$ and $\jmath^{U}_{CH+1:\Omega_{pr}}(k)$. However being in the time instant k which is within the occupation interval, the cumulative costs $\jmath^{U}_{1:CH}(k)$ and $\jmath^{U}_{CH+1:\Omega_{pr}}(k)$ are bounded within thermal comfort criterion however as the nodes within $i = K+PH-\Omega_{pr}$ to $i = K+PH$ steps are outside of occupation period the restriction are not applied in order to calculate the term $\jmath^{U}_{\Omega_{pr}+1:PH}(k)$. An initial estimate of the optimal cumulative cost from step $CH+1$ to PH in a case that $\Omega_{pr} > CH$ is calculated as the the sum $\jmath^{U}_{CH+1:\Omega_{pr}}(k)$ and $\jmath^{U}_{\Omega_{pr}+1:PH}(k)$. Regarding these considerations, an estimate of the lower bound on the cumulative cost from step i to PH, $\jmath^{L}_{i:PH}(k)$ is computed. After all the conditions in the equations (3.20) and (3.21) are evaluated in order to decide if the solution search will follow a particular branch. A possible implementation of the procedures described above is listed in algorithm (6.4). The condition in line 14 restrict only those nodes within the occupation periods otherwise the objective is just to minimize the energy hence the cumulative cost is calculated in inasmuch as reduce the objective function.

In the typical implementation of BaB, when the algorithm encounter a violation of at least one restriction, the tree is pruned thus the candidate branch is eliminated. Due to this reason, it may be expected that the restricted problem formulation will be computationally cheaper when compared to the modified BaB. This case can not be problematic in the case of timing as branching is only performed until the control horizon is reached and henceforth the last control combination, $u(k+CH-1)$, should be applied successively to the system model until the prediction horizon is reached. Furthermore the improved version of BaB significantly decreases the energy consumption and its correspondent prices as it does not bound the control actions to fit in the range of thermal comfort outside of the occupation hours thereby the HVAC systems run for less hours.

6.5 Simulation results

In order to evaluate the efficiency of the developed methodologies, several experiments were conducted. These experiments were carried out to find out which of the these approaches best results in lower energy consumption and prices while providing thermal comfort while for occupants's arrival. As discussed earlier , the best objective function formulated for this problem is a cost-oriented structure built on a steady-state energy

Algorithm 6.4. Modified MBPC Algorithm

$(\jmath^U_{1:PH}, U) \Leftarrow \sum_{i=k+1}^{K+\Omega_{pr}} \min_{u(i-1)=AP_j}\{\hat{J}(i)\}_{i=1}^{nao} + \sum_{i=k+\Omega_{pr}+1}^{K+PH} \min_{u(i-1)=AP_j}\{\hat{J}(i)\}_{i=1}^{nao}$
$\jmath^U_{CH+1:PH} \Leftarrow \jmath^U_{1:PH} - \jmath^U_{1:CH}$
$BestNode.\jmath \Leftarrow \jmath^U_{1:PH}$
$BestNode.U \Leftarrow U$
$(node.i, node.U, node.\jmath) \Leftarrow (0, [], 0)$
$NodeList \Leftarrow \{node\}$
while do $len(NodeList) \neq 0$
  $node \Leftarrow NodeList.PopFirst$
  $node.i \Leftarrow node.i + 1$
  for $j = 1$ to nao **do**
    $NewNode \Leftarrow node$
    $NewNode.U \Leftarrow [NewNode.U\ A_i^T]$
    $NewNode.\jmath \Leftarrow NewNode.\jmath + \hat{J}^e$
    if $t_{os} \leq NewNode.k \leq t_{oe}$ **then**
      if $\mid NewNode.\hat{\Theta} \mid \leq \Theta_T$ **then**
        if $(NewNode.\jmath + \jmath^U_{CH+1:PH}) < \jmath^U_{1:PH}$ **then**
          $NewNode.\jmath \Leftarrow NewNode.\jmath + \hat{J}^m$
          if $(NewNode.\jmath + \jmath^U_{CH+1:PH}) < \jmath^U_{1:PH}$ **then**
            if $NewNode.i = CH$ **then**
              $BestNode \Leftarrow NewNode$
              $\jmath^U_{1:PH} \Leftarrow BestNode.\jmath$
              $\jmath^U_{CH+1:PH} \Leftarrow \left(\sum_{i=1}^{PH} min_{u(i-1)=A_j}\{\hat{J}(i)\}_{i=1}^{nao}\right)\Big|_{BestNode.U}$
              $\jmath^U_{1:PH} \Leftarrow \jmath^U_{1:PH} + \jmath^U_{CH+1:PH}$
            else
              $NodeList \Leftarrow \{NodeListNewNode\}$
            end if
          end if
        end if
      end if
    else
      if $(NewNode.\jmath + \jmath^U_{CH+1:PH}) < \jmath^U_{1:PH}$ **then**
        $NewNode.\jmath \Leftarrow NewNode.\jmath + \hat{J}^m$
        if $(NewNode.\jmath + \jmath^U_{CH+1:PH}) < \jmath^U_{1:PH}$ **then**
          if $NewNode.i = CH$ **then**
            $BestNode \Leftarrow NewNode$
            $\jmath^U_{1:PH} \Leftarrow BestNode.\jmath$
            $\jmath^U_{CH+1:PH} \Leftarrow \left(\sum_{i=1}^{PH} min_{u(i-1)=A_j}\{\hat{J}(i)\}_{i=1}^{nao}\right)\Big|_{BestNode.U}$
            $\jmath^U_{1:PH} \Leftarrow \jmath^U_{1:PH} + \jmath^U_{CH+1:PH}$
          else
            $NodeList \Leftarrow \{NodeListNewNode\}$
          end if
        end if
      end if
    end if
  end for
end while

estimation method presented in this work thereby it is applied for all the simulations in order to choose the best control action in each step. Four experiments were conducted within 2 days in January in order to evaluate the proposed control approaches in different circumstances. In order to initialize the predictive models, real data was obtained from the database. Each experiment simulates four methodologies, standard MBPC, scheduled MBPC 4 hours and 2 hours before the occupation as well as the modified MBPC algorithm.

An energy calculation has been done according to the procedure suggested by Mitsubishi which was given in the previous chapter. In order to utilize this formulation the HVAC system on/off as well as the thermostat state of each internal machine connected to the corresponding external unit are needed. Thus in order to estimate the energy consumption of the controlling unit, the control actions along with the on/off and thermostat bits of the other internal units were directly taken from the database thereby the external unit total energy consumption is divided by the suggested formulation among the internal machines as discussed in equation (5.17).

The first scenario considers a case that the controlling room is expected to be occupied for a duration of 140 minutes starting at 21:30 and finishing at 23:50 of a night in January. Figure (6.4) depicts the HVAC system on/off state from 4 hours before occupation. For the purpose of clarity, the plots of standard MBPC, scheduled MBPC 4 hours, scheduled MBPC 2 hours and modified MBPC are distinguished in different levels of 0.9, 1, 1.1 and 1.2 respectively. As it can be seen from the plot, scheduled MBPC 4 hours is operating for 72.34% of the time before the occupancy while this value is equal to 29.79% and 21.28% for scheduled MBPC 2 hours and Modified MBPC respectively. The standard MBPC is off for whole this period, as the control algorithm only starts in the beginning of the occupancy however in order to compensate for the discomfort in the rooms, the HVAC has to operate for 75% within this period, whereas scheduled MBPC 4 hours, scheduled MBPC 2 hours and modified MBPC are running for 35.71%, 14.29% and 35.71% within occupied times respectively.

For visual representation of the thermal comfort criterion, PMV index for all the approaches are plotted in (6.5) in which standard MBPC is out of comfort zone for 53.57% of the occupation period and although the HVAC system is operating for 75% inside the occupation period. This happens notwithstanding that all the developed scheduled MBPC methodologies lead the system to lie in thermal comfort zone for whole the considerer period.

Numerical values for the energy consumption as well as the commensurate costs distinguished in two parts of 4 hours prior to occupation and within occupation are represented in table (6.1). As it can be seen from the table, standard MBPC has the lowest energy

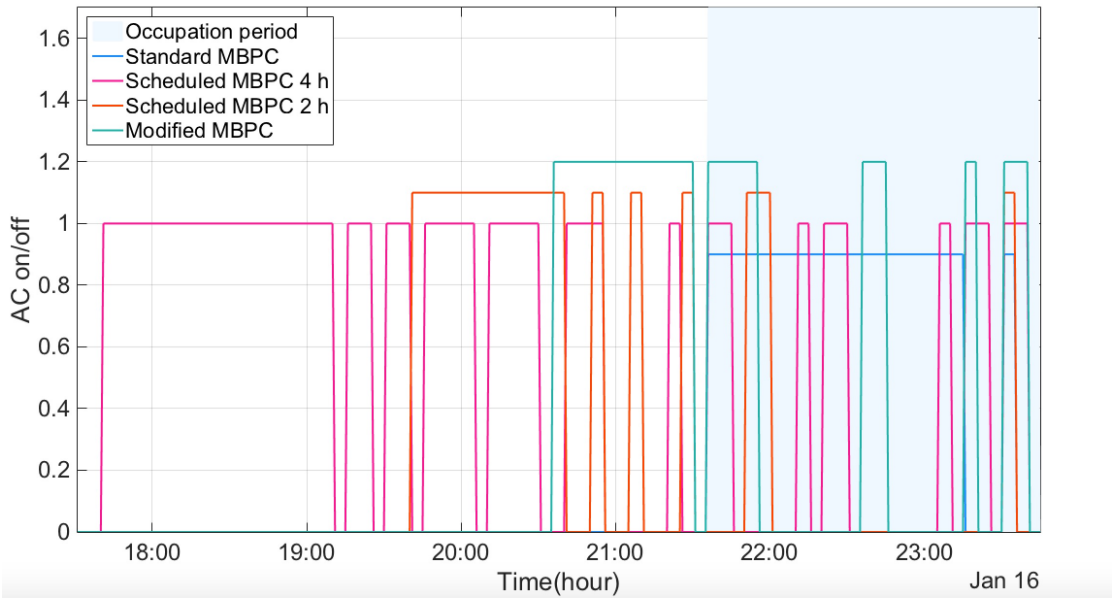

FIGURE 6.4: A comparison between HVAC system on/off state applying different MBPC methodologies developed in this work compared with the MBPC with regular BaB algorithm for experiment 1. In order the plot to be discernible, standard MBPC, scheduled MBPC 4 hours, scheduled MBPC 2 hours and modified MBPC on/off states are distinguished in different levels of 0.9, 1, 1.1 and 1.2 respectively.

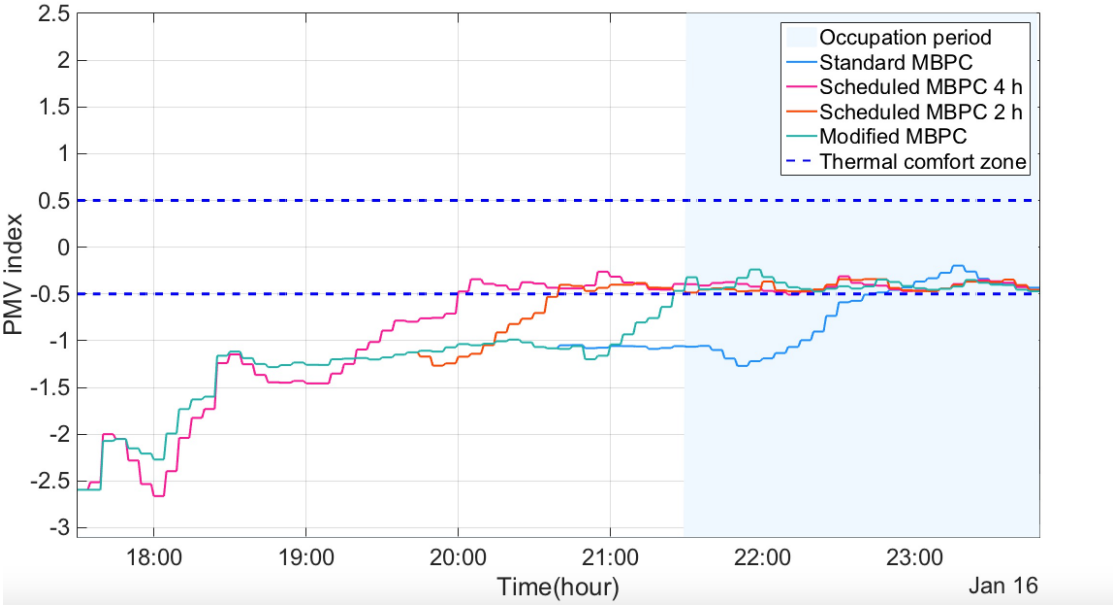

FIGURE 6.5: PMV evolution employing different MBPC methodologies developed in this work compared to the standard MBPC within the occupation period for experiment 1.

consumption and price among the all equal to $3.15\,kWh$ and 0.25 € notwithstanding that the rooms is not in thermal comfort for 53.57% of the occupation time. However modified MBPC has the total lower energy consumption of $4.46\,kWh$ and price of 0.64 €

thereby can be considered as the most efficient control methodology in terms of thermal comfort as well as the energy consumption and expenses.

Control approach	4 **hours before occupation**		**within occupation**	
	Energy (kWh)	**Price (€)**	**Energy (kWh)**	**Price (€)**
Standard MBPC	0.00	0.00	3.15	0.25
Scheduled MBPC 4 hours	8.47	1.19	1.64	0.13
Scheduled MBPC 2 hours	4.45	0.90	0.45	0.04
Modified MBPC	2.98	0.51	1.48	0.13

TABLE 6.1: Energy consumptions and their corresponding prices employing different MBPC methodologies developed in this work compared to the standard MBPC distinguished in two parts of 4 hours prior to occupation and within occupation for experiment 1.

Second scenario has a considerably longer duration and it includes 2 occupation periods. The first expected occupancy is in the morning at 7:00 ending up till 13:30 for 6 hours and 30 minutes, having a pause of only 110 minutes, the room is supposed to be occupied again for a period of 11 hours from 15:20 till 2:20 a.m of the next day. HVAC system on/off state depicted in figure (6.6) illustrates that, employing scheduled MBPC 4 hours, the HVAC system runs for the significant amount of time before the occupation (49.30% of time for both occupancy intervals) while this value is only 16.19% within total occupation hours. However by applying scheduled MBPC 2 hours and modified MBPC, the HVAC system's behavior is more or less the same and the AC operates for 22.54% and 25.35% of time prior to two occupancy periods in total and 9.05% and 8.1% along the both occupation periods respectively. Standard MBPC only start in the beginning of each pre-scheduled occupancy time, so the HVAC system is running for total 58.57% of times within both occupations.

A comparison between thermal comfort conditions using each method is plotted in (6.7) showing that 3 scheduling approaches lie in thermal comfort zone for whole the occupation periods in contrast of employing the standard MBPC in which for the first expected occupation period, the room is not in thermal comfort for 52.56% of the time while this violation is about 19.52% considering both the occupation intervals.

Table (6.2) summarizes the energy consumption and the related expenses of each control methodology. Numerical values represent that notwithstanding the energy consumption and price before the occupation is zero for standard MBPC but however in order to compensate the discomfort, the HVAC system needs to operate for most of the occupation intervals leading to consume $18.07\,kWh$ energy with cost of 2.02 €. As can be seen from the table, modified MBPC leads to the less energy consumption of $4.46\,kWh$ and price of 0.41 € in total. However these values are marginally lower than the energy consumption and price of the scheduled MBPC 2 hours which are equal to $4.77\,kWh$ and 0.47 € respectively. The total energy and price for scheduled MBPC 4 hours is however

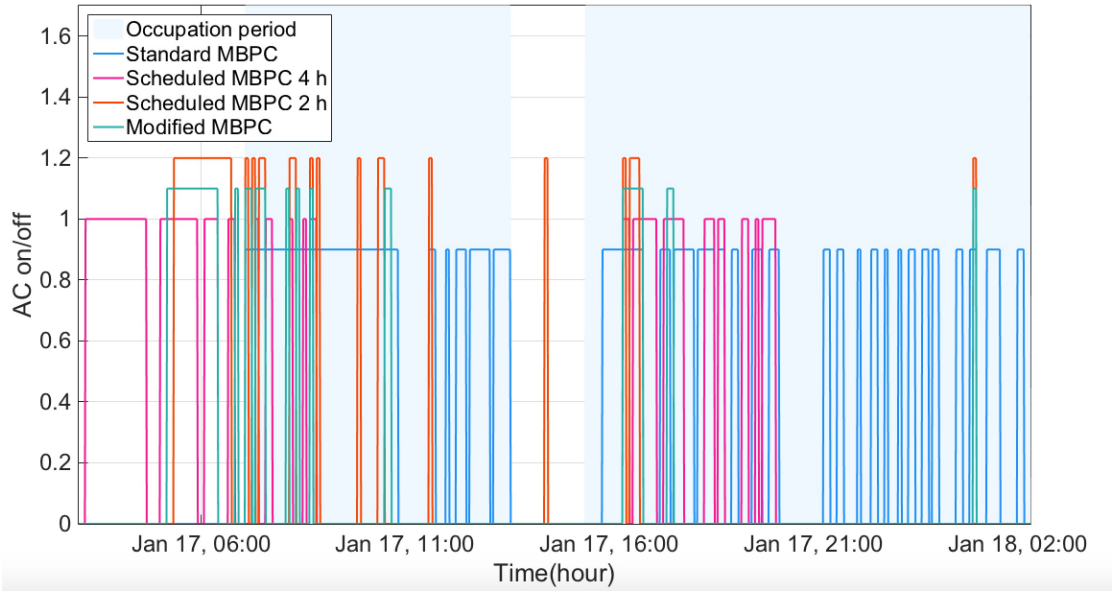

FIGURE 6.6: A comparison between HVAC system on/off state applying different MBPC methodologies developed in this work compared with the MBPC with regular BaB algorithm for experiment 2. In order the plot to be discernible, standard MBPC, scheduled MBPC 4 hours, scheduled MBPC 2 hours and modified MBPC on/off states are distinguished in different levels of 0.9, 1, 1.1 and 1.2 respectively.

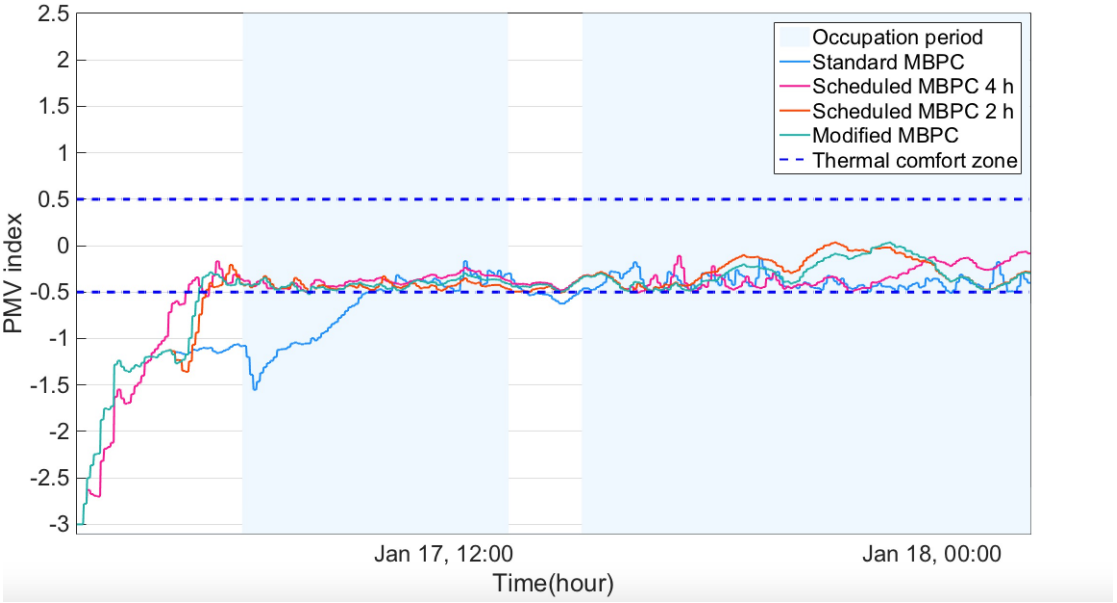

FIGURE 6.7: PMV evolution employing different MBPC methodologies developed in this work compared to the standard MBPC within the occupation period for experiment 2.

a bit higher, although considerable compared to standard MBPC, equal to 6.24 kWh and 0.64 €.

Control approach	4 **hours before occupation**		**within occupation**	
	Energy (kWh)	**Price (€)**	**Energy (kWh)**	**Price (€)**
Standard MBPC	0.00	0.00	18.07	2.02
Scheduled MBPC 4 hours	1.81	0.12	4.43	0.52
Scheduled MBPC 2 hours	1.88	0.14	2.89	0.33
Modified MBPC	1.45	0.10	3.01	0.31

TABLE 6.2: Energy consumptions and their corresponding prices employing different MBPC methodologies developed in this work compared to the standard MBPC distinguished in two parts of 4 hours prior to occupation and within occupation for experiment 2.

Taking advantage of a whole day experiment with longer occupation periods in different time of the day while the duration between two occupancy is less than 2 hours, we can conclude that beneficing from scheduled control methodologies, the room is guaranteed to be in thermal comfort within the occupation periods. On the other hand taking advantage of flexibility over possible times to turn on the HVAC system, the control algorithm is able to shift the major operating time to low energy-rate intervals if conceivable according to thermal comfort limitations.

As it was mentioned before, the first goal of control strategy is to provide thermal comfort within the occupation periods. Consider $\Gamma_{j,k}(i)$ as the PMV failure resulted from applying the control algorithm j in the instant i of the experiment k where $j = 1, 2, 3, 4$ refers to standard MBPC, scheduled MBPC 4 hours , scheduled MBPC 2 hours as well as modified MBPC respectively:

$$\begin{gathered}\Gamma_{j,k}(i) = \begin{cases} 0 & \text{if} \quad |\Theta_{j,k}(i)| \leq \Theta_T \\ 1 & \text{if} \quad |\Theta_{j,k}(i)| \geq \Theta_T \end{cases} \\ k = 1, 2, 3, 4 \quad i \in [1, \ell_k] \\ j = 1, 2, 3, 4 \end{gathered} \tag{6.3}$$

In which i is a notation representing each instant within the experiment k which ranges between $[1, \ell_k]$ where ℓ_k is the length of experiment k. $\Theta_{j,k}(i)$ demonstrates the PMV values resulted from applying the control rule j within in the instant i of the experiment k and Θ_T expresses the PMV threshold value. The PMV failure percentage correspondent to the experiment k applying the control methodology j, $\hbar_\Gamma(j, k)$, can be calculated as:

$$\hbar_\Gamma(j, k) = \frac{\sum_{i=1}^{\ell_k} \Gamma_{j,k}(i)}{\ell_k} \times 100 \tag{6.4}$$

According to (6.4), $\hbar_\Gamma(j, k)$ values related to 2 considered experiments earlier employing 4 presented MBPC algorithms were calculated. As follows from the numerical values,

considering that the standard MBPC initializes only in the beginning of the occupation period, the PMV has been violated from thermal comfort area for 53.57% within occupation interval of experiments 1 and 52.56% of the first occupation period of experiment 2 which is 19.52% of total occupied intervals in this experiment whereas scheduled MBPC control methodologies demonstrate zero violation along the both experiments.

The second goal of the control algorithm is to decrease the energy consumption and expenses as much as feasible. In order to sum up the simulation results, it is needed to evaluate the efficiency of developed methods. Considering $E_{schd}(j,k)$ as a sequence of energy consumption values correspondent to each of the developed scheduled MBPC algorithms j and experiment k, the energy rise/fall percentage of each developed method compared to standard MBPC is noted as $\Lambda_E(j,k)$ and can be calculated by:

$$\Lambda_E(j) = \frac{E_{reg}(k) - E_{schd}(j,k)}{max(E_{reg}(k), E_{schd}(j,k))} \times 100 \quad \begin{matrix} j = 1,2,3 \quad k = 1,2,3,4 \end{matrix} \tag{6.5}$$

where $E_{reg}(k)$ is the energy consumption value applying the standard MBPC algorithm of the experiment k while three concept are introduced as:

$$\begin{cases} rise \quad \text{if} \quad \Lambda_E(j) \geq 0 \\ equal \quad \text{if} \quad \Lambda_E(j) = 0 \\ fall \quad \text{if} \quad \Lambda_E(j) \leq 0 \end{cases} \tag{6.6}$$

where *rise* means that the correspondent scheduling MPBC algorithm has a rise in energy efficiency compared to the standard MBPC by amount of $\Lambda_E(j,k)$ for th experiment k. On the contrary, *fall* means that the correspondent scheduling MPBC algorithm has decreased the efficiency compared to the standard MBPC by amount of $\Lambda_E(j,k)$. At last *equal* illustrates the condition that the efficiency of both comparing algorithms are equal. Equally we shall write the above expressions to evaluate energy expenses as:

$$\Lambda_P(j) = \frac{P_{reg}(k) - P_{schd}(j,k)}{max(P_{reg}(k), P_{schd}(j,k))} \times 100 \quad \begin{matrix} j = 1,2,3 \quad k = 1,2,3,4 \end{matrix} \tag{6.7}$$

where $\Lambda_P(j)$ stands for price efficiency rise/fall percentage of each developed method, j compared to standard MBPC and $P_{reg}(k)$ is the energy price by employing the standard MBPC in each experiment k. Furthermore energy price resulted from scheduling type control algorithm j is noted by $P_{schd}(j,k)$. Simultaneously to (6.6), following condition can be rewritten in order to evaluate the price efficiency:

$$\begin{cases} rise & \text{if} \quad \Lambda_P(j) \geq 0 \\ equal & \text{if} \quad \Lambda_P(j) = 0 \\ fall & \text{if} \quad \Lambda_P(j) \leq 0 \end{cases} \tag{6.8}$$

Considering the above discussion, table (6.3), outlines the effectiveness of each developed control strategy compared to the standard MBPC. Numerical values demonstrate that although this may be true that in the first experiment all the scheduled MBPC methodologies consume more energy leading to have higher expenses, however as the first goal of the control algorithm is thermal comfort within the occupation times, this can be neglected. Furthermore as can be seen from the table, in longer periods of time, scheduled MBPC approaches lead the HVAC system to decrease the energy consumption and price to minimum of 65% and 68% respectively. The table indicates that scheduled MBPC 2 hours and modified MBPC algorithms result in lower energy consumption an price however inasmuch as modified MBPC has the lowest consumption and cost while maintaining the thermal comfort withing all the occupation periods in both experiments, this approach is chosen as the best control methodology among the studied MBPC approaches.

Experiment	**Scheduled MBPC** 4 **hours** ($j = 1$)		**Scheduled MBPC** 2 **hours** ($j = 2$)		**modified MBPC** ($j = 3$)	
	Energy (%)	**Price**(%)	**Energy** (%)	**Price**(%)	**Energy** (%)	**Price**(%)
$k = 1$	-68	-82	-19	-68	-13	-49
$k = 2$	65	68	76	79	79	84

TABLE 6.3: Energy consumption and corresponding price saving percentages employing different MBPC methodologies developed in this work compared to the standard MBPC within 4 presented experiments.

6.6 Concluding remarks

Based on the results, it can be concluded that the research on scheduling MPBC as well as modifying the search methodology of BaB algorithm in air-conditioning applications has been very successful. From the outcome of our investigation it is possible to conclude that taking into account the occupation periods in controlling the HVAC systems of the buildings significantly reduces the energy consumption and thereby building expenses.

The findings of our research are quite convincing, and thus the following conclusions can be drawn according to the experiments carried out. Standard MBPC only initializes in the beginning of the occupation period though employing this approach, the system endure PMV violation for significant amount of time of starting each occupancy period if

the room is not already in thermal comfort. Employing scheduled MBPC 4 hours, on the positive side makes the system to maintain the thermal comfort within all the occupation periods however on the negative side as the system has started 4 hours before and best control actions are only chosen based on the weather predictions, thereby may lead the system to over work sometimes and though the energy consumption and price is higher that the other two developed approaches. Scheduled MBPC 2 hours and modified MBPC algorithm make the system to maintain the thermal comfort within all the occupation periods inasmuch as the later approach saves the most energy consumption and its related costs among all the studied approaches, thus this method has been chosen to apply in real time control.

7

Conclusions and future works

7.1 Conclusions

Model based predictive control is nowadays perceived in the literature as the best method for HVAC control when the minimization of energy consumption is one of the requirements. In order to take fully advantage of this methodology, the most possible accurate predictive models are required, as the control solutions highly depend on the quality of the predictions. The model based predictive control employed in this thesis involves five site-specific predictive models for thermal dynamics of the given building in order to forecast inside climate and outside weather within the prediction horizon, in addition to predicted mean vote model in order to evaluate the thermal comfort conditions within the prediction horizon. These predictive models had already obtained been using radial basis artificial neural networks developed by means of an implementation of multi-objective genetic algorithm in CSI research center in UAlg. Multi-objective genetic algorithms were employed in order to choose the models structure, that is their number of neurons, used variables and lagged input terms.

The data yielded by this study provided convincing evidence that the energy consumption is completely independent from the deviation of the average inside air temperature over the integration period to its setpoints. Therefore as this dissertation studies a

multi-zone building, thereby in order to deal with subsystem interactions, an adequate estimation of the energy consumption of the external device which supplies the air with desired temperature to multiple indoor units was essential. This energy highly depended on the number of operating internal machines in each control step. This issue been addressed in this thesis by using dynamic and static models.

Furthermore, the outright cost benefit analysis should not only contain energy savings but also the economical cost of the control actions chosen by MBPC. This thesis demonstrated that peak electricity demand in building climate control corresponding to a given reference load curve could successfully be decreased by incorporating a conveniently designed variable electricity tariff straightly into the objective function of an MBPC setup. This load shifting effort for thermal loads resulted in lower electricity costs.

Discretizing the control space into a finite set of control alternatives enables us to apply search techniques in order to obtain an appropriate control solution to be implemented by the actuators. The branch-and-bound method had been suggested in the previous version of this work ([1]) in order to search out for the optimal solution to the formulated PMV restricted predictive control problem.

Assorted improvements were introduced to the initial control problem formulation with the goal of reducing the energy consumption as well as costs required to achieve a predefined PMV index bound. An alternative to solve this issue would be to take into account the occupation scheduling of the building. To address this problem, two different scheduling, regarding the time prior to occupation were introduced. It was confirmed by simulations that these approaches provided thermal comfort in the beginning of occupancy times and maintain the comfort within all the pre-scheduled intervals. However, another improvement was proposed in the optimization algorithm in order to decrease the energy as well the corresponding prices. The idea was to improve the branch and band search paradigm in order not to bound the control actions to fit in the range of thermal comfort outside of the occupation hours. The simulation results indicated that the suggested scheme was well set off to attain the aim of load shifting and reducing of peak electricity demand regarding a given load profile.

7.2 Future work

In practical problems, it is typical to detect that the required constraints are inconsistent; namely, they cannot all be satisfied simultaneously. In the circumstance that constraints do not agree on a solution, then the MBPC optimization is poorly situated and has no solution. However this cannot occur on a real process as the control output would be

haphazard. In modified BaB developed in this work, the PMV values are not bounded outside the occupied periods. Furthermore a conservative alternative approach is made in case that no control action is found within the required time respecting the constraints, that is to apply the predefined setpoints by the control algorithm. However the control performance can be improved by considering some soft constraints that can be violated though at some small penalty which can be prioritized into a ranking of importance.

The predictive models are crucial portions of the overall control solution proposed. The prediction performance improvement undoubtedly would be translated in an improvement of the accuracy of the control system. Problems of uncertainty in future output predictions come from the uncertainty in the model due to the influence of manipulated variables on process outputs as well as the uncertainty in future disturbances. Model uncertainty can be explained as parametric uncertainty. Analogously, disturbance uncertainty may be characterized regarding a stochastic model, whereas that model may change drastically with time. Thus, quantification of the uncertainty of future output predictions cannot conceivably apprehend all possible cases. Therefore the forecasts could be seen as stochastic variables and thus it could be interesting as well to develop a stochastic predictive model for occupancy forecasts in order to take into account the the internal thermal load changes produced by occupations and activities.

Bibliography

[1] P. M. Ferreira, A. E. Ruano, S. Silva, and E. Z. E. Conceicão, "Neural networks based predictive control for thermal comfort and energy savings in public buildings," *Energy and Buildings*, vol. 55, p. 238–251, 2012.

[2] P. M. Ferreira, *Application of computational intelligence methods to greenhouse environmental control*. PhD thesis, The University of Algarve, 2007.

[3] ISO, Geneve, Switzerland, *Iso 7730: Moderate thermal environments determination of the pmv and ppd indices and specification of the conditions for thermal comfort*, 1994.

[4] B. Atanasiu, C. Despret, M. Economidou, J. Maio, I. Nolte, and O. Rapf, *Europe's buildings under the microscope*. Buildings Performance Institute Europe (BPIE), 2011.

[5] F. Haghighat, "Thermal comfort in housing and thermal environments," *Sustainable build environment*, vol. I.

[6] P. O. Fanger, *Thermal comfort: analysis and applications in environmental engineering*. McGraw-Hill, 1972.

[7] F. Oldewurtel, *Stochastic model predictive control for energy efficient building climate control*. PhD thesis, ETH Zurich, 2011.

[8] M. S. Owen, *ASHRAE handbook–fundamentals*. ASHRAE, si ed., 2009.

[9] A. Aswani, N. Master, J. Taneja, D. Culler, and C. Tomlin, "Reducing transient and steady state electricity consumption in hvac using learning-based model-predictive control," *Proceedings of the IEEE*, vol. 100, pp. 240–253, 2012.

[10] J. R. Ma, J. Qin, T. Salsbury, and P. Xu, "Demand reduction in building energy systems based on economic model predictive control," *PChemical Engineering Science*, vol. 67, pp. 92–100, 2012.

[11] R. W. Payne and J. J. McGowan, *Energy management and control system handbook*. Lilburn, GA: The Fairmont Press, 1988.

[12] M. Zaheer-Uddin and G. Zheng, "Optimal control of time-scheduled heating, ventilation and air conditioning processes in buildings," *Energy Conversion & Management*, vol. 41, pp. 49–60, 2000.

[13] W. Grünenfelder and J. Tödtli, "The use of weather predictions and dynamic programming in the control of solar domestic hot water systems," 1985.

[14] R. V. Andersen, B. Olesen, and J. Toftum, "Simulation of the effect of occupant behaviour on indoor climate and energy cosumption," in *Cima 2007 Well Being Indoors*, (Helsinki, Finland), 2007.

[15] D. Bourgeois, C. Reinhart, and I. Macdonad, "Adding advanced behavioural models in whole building energy simulation: A study on the total energy impact of manual and automated lighting control," *Energy and Buildings*, vol. 38, p. 814–823, 2006.

[16] S. H. Cho and M. Zaheer-uddin, "Predictive control of intermittently operated radiant floor heating system," *Energy and Conversion Management*, vol. 49, pp. 1333–1342, 2003.

[17] M. Gwerder and J. Todtli, "Predictive control for integrated room automation," in 8*th REHVA World Congress for Building Technologies, CLIMA 2005*, (Lausanne), 2005.

[18] G. P. Henze, D. E. Kalz, S. Liu, and C. Felssman, "Experimental analysis of model-based predictive optimal control for active and passive building thermal storage inventory," *HVAC & RESEARCH*, vol. 11, pp. 189–213, 2005.

[19] A. E. D. Madyn, G. M. Provan, C. Ryan, and K. N. Brown, "Stochastic model predictive controller for the integration of building use and temperature regulation," in *in Proceedings of the Twenty-Fifth AAAI Conference on Artiffcial Intelligence*, 2011.

[20] Y. Ma and F. Borrelli, "Fast stochastic predictive control for building temperature regulation," in *American Control Conference*, (Canada), pp. 3075–3080, 2012.

[21] F. Oldewurtel, A. Parisio, C. N. Jones, D. Gyalistras, M. Gwerder, V. Stauch, B. Lehmann, and M. Morari, "Use of model predictive control and weather forecasts for energy effcient building climate control," *Energy and Buildings*, vol. 45, pp. 15–27, 2012.

[22] A. Parisio, M. Molinari, D. Varagnolo, and K. H. Johansson, "A scenario-based predictive control approach to building hvac management systems," in *IEEE Conference on Automation Science and Engineering (CASE)*, 2013.

[23] Internation Organization for Standardization, *Ergonomics of the thermal environment-analytical determination and interpretation of thermal comfort using calculation of PMV and PPD indices and local thermal comfort criteria*, 2005. ISO7730.

[24] American Society of Heating, Refrigerating and Air-Conditioning Engineers, Atlanta, USA, *ASHRAE fundamentals*, 2005.

[25] American Society of Heating, Refrigerating and Air Conditioning Engineers, *Standard 55-2004*, 2004.

[26] R. Freire, G. Oliveira, and N. Mendes, "Predictive controllers for thermal comfort optimization and energy savings," *Energy and Buildings*, vol. 40, p. 1353–1365, 2008.

[27] M. Castilla, J. Álvarez, M. Berenguel, F. Rodríguez, J. Guzmán, and M. Pérez, "A comparison of thermal comfort predictive control strategies," *Energy and Buildings*, vol. 43, p. 2737–2746, 2011.

[28] D. Rijksen, C. Wisse, , and A. V. Schijndel, "Reducing peak requirements for cooling by using thermally activated building systems," *Energy and Buildings*, vol. 42, p. 298–304, 2009.

[29] J. E. Braun, "Load control using building thermal mass," *Journal of Solar Energy Engineering*, vol. 125, pp. 292–301, 2003.

[30] J. Ma, S. Qin, B. Li, and T. Salsbury, "Economic model predictive control for building energy systems," *IEEE*, vol. 42, p. 1–6, 2011.

[31] P. D. Morošan, R. Bourdais, D. Dumur, and J. Buisson, "Building temperature regulation using a distributed model predictive control," *Energy and Buildings*, vol. 42, p. 1445–1452, 2010.

[32] P. D. Morošan, R. Bourdais, D. Dumur, and J. Buisson, "A distributed mpc strategy based on benders' decomposition applied to multi-source multi-zone temperature regulation," *Process Control*, vol. 21, p. 729–737, 2011.

[33] P. M. Ferreira, S. M. Silva, A. E. Ruano, A. T. Négrier, and E. Z. E. Conceicão, "Neural network pmv estimation for model-based predictive control of hvac systems," (Brisbane, Australia), 2012.

[34] A. E. Ruano, G. Mestre, H. Duarte, S. Silva, P. M. F. S. Pesteh, H. Khosravani, and R. Horta, "A neural-network based intelligent weather station," (Siena), pp. 1–6, 2015.

[35] P. M. Ferreira and A. E. Ruano, "Evolutionary multiobjective neural network models identification: Evolving task-optimised models," in *New Advances in Intelligent Signal Processing, ser. Studies in Computational Intelligence*, vol. 372, p. 21–53, 2011.

[36] P. M. Ferreira, A. E. Ruano, and C. Fonseca, "Genetic assisted selection of rbf model structures for greenhouse inside air temperature prediction," (Istanbul, Turkey), p. 576–581, 2003.

[37] P. M. Ferreira, A. E. Ruano, and C. M. Fonseca, "Evolutionary multi-objective design of radial basis function networks for greenhouse environmental control," in *The 16th IFAC World Congress on Automatic Control*, vol. 16, (Prague, Czech Republic), 2005.

[38] P. M. Ferreira and A. E. Ruano, "Discrete model-based greenhouse environmental control using the branch & bound algorithm," in *Proceedings of the 17th World Congress*, (Seoul, Korea), 2008.

[39] P. M. Ferreira, S. M. Silva, and A. E. Ruano, "Model based predictive control of hvac systems for human thermal comfort and energy consumption minimisation," in *Proceedings of the 1st IFAC Conference on Embedded Systems, Computational Intelligence and Telematics in Control - CESCIT*, (Würzburg, Germany), 2012.

[40] P. M. Ferreira, S. M. Silva, and A. E. Ruano, "Energy savings in hvac systems using discrete model-based predictive control," in *WCCI 2012 IEEE World Congress on Computational Intelligence*, (Brisbane, Australia), 2012.

[41] A. E. Ruano, S. Silva, S. Pesteh, P. M. Ferreira, H. Duarte, G. Mestre, H. Khosravani, and R. Horta, "Improving a neural networks based hvac predictive control approach," in *2015 IEEE 9th International Symposium on Intelligent Signal Processing (WISP)*, (Siena), pp. 1–6, 2015.

[42] J. Maciejowski, *Predictive control with constraints*. England: Prentice Hall, 2002.

[43] J. B. Rawlings and D. Q. Mayne, *Model predictive control: theory and design*. Nob Hill Publishing, 2009.

[44] J. Kang, Y. Kim, H. Kim, J. Jeong, and S. Park, "Comfort sensing system for indoor environment," in *International Conference on Solid State Sensors and Actuators*, vol. 1, p. 311–314, jun 1997.

[45] T. Bedford and C. Warner, "The globe thermometer in studies of heating and ventilation," *Journal of Hygiene*, vol. 34, no. 4, p. 458–473, 1934.

[46] K. Cena and J. Clark, "Bio engineering, thermal physiology and comfort," *Elsevier*, vol. 10, 1981.

[47] J. A. Orosa and A. C. Oliveira, "Software tools for hvac research". in: Advances in engineering software," *Process Control*, vol. 42, p. 846–851, 2011.

[48] K. Levenberg, "A method for the solution of certain non-linear problems in least squares," *The Quarterly of Applied Mathematics*, vol. 2, p. 164–168, 1944.

[49] D. W. Marquardt, "An algorithm for least-squares estimation of nonlinear parameters," *Journal of the Society for Industrial and Applied Mathematics*, vol. 11, no. 2, p. 431–441, 1963.

[50] A. Ruano, D. Jones, and P. Fleming, "A new formulation of the learning problem of a neural network controller," in *Proceedings of the 30th IEEE Conference on Decision and Control*, vol. 1, p. 865–866, 1991.

[51] P. M. Ferreira and A. E. Ruano, "Exploiting the separability of linear and non-linear parameters in radial basis function neural networks," (Canada), pp. 321–326, 2000.

[52] T. M. Cover, "Geometrical and statistical properties of systems of linear inequalities with applications in pattern recognition," *IEEE Transactions on Electronic Computers*, p. 326–334, 1965.

[53] C. A. Micchelli, "Interpolation of scattered data: distance matrices and conditionally positive functions," *Constr. Approx*, vol. 2, pp. 11–22, 1965.

[54] S. Haykin, *Learning in neural networks: a comprehensive foundation*. Prentice Hall, 1999.

[55] P. M. Ferreira, E. Faria, and A. E. Ruano, "Neural network models in greenhouse air temperature prediction," *Neurocomputing*, vol. 43, no. 1-4, p. 51–75, 2002.

[56] A. E. Ruano, P. M. Ferreira, and C. Fonseca, "An overview of non-linear identification and control with neural networks," *A.E. Ruano (Ed.), Intelligent Control Using Soft-Computing Methodologies, IEE Publishing*, vol. 70 of Control Series, p. 37–87, 2005.

[57] P. M. Ferreira and A. E. Ruano, "Application of computational intelligence methods to greenhouse environmental modelling," in *IEEE International Joint Conference on Neural Networks (IJCNN 2008)*, p. 3582–3589, 2008.

[58] J. Clausen, "Branch and bound algorithms – principles and examples," 1999. Lecture notes.

[59] J. M. Sousa, R. Babuška, and H. B. Verbruggen, "Fuzzy predictive control applied to an air-conditioning system," *Control Engineering Parctice*, vol. 5, p. 1395–1406, 1997.

[60] J. A. Roubos, S. Mollov, R. Babuška, and H. B. Verbruggen, "Fuzzy model-based predictive control using takagi-sugeno models," *International Journal of Approximate Reasoning*, vol. 22, p. 3–30, 1999.

[61] J. M. Sousa, "Optimization issues in predictive control with fuzzy objective functions," *International Journal of Intelligent Systems*, vol. 15, p. 879–899, 2000.

[62] L. Ljung, *System identification toolbox user's guide*. MathWorks, third ed., 1995.

[63] T. Salsbury, "A survey of control technolsogies in the building automation industry," in *IFAC World Congress*, (Prague, Czech Republic), 2005.

[64] J. I. Aunon, C. D. McGillem, and D. G. Childers, "Signal processing in evoked potential research: averaging and modeling," *Averaging and modelling, CRC Crit Rev Bioeng*, vol. 5, pp. 323–367, 1981.

[65] M. Electric, *Electric, how to calculate the electric energy consumption ratio of city multi by BMS via LMAP02*, 2001.